Elucidation of the structure and mechanism of the MtrCDE multi drug transporter in Neisseria gonorrhoeae

Zhang, Li

Durham University

Elucidation of the structure and mechanism of the MtrCDE multidrug transporter in *Neisseria gonorrhoeae*

By

Li Zhang

Xi'an JiaoTong University, MD in Clinical Medicine

Xi'an JiaoTong University, M.Sc in Medical Microbiology

A thesis submitted for the degree of Doctor of Philosophy

In

The School of Biological and Biomedical Sciences

Durham University

Contents

September 2008

Declaration

I declare that the work presented herein is my own, except where stated by citation or statement, and has not been submitted for another degree in this or any other university.

Acknowledgements

This PhD was undertaken at the School of Biological and Biomedical Science, Durham University. The author was a recipient of a University doctoral fellowship.

I am indebted to Professor Adrian Walmsley for providing me with the opportunity to study for this PhD and for his guidance throughout the development of my study; to my colleagues, past and present, Dr Ines Borges-Walmsley, Dr John Gatehouse, Dr Dijun Du, Dr Daliang Chen, Dr Kenny McKeegan, Dr Gary Sharples, Dr Teresa Massam-Wu, Emma Cunningham, Dr Hong-Ting Lin, Dr Thamarai J Kanan, Jungwoo Yang, Dr Fiona Curtis and Helen Frankish for their invaluable sources of information and direction; Further thanks to Ms Diane Hart and Mr Simon Padbury for their indispensable assistance. Finally, I express my sincere thanks to all my family and friends for their inspiration and love. My reverence extends to my husband Yingwei Zhang for his immense love, patience and support.

Publishments arising from this thesis

1. Zhang, L., Barrera, N.P., Bavro,V.N. Zhang B, Janganan T.K., Matak-Vinkovic D., Robinson C.V., Borges-Walmsley M.I. and Walmsley, A.R. The MtrC-hairpin domain activates the MtrCDE tripartite multidrug pump from Neisseria gonorrhoeae. Submitted to *Journal of Mol Biology*
2. McKeegan, K.S. , Zhang L. , Burton M.F., Steel P.G. , Sharples G.J., Borges-Walmsley M.I. and Walmsley A.R. Evolution of a repressor for co-ordinated transcriptional regulation of both chromosomal and plasmid encoded resistance determinants in *Neisseria gonorrhoeae*. Submitted to *Microbiology*.

Abstract:

The Mtr (Multiple transferable resistance) transport system in *Neisseria gonorrhoeae* was found to confer the resistance of gonococci to penicillin and structural diverse hydrophobic agents (HAs), such as drugs, dyes, detergents and host-derived compounds (fatty acids and bile salts), as well as some cationic antimicrobial peptides. The *mtr* operon encodes an energy-dependant efflux pump system and this MtrC-MtrD-MtrE system is negatively regulated by the transcriptional repressor MtrR.

The first part of this thesis presents insights into a structural study of the two membrane components, the inner membrane protein MtrD and the outer membrane protein MtrE. MtrD and MtrE have been overexpressed, purified and crystallized using the sitting-drop vapour-diffusion method. Unfortunately, due to the difficulty of membrane protein crystallography, the best resolution of the MtrE crystals was only 8Å and of the MtrD crystals was 20Å, so the structures of both MtrE and MtrD haven't been solved yet. However, this preliminary X-ray analysis leads to the possibility of solving these structures in the near future. In the mean time, using pull-down assay、 growth curve analyses and ITC(Isothermal Titration Calorimetry), we established that the antiporter MtrD, the adaptor MtrC and the outer membrane protein MtrE form a contiguous complex. Assembly of the pump is constitutive, even in absence of substrate. Without the assistance of MtrC, MtrD was unable to export its substrate, Nafcillin, and the efficiency of this assembly could be enhanced by the presence of the outer membrane protein MtrE. MtrD could interact with MtrE independently in pull-down assays, showing they can form a complex even in the absence of MtrC. This behaviour is consistant with the increased hypersensitivity to Vancomycin of the recombinant strain expressing MtrE-MtrD, which indicated that MtrE could be opened by MtrD in the presence of the substrate. However, the interaction between them was not detected by ITC, suggesting this interaction is weak or energetically unfavourable. The α-helical hairpin domain of MtrC was also overexpressed and purified to test for its interaction with MtrE or MtrD. Fascinatingly, the cross-linked hairpin formed a hexamer and AFM (Atomic Force Microscopy) studies revealed it arranged into a cylindrical structure. In addition, ITC studies revealed that the hairpin domain could bind to both MtrE and MtrD, suggesting that MtrC

might form a channel, one end of which interacts with MtrD and the other with MtrE. Growth curves also showed that the periplasmic hairpin domain could enhance the transport activity of MtrCDE, but couldn't activate the transport of MtrD, indicating it probably works by stabilizeing the open form of MtrE.

The expression of *mtrCDE* is believed to be under the control of a TetR-type transcriptional regulator repressor, *mtrR*. MtrR forms a dimer but with presence of dsDNA, it forms a tetramer. Fragments of the antimicrobial polypeptide LL-37 were synthesized and tested by titrating to MtrR by ITC. The C-terminal of LL-37(29-37) is the part that binds to MtrR and N-terminal (1-11) is not. Interestingly, interaction of MtrR with Penicillin G demonstrated for first time that MtrR might work as a β-lactamase; with its enzyme activity reduced after mutanting His105 to Tyr, which was reported to be found naturally in penicillin sensitive *N. gonorrhoeae* strains.

Chapter 1 Introduction-Antibiotic resistance

1.1 antibiotics and antibiotics resistance

An antimicrobial is a substance that can either kill or inhibit the growth of microorganism, such as bacteria, fungi. The discovery of antibiotics started with the observation that the growth of one type of bacteria can inhibit the growth of another. In term of usage, antibiotic refers to any drugs that cure a bacterial infection.

Among the antimicrobial, the antibiotics are natural or synthetic compounds that kills or inhibits the growth of bacteria. The most well-known antibiotic is penicillin, which was adopted as a medicine in 1940'. Following the success of the penicillin, a lot of antibiotics were discovered by screening a bacteria extract against other bacteria. The antimicrobial agents are categorized by their principle mechanisms of action, which include interference with the synthesis of the cell wall; the inhibition of the synthesis of proteins or nucleic acids; the inhibition of metabolic pathway or disruption of bacterial membranes. The use of antibiotics has created a possibility for human beings to combate bacterial infections. However, nowadays, the treatment of bacterial infection is increasly complicated by the development of resistance of bacteria to antimicrobial agents. Antibiotic resistance is an ability of microorganism to withstand the existence of the antibiotic, and is a consequence of mutation and natural selection.

1.2 Mechanisms of antibiotics resistance

Microorganism may aquire resistance to antimicrobial agents through a variety of mechanisms. The four main mechanisms are described below.

Drug inactivation or modification

Production of beta-lactamases is one of the commonest mechanisms of bacterial resistance to beta-lactam antibiotics. They work on beta-lactam antibiotics by breaking the beta-lactam ring open. Among the gram negative bacteria, it appeared initially in a limited

number of bacterial species (E. cloacae , *C. freundii*, *S. marcescens*, and *P. aeruginosa*) that could mutate to hyperproduce their chromosomal class C β-lactamase. A few years later, resistance appeared in bacterial species not naturally producing AmpC enzymes (*K. pneumoniae*, *Salmonella spp.*, *P. mirabilis*) due to the production of extended-spectrum beta-lactamases (ESBLs)(Philippon *et al.*, 2002).

Alteration of target site

Modifying the target sites of antibiotics is another common mechanism of antibiotic resistance. In addition to the production of beta-lactamases, the resistance to beta-lactam antibiotics can also result from mutations in Penicillin Binding Proteins (PBP). Penicillin Binding Proteins (PBPs) are a group of proteins that can bind Penicillin, they can catalyze the polymerization of the glycan strand and the cross-linking between glycan chains. Upon binding with Penicillin their peptidoglycan cross-linking capability can be impaired, therefore disrupt the construction of cell wall. It has been found that in many beta-lactam antibiotics resistant strains, like *Streptococcus pneumoniae*(Frere, 1995; Ward *et al.*, 2007; Zaitseva *et al.*, 2005) , *Neisseria gonorrhoeae*(Fontana et al., 1990; Takahata et al., 2006) and in *Enterococci faecalis*(Reichmann et al., 1996), the alterations mainly cause a decreased in affinity of the PBP for beta-lactam antibiotics.

The resistance to glycopeptide antibiotics was considered to be related to the various changes in the target of Vancomycin, the D-Ala-A-Ala terminus of the stem peptide of the peptideoglycan precursor. In glycopeptide resistant *Staphylococcus aureus* strains, the cell wall was found to have an increased content of glutamate, a decreased level of cross-linking of peptidoglycan and a decreased dimeric muropeptide/monomeric muropeptide ratio(Boyle-Vavra et al., 2001; Hanaki et al., 1998). All of this contributes to the lower binding affinity to cell wall or decreased amount of vancomycin available to reach D-Ala-A-Ala peptidoglyan precursor target.

In the study of DNA gyrase and topoisomerase IV, which are the two enzymes involved in bacterial DNA synthesis and also the target of quinolone antimicrobial agents, the mutation was found to be related to a reduced binding of drugs to the DNA-gyrase complex(Willmott and Maxwell, 1993).

Alteration of metabolic pathway

The sulfa drugs are used to treat the infection that is caused by bacteria and diseases that are caused by eukaryotes, such as, the cause of the pneumonia in HIV patients. The targets of sulfa antibiotics are two enzymes in the folic acid synthesis pathway, dihydropteroate synthase (DHPS) and the dihydrofolate reductase (DHFR). They can compete with the natural substrate para-aminobenzoic acid (pABA), therefore depletes the cell of folates, causing death(Patel et al., 2003).

In addition to the sequence alteration in DHPS caused by mutation, the utilisation of exogenous folic acid has also been found to be one mechanism of sulfa drug resistance. In DHPS and DHFR knock out Pneumocystis carinii, which lack the related synthesis pathway, the selected mutants can grow with the presence of folic acid in the medium(Bayly et al., 2001; Bayly and Macreadie, 2002), indicating that the cells can utilise the preformed folic acid like mammalian cells.

Reduced drug accumulation

Reducing the drug accumulation can be achieved by either changing the permeability of the cell membrane or by activating drug efflux pumps.

In *Pseudomonas aeruginosa*, drug resistance can be caused by a lack of the D2 porin protein in the outer membrane protein(Trias and Nikaido, 1990b), which plays a physiologically significant role in the uptake of basic amino acids and peptides containing these amino acids across the outer membrane(Trias and Nikaido, 1990a). This outer membrane protein is also used to take up drugs, therefore lack of it can prevent the drugs to get through outer membrane and reach their targets.

Another way to reduce drug accumulation is via energy-driven antibiotic efflux pumps, which are found in both gram positive and negative bacteria. According to the bioenergetic requirement, the multidrug transporters can be classified into primary and secondary-active transporters. In the primary-active transporters, such as ABC (ATP-binding cassette) transporters, the energy that is used to drive the transport of substrates directly comes from the hydrolysis of ATP; however, in secondary transporters, the transport is driven by chemiosmotic energy produced by electrochemical gradient of proton/sodium ions.

1.3 Multidrug transporters

The active efflux of drugs has been considered as a major mechanism of multidrug resistance. It has been found ubiquitously from microorganisms to human caner cell. As described before, they can be classified into primary and secondary active pumps by the resource of the energy that is used to drive the substrates efflux. The primary active pumps include ABC pumps that utilise the hydrolysis ATP as driving energy; the secondary active pumps include proton driven transporters, including the Resistance-nodulation-cell division (RND) super family, the Major facilitator super family (MFS) and the Small multidrug resistance super family (SMR). There is another super family called the Multidrug and toxic compound extrusion (MATE) super family that are driven by a sodium gradient (Borges-Walmsley *et al.*, 2003; Cattoir, 2004; Hasdemir, 2007).

Figure 1.1 Five well-characterised super families involved in multidrug efflux (McKeegan *et al.*, 2004)

A highly simplified representation of the five major super families that are included in multidrug transport. The RND family is shown as a tripartite complex in gram negative cells, which have an inner and outer membrane. The complex is formed by three components, an outer membrane protein (OMP), an inner membrane protein (IMP) and a membrane fusion protein (MFP).

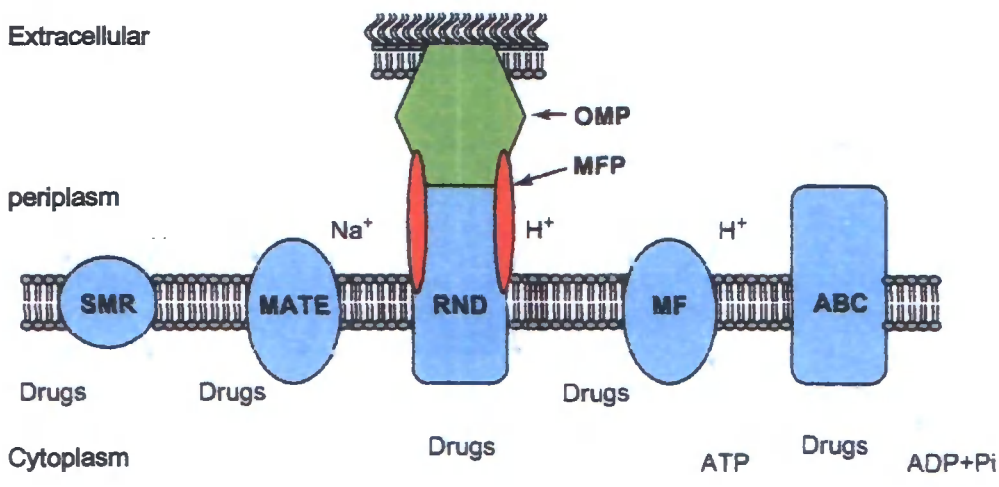

1.3.1 ATP-binding cassette (ABC) transporters

ABC transporters are a group of integral membrane protein that use the energy from ATP hydrolysis to transport substrates across biological membranes. The core of this group of membrane transporters is composed of two domains according to their position and functions, the transmenbrane domains (TMDs) and the nucleotide-binding domains (NBDs). Based on the direction of transport activity, ABC transporters can be divided into two subtypes, importers and exporters. In ABC importers, the TMDs and NBDs are separate polypeptides and transport needs the assistance of a substrate binding protein, but in bacterial exporters, a single gene usually encodes both the transmembrane domain and its partner ATP-binding domain, so that one TMD is fused to one NBD and the substrates are delivered directly from the cytoplasm.(Davidson and Maloney, 2007; Hollenstein *et al.*, 2007a).

To date, the structures of six ABC transporters are available. Four of them are importers: the Vitamin B_{12} transporter BtuCD from *Escherichia coli* (Hvorup *et al.*, 2007; Locher *et al.*, 2002), the putative metal-chelate-type transporter HI1470/1 from *Heamophilus influenzae* (Pinkett *et al.*, 2007), the molybdate transporter $ModB_2C_2$ from *Archaeoglobus fulgidus* (Hollenstein *et al.*, 2007b) and the maltose uptake system $MalFGK_2$ from *Escherichia coli* (Oldham *et al.*, 2007). There are currently two structures for ABC exporters, the multidrug transporter Sav1866 from *Staphylococcus aureus* (Dawson and Locher, 2006) and the lipid flippase MsbA from *Escherichia coli, Salmonella typhimurium* and *vibrio cholerae* (Ward *et al.*, 2007). We will now discuss the structurally relevant features and a common mechanism that rationalize the ATP-driven substrate transport.

Figure 1.2 Six currently available crystal structures of ABC transporters, with the tranporter name, organism source and putative function indicated below each graph(Dawson and Locher, 2006; Hollenstein *et al.*, 2007b; Hvorup *et al.*, 2007; Oldham *et al.*, 2007; Pinkett *et al.*, 2007; Ward *et al.*, 2007).

Import ABC transporters

Except HI1470/1, the other three transporters are all complex with the correspondence binding protein. The TMDs and NBDs are separate subunits.

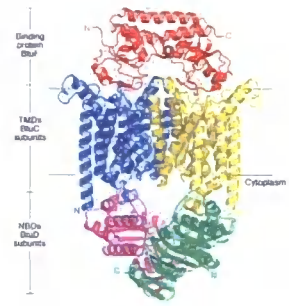

BtuCD-BtuF *E.coli*

Vitamin B_{12} transporter

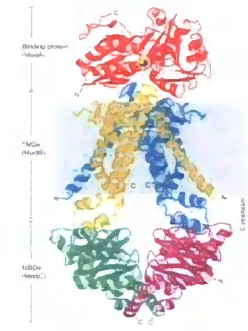

$ModB_2C_2$ *Archaeoglobus fulgidus*

molybdate transporter

HI1470/1 *Heamophilus influenzae*

metal-chelate-type transporter

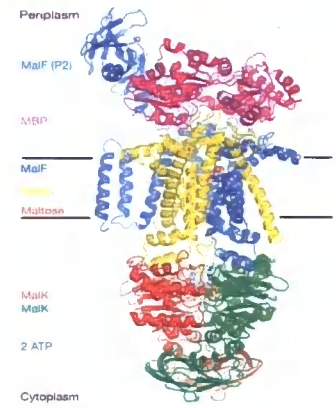

$MalFGK_2$ *E.coli*

maltose uptakeing system

Export ABC transporter

The TMDs of exporters are fused to the NBDs.

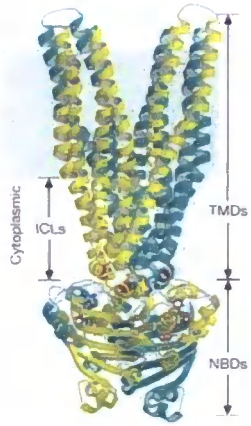

Sav1866 *staphylococcus aureus*

multidrug transporter

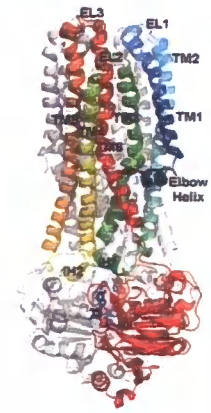

MsbA（Nucleotide bound ）*Salmonella typhimurium*

lipid flippase

Nucleotide-binding domains

Typically, the functional form of the ABC tranporters consists of two hydrophilic nucleotide-binding domains that are located at the cytoplasmic side of the membrane and two hydrophobic transmembrane domains that are considered to form the translocation pathway and define the substrate specificity. The nucleotide-binding domain is known to hydrolyze ATP, coupling this to transport. Although the ABC superfamily can be divided into several subfamilies, their primary sequences of Nucleotide-binding domain are highly conserved.

The most prominent among the conserved features are the Walker A and Walker B motifs, which are also found highly conserved in many enzymes that employ ATP in catalysis. The Walker B motif is able to bind both ADP and ATP as required for catalysis; whilst the walker A motif is considered to involved in the regulation of ATP synthase activity(Walker *et al.*, 1982). Within the consensus G××G×GC/KT sequence of the Walker A motif, it has been found that the cysteine/lysine residue plays a critical role in ATP hydrolysis(Jha *et al.*, 2003). After substituting the lysine of the maltose transporter, MalK from *Salmonella typhimurium*, to arginine, although it still retains the capability to bind nucleotides, the ATPase activity was greatly reduced(Schneider *et al.*, 1994). In the mouse MDR1 protein, mutants that bear the lysine to arginine completely abrogate the ability to confer multidrug resistance(Azzaria *et al.*, 1989). The other conserved ATP-binding signature, the Walker B motif, is downstream of the Walker A motif. The Walker B motif terminates with an Asp residues (NBD1), which has been found to be the catalytic base for ATP hydrolysis. It interacts with the Mg^{2+} that chelated the bound ATP. The Glu following Asp is also highly conserved, it hydrogen bonds with water and is most the likely candidate for 'attacking'water during ATP hydrolysis(Smith *et al.*, 2002). After being changed to various of amino acids, although each mutant is able to trap a high amount of nucleotide, the nucleotide species trapped is exclusively the ATP form, which indicates the importance of the Glu residue of the Walker B motif in ATP hydrolysis(Orelle *et al.*, 2003; Payen *et al.*, 2003).

Another highly conserved motif, known as the C-loop or family signature motif, is a unique feature of each ABC transporter. It has been found in the active conformation of NBDs, the signature motif (LSGGQ) from one subunit forms a "nucleotide sandwich" with the walker A motif from another subunit(Smith *et al.*, 2002). This was also proved by

cross-linking analysis after pairs of cysteines were introduced into the signature motif of human multidrug resistance P-glycoprotein (P-gp) and its opposing Walker A motif. This indicates that the signature motifs are adjacent to the opposing Walker A site(Loo *et al.*, 2002). They likely participate in forming the ATP-binding site and are displaced by ATP hydrolysis (Buchaklian and Klug, 2006). Numerous of studies have been undertaken to substitute the conserved residues in the signature motif to various amino acids. These studies have established that the fourth residue glycine plays an important role in the posthydrolytic complex formation and is part of the conformational network, which is responsible for the accelerated hydrolytic activity upon interaction of transporter with its transported substrates(Szentpetery *et al.*, 2004). Some mutagenesis studies have been done to show the functions of this motif. It is quite clear that the signature motif is involved in ATP hydrolysis during transport. Moreover, some researchers also suggested that this motif is directly involved in the transporter function; for example, by acting as a signal transducer between the hydrophobic domain and the NBD of the transporter(Browne *et al.*, 1996).

Transmembrane domains (TMD)

Unlike the NBDs, the transmembrane domains of ABC transporters vary in primary sequence, length and architecture, and the number of transmembrane helix.

In the two reported exporter structures, Sav1866 from *Staphylococcus aureus* and MsbA from *E.coli*, it has been found that they share high similarity. Their TMDs traverse the lipid bilayer six times to yield 6 transmembrane helices; for these homodimer transporters, each bundle of TM helices consists of TM1-2 from one subunit and TM3-6 from the other subunit. Both of them interact with the NBDs through the intracellular loop 1 (IL1, between TM2 and TM3) and the intracellular loop 2 (IL2, between TM4 and TM5). They both revealed the existence of domain swapping, with one intracellular loop reaching across and contacting the opposite NBD. Because the open inward-facing and close inward-facing conformations of MsbA have also been reported, it is possible for us now to have a deep look into the conformational change that occurs during the substrate translocation, which will be discussed in the following section(Dawson and Locher, 2006; Ward *et al.*, 2007).

From the reported structures of importer ABC transporters, the number of transmembrane helices vary from six to ten ($ModB_2C_2A$ and MalG have 6 TM helices; MalF

has 8 and 10 in the cases of BtuCD and HI1470/1471). The overall architecture of the intact metal-chelate-type ABC transporter HI1470/1 resembles that of the Vitamin B_{12} transporter BtuCD. They both have 10 transmembrane helices and a pseudo-two-fold rotation axis relates two groups of transmembrane helices and their connecting loops in one subunit (the first group comprises TM2 through TM5, whlist the second group comprises TM7 through TM10, but TM1 and TM6 are not related by this symmetry). The interface between the two membrane-embedded subunits is formed by TM5 from one subunit and TM10 from the other one, with residues from TM3 and TM8 lining the permeation pathway. Although these two structures have similarities, there are still some detailed differences in the tertiary and quaternary arrangements between them that may be functionally relevant. An important one is that HI1470/1 and BtuCD adopt inward- and outward-facing conformations respectively. In the reported structure of a putative molybdate transporter $ModB_2C_2$, each ModB subunit crosses the membrane 6 times for a total of 12 transmembrane helices in the transporter, which doesn't resembles the structures of other reported ABC transporters. The two ModB subunits form a large inward-facing cavity, which is presumed to be the translocation pathway. The cavity forms a closed "gate" underneath the interface with the substrate binding protein ModA. This gate is composed of four converging protein stretches, two from each ModB subunit. Among the four importer ABC transporters, the maltose transporter $MalFGK_2$ is a unique one. Unlike the other three transporters, the TMDs of MalFGK2 are not assembled from homodimer, but from a heterodimer; the two TM subunits, MalF and MalG are not arranged side-by-side and MalF has eight transmembrane helices whilst MalG only has six.

As mentioned before, the TMDs of the exporter ABC transporters in the nucleotide-binding state interact with the opposite NBDs via intracellular loops. In the importer ABC transporters, their interface is common between TMDs and NBDs. From the four reported structures, the interface residues of the NBDs are all located in the Q-loop. The conformational switching of the Q-loop, that has been found may mediate communication between the TMDs and NBDs of ABC transporters, and may be involved in the movement of the highly conserved glutamine in and out of the catalytic site due to the conformational change(Jones and George, 2002). The cytoplasmic loops in TMDs represent a general interface with the Q-loop, between the ABC cassette and membrane-spanning domains. It is

between TM7 and TM8 in BtuC, HI1471 and MalF, but between TM4 and TM5 in the cases of ModB and MalG. This cytoplasmic loop consists of two short helices and has been found to undergo conformational changes in order to communicate structural changes in the two NBDs upon ATP binding to the two TMDs in $MalFGK_2$ transporter(Daus *et al.*, 2007).

Mechanism of ABC transporters

As mentioned before, the ABC transporters can be divided into two groups on the basis of their transport direction and the reaction mechanism. ABC importers need to recruit a periplasmic binding-protein to deliver the substrates to the system, while ABC exporters don't need.

Figure 1.3 A model for maltose transporter(Davidson and Maloney, 2007).

(a) The resting state, the MBP closes after the binding of a maltose and transfers it to the transporter.

(b) The transition state, after the binding of MBP and ATP, the two subunit of the ATP binding cassette close, the ATP-activity is activated; the conformational change of the TM helices to form a translocation pathway that faces the periplasm; MBP releases the maltose into the transporter.

(c) The posthydrolysis state, following ATP hydrolysis, in which the maltose and ADP are released to the cytoplasm; the MBP dissociates from the transporter; the translocation pathway changes to face the cytoplasm.

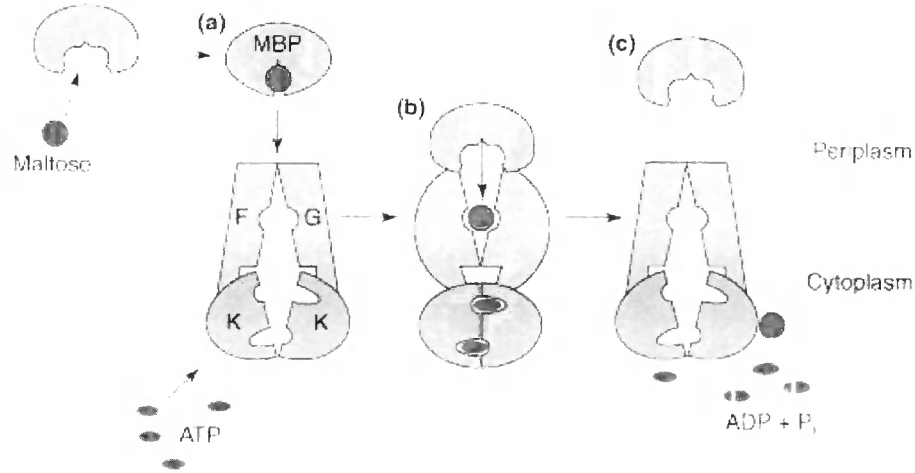

Among the ABC importers, the best-studied model is the maltose transporter, MBP-MalFGK$_2$. The following model (Davidson and Maloney, 2007) is based upon several important informations that have been found. First, only the ATP and ATP/Mg^{2+} binding state of the NBDs form a dimer, while the nucleotide –free and ADP state are monomeric proteins (Zaitseva *et al.*, 2006); second, the interaction of the MBP with MalFGK$_2$ stimulates its ATPase activity by stabilizing the transition state conformation of the transporter, there by lowering the activation energy for hydrolysis(Chen *et al.*, 2001); third, the MBP binds to maltose with high-affinity, acts "open cleft" (without bound sugar) and closed (with bound sugar) conformations through a flexible hinge(Spurlino *et al.*, 1991); last, the crystal structure of HI1470/1 and ModB_2C_2A have revealed the resting state conformation and the transition state is based on the structure of MBP-MalFGK$_2$(Hollenstein *et al.*, 2007b; Oldham *et al.*, 2007; Pinkett *et al.*, 2007).

After the report of the three structures of MsbA, in the open, closed and the nucleotide bond states(Ward *et al.*, 2007). it is now possible to set up a model of the mechanism of the exporter ABC transporters. Unlike the importer transporters, exporters do not recruit cognate proteins (such as maltose binding protein in maltose transporter MalFGK$_2$) to deliver the substrate to themselves. In order to achieve the extrusion of the substrates, exporters need to commit significant conformational changes.

Figure 1.4 summary of conformational change in MsbA(Ward *et al.*, 2007)

(A) The conformational changes of MsbA from inward to outwards-facing. The TM helices of one monomer are highlighted in cyan. Both the open and closed Apo protein form a cytoplasmic-facing V chamber between TM4/5 and TM3/6, which is represent by a red asterisk. After the binding of nucleotide, The TM4/TM5 moves and TM3/TM6 splits away from TM1/TM2. At the same time, the cytoplasmic end of the TMDs closes and the periplasmic end widens, thereby forming an outward-facing V chamber.

(B) The cartoon view to elucidate the model above.

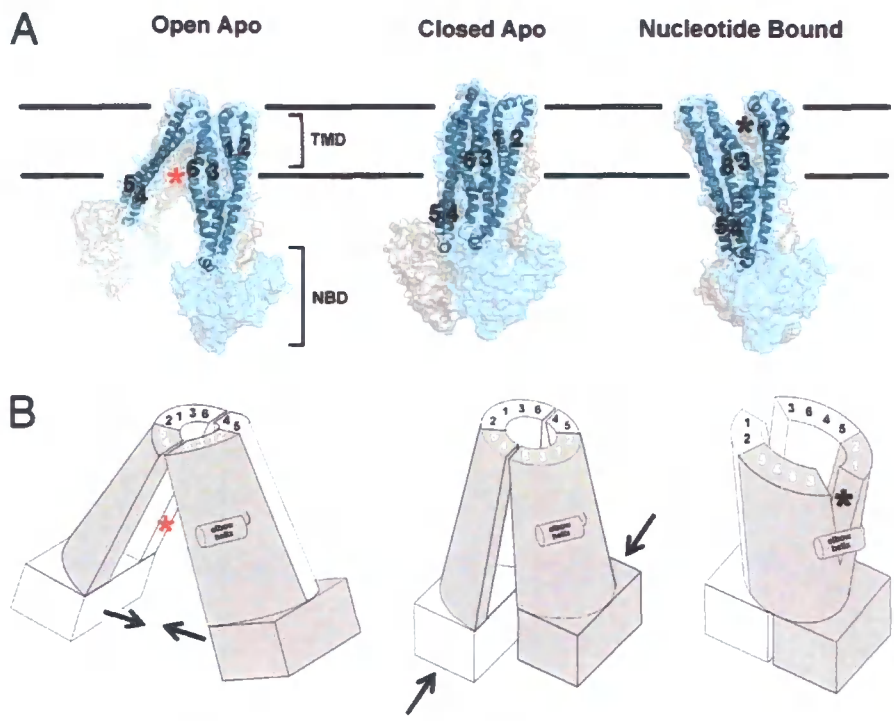

The model of MsbA conformational changes are supported by structural and biochemical studies. It has been found that in the resting state of MsbA, the top of the helical bundles is closed (Buchaklian et al., 2004) and form a V shaped conformation that faces the cytoplasm(Dong et al., 2005). *Dong J.* et al has provided the evidence for a large conformational change upon the binding of nucleotide by electron paramagnetic spin resonance (EPR), which is consistent with the change from the open apo conformation to the nucleotide bound conformation(Dong et al., 2005). Moreover, this structural transition also consistant with the distance measurements by pulse dipolar spectroscopy and fluorescence homotransfer, which indicates that the substrate binds to the open chamber at the cytoplasmic side of MsbA and they undergo a significant conformational change to form a dimer after the binding of ATP(Borbat et al., 2007). Large conformational changes (50 Å) of domains in a transporter during its transport cycle have also been observed for P-type ATPases such as the Ca^{2+}-ATPase(Toyoshima and Inesi, 2004).The structure of the ABC exporter Sav1866 demonstrates the structure of the nucleotide bound conformation, in which there is dimerization of the NBDs with bound nucleotide, whilst the periplasmic facing chamber is also in agreement with the nucleotide binding conformation of MsbA(Dawson and Locher, 2006). However, some biochemical studies are not consistent with this model, they mainly

question the existence of the cytoplasmic facing chamber and the big conformational change upon the binding of ATP(Buchaklian and Klug, 2006; Eckford and Sharom, 2008). Further studies on other ABC exporters will be required to evaluate the relevance of these studies for other members in the ABC transporter family.

1.3.2 Proton driven transporters

This group of transporters belongs to the secondary active transporters. Unlike primary active transporters, such as ABC transporters that we described before, there is no direct coupling of ATP; instead, the potential proton difference created by pumping ions out of the cell is used. These pumps are often termed H^+ antiporters and can be categorized into a number of families based on their primary structure: SMR (small multidrug resistance) family, MF (major facilitator) family and RND (resistance nodulation) family.

1.3.2.1 Small Multidrug Resistance (SMR) Family

The transporters belong to the SMR family are much smaller than those belong to other families. Members of the SMR family generally contain 100-120 amino acid residues, which are organised into four transmembrane helices. Amongst them, the best characterized one is EmrE from *Escherichia.coli*, which confer resistance to EtBr (ethidium bromide) and Methyl Viologen with the coupling of the proton electrochemical gradient(Yerushalmi *et al.*, 1995). Another transporter, EbrAB from *Bacillus subtilis*, is found to belong to the SMR family as well. However, EbrAB likely forms a heterodimer in contrast to the EmrE homodimer (Masaoka *et al.*, 2000).

The basic functional unit of EmrE has been shown to be an oligomer, most likely a homodimer, which appears to be supported by Cryo-electron microscopy, high-resolution size-exclusive chromatography, substrate binding analyses and X-ray crystallography(Butler *et al.*, 2004; Chen *et al.*, 2007; Tate *et al.*, 2001; Ubarretxena-Belandia *et al.*, 2003).

Figure 1.5 the structure of the EmrE homodimer with bound TPP(Chen *et al.*, 2007)

A: The antiparallel homodimer of EmrE, the two monomers are colored yellow and blue, the bound TPP is pink.

B: Docking the EmrE-TPP X-ray structure into the EM density map, the two monomers are distinguished by asterisks. The red arrow represents the bound substrate in the EM map, which is in agreement with the position of TPP in X-ray structure.

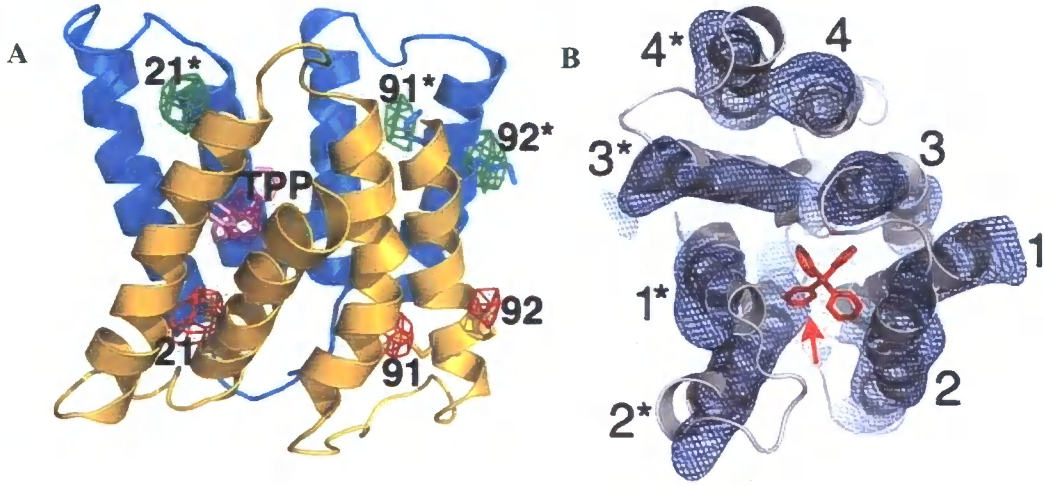

From the EM data (2D-crystal) and X-ray data, the structure of EmrE is an asymmetric antiparallel homodimer, consisting of a bundle of eight transmembrane helices with one substrate bound near the centre. The substrate binding chamber is formed from six helices, three from each monomer. The two TM4 helices are not involved in forming the binding site but only participate in the dimerization interaction with TM1-TM3. At the same time, the antiparallel configuration shows that the EmrE protein is inserted into the *E.coli* membrane in two orientations, in common with the report by Gunnar von Heijne group that EmrE has a dual topology(Rapp *et al.*, 2007).

Although the antiparallel topology is supported by lots of data, other studies have been done and the results indicate that EmrE might have a parallel topology in functional dimer. It has been reported by Schuldiner's group that the carboxy-terminus of EmrE faces the cytoplasm while the first loop between TM1 and TM2 faces the periplasm, which indicates that EmrE has a Nin/Cin topology(Ninio et al., 2004). Subsequently, they found, that EmrE with a parallel topology is fully functional using a chemical cross-linking analysis after introducing cysteines into positions not permissible by an antiparallel topology (Soskine et al., 2006). Most recently, the same group tested the transport activity of a tandem EmrE that was built with two identical monomers genetically fused head to tail with a hydrophilic linker. They found the obligating EmrE parallel dimer still confered resistance to ethidium.

Interestingly, after mutates the essential glutamate of this tandem EmrE, it could only transport monovalent substrates and displayed a modified stoichiometry, which also supports the conclusion that the transporter is functional(Steiner-Mordoch et al., 2008). However, by a series of in vivo complementation studies with the EmrE protein subtly mutated to obtain a unique orientationvon, Heijne and colleagues showed that only an antiparallel arrangement of the EmrE subunits is functional(Rapp et al., 2007). This conclusion is also supported by recent data of zhang et al(Zhang et al., 2007). It has been suggested that parallel topology is based on mainly cross-linking results with protein in the detergent-solubilized state, a nonnatural environment, whilst antiparallel topology is more reliable because the usage of the native lipid membrane.Nevertheless, the antiparallel topology hypothesis is still faced a tricky question about the insertion and assembly of these proteins in the membrane(Schuldiner, 2007).

Due to the small size of SMR transporters, another question has been raised, how does such a small protein do such a big jobs? For example, the substrates of EmrE are all large hydrophobic cations, like tetraphenylphosphonium (TPP^+), ethidium, propidium and dequalinium. It is unlikely that one monomer of EmrE with four transmembrane helices could perform the translocation of the substrates, considering both the size of the transporter and the character of the molecule, which has been shown not to contain any hydrophobic core(Chen *et al.*, 2007). As described before, it has been reported in many studies that EmrE forms oligomers as a functional unit, most likely a dimer. From the Cryo-electron-microscope, electron crystallography and X-ray data, the substrates bind to the centre of the dimer within the same pocket (Chen *et al.*, 2007; Korkhov and Tate, 2008; Ubarretxena-Belandia *et al.*, 2003). The electron crystallography studies also revealed that, while retaining the overall fold of the protein, the binding of drugs is accompanied by a small arrangements of the transmembrane domains(Korkhov and Tate, 2008; Tate *et al.*, 2003).

It has been found that the proton and substrates share the same binding site in EmrE and one monomer releases a proton upon substrate binding (Soskine *et al.*, 2004). In the same year, studies of proton-substrate antiport for EmrE reconstituted into proteoliposomes by same group, found the protein to be electrogenic for monovalent and electroneutral for divalent substrates(Rotem and Schuldiner, 2004). This lead to the conclusion, that during one

transport cycle, two protons are exchanged with one substrate molecule, therefore the basic functional unit of EmrE is a dimer with both monomers participating in a single binding site shared by protons and substrates.

EmrE has eight charged residues, five basic (Lys-22, Arg-29, Arg-8, Arg-106 and His-110) and three acidic (Glu14, Glu-25 and Asp-84), seven of these residues are located in the hydrophilic loops and can be replaced by with either cysteine or other amino acids bearing the same charge, without significant decreas in either resistance or uptake activity. Glu-14 is the only charged residue in TM1 of the transmembrane domain and is highly conserved in the SMR family(Ninio *et al.*, 2001), which suggests the functional importance of this residue. From the recently published structure of EmrE, with bound TPP, both Glu-14 residues point toward the binding chamber and appear well placed to form ionic contacts with the positively charged TPP molecule (figure 1.6).

Figure 1.6 "Top" view of EmrE-TPP structure(Sennhauser *et al.*, 2007)

The two monomers are represented in yellow and blue, the TPP molecule is colored pink.

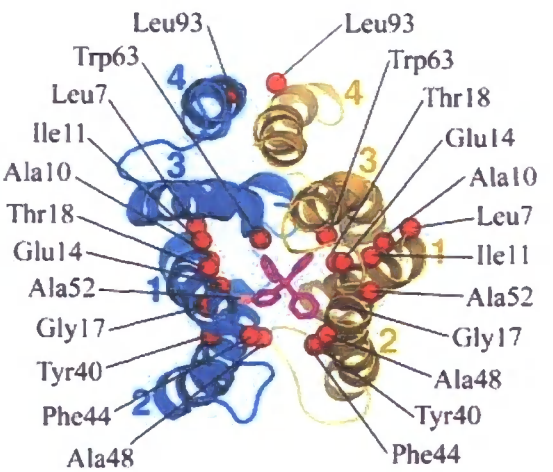

Many biochemical studies are also indicative of the importance of the Glu-14 residue: after finding an unusually high p*K* for Glu-14 of 8.5, the stoichiometry of the proton release and PH dependence were measured in the wild type protein as well as in a fully active mutant only with a single carboxyl at position 14 with a lower p*K*, the results showed that the high p*K* of the carboxyl at position 14 is essential for coupling the fluxe of the proton and substrates(Soskine *et al.*, 2004). After finding this, the study by the same research group using

dicyclohexylcarbodiimide (DCCD), which is known to react with carboxyl, it showed that binding of substrates limits the accessibility of DCCD to its site of action, Glu-14, also suggesting that this residue is part of the substrate binding site(Yerushalmi *et al.*, 2001). An analyses of substrates transport also demonstrated reduced activity and different PH profile after replacing the Glu-14 with various amino acids (Yerushalmi and Schuldiner, 2000). In order to determine the number of Glu-14 residues reacting in the functional unit, electrospray ionization mass spectrometry was exploited with the carboxyl-specific modification reagent DiPC. The results showed that Glu-14 is modified by DiPC and the modification can be reduced by 80% upon the binding of TPP, indicating that both Glu-14 residues in the functional unit are close enough to the binding sites that TPP prevents their modification(Weinglass *et al.*, 2005).

1.3.2.2 Major Facilitator (MF) Family

The MF family transporters are much larger than those belong to the SMR family. They are normally composed of 400 amino acids and putatively arranged into 12 transmembrane helices, with a cytoplasmic loop between helice 6 and 7. As the two halves of the transporter have similar sequence, this indicates that this structure was most likely arisen by gene duplication(Pao *et al.*, 1998). Like the transporters in the SMR family, MF transporters are proton driven secondary active transporter, which means the transport of the substrates is accompanied by H^+ influx.

To date, the structure of three MF transporters has been reported: the Lactose permease LacY from *Escherichia coli*(Abramson et al., 2003), the Glycerol-3-Phosphate transporter GlpT from *Escherichia coli*(Huang et al., 2003), and the amphipathic compound transporter EmrD from *Escherichia coli* (Yin *et al.*, 2006a). Among them, LacY adopted a mutant C154G, which binds substrate with high affinity but catalyzes little or no transport, whilst structures for GlpT and EmrD are proteins without bound substrates. Both the LacY and GlpT represent inward-facing conformations and EmrD is not in a V shape and consquently probably represents an structure of intermediate state. (figure 1.7)

Figure 1.7 Overall structures of LacY, GlpT and EmrD(Abramson *et al.*, 2003; Huang *et al.*, 2003; Yin *et al.*, 2006a)

A: (1) Ribbon presentation of LacY viewed parallel to the membrane. Substrate TDG is represented by black sphere.

(2) Ribbon presentation of LacY viewed from cytoplasmic side. Substrate TDG is represented by black sphere.

B: (1) Ribbon presentation of GlpT viewed parallel to the membrane.

(2) Ribbon presentation of GlpT viewed from cytoplasmic side.

C: (1) Ribbon presentation of EmrD viewed parallel to the membrane.

(2) Ribbon presentation of EmrD viewed from periplasmic side.

A (1)

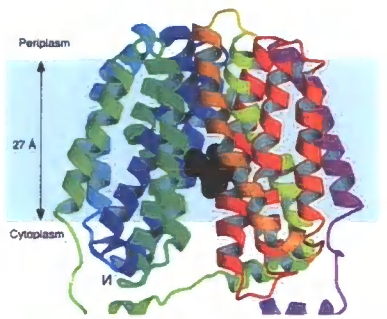

A (2)

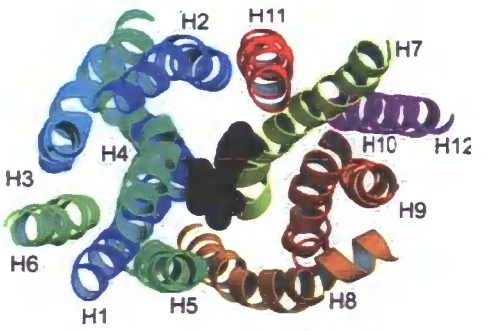

B (1)

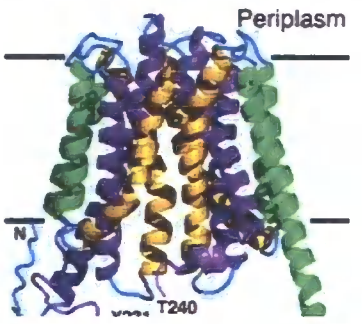

B (2)

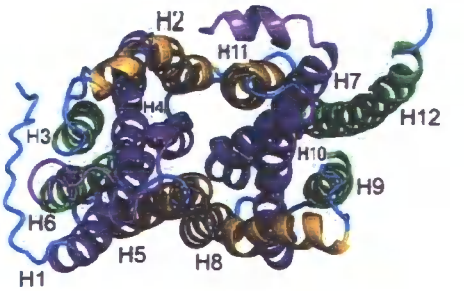

C (1)

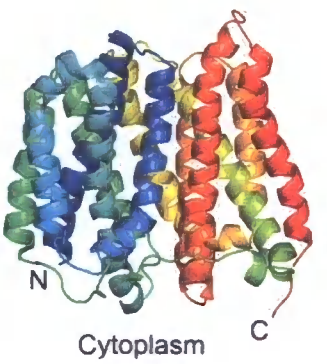

C (2)

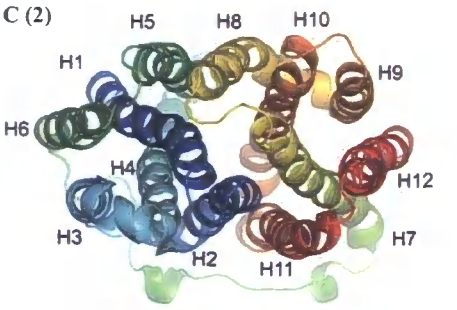

From the structures above, these three transporters are all composed of 12 transmembrane helices with a large cytoplasmic loop between H6 and H7. The structures of LacY and GlpT form a "V" shape inward-facing conformation, which support the alternating access model of transporters, whereby the substrate-bind site is accessible from one side of the membrane at one time.

The arrangements of the transmembrane helices of these three transporters share similarity as well. The 12 transmembrane helices organize into two pseudo symmetric α-helical bundles, with helices H3, H6, H9and H12 facing away from the interior(Guan *et al.*, 2007), while the remaining transmembrane helices form the internal cavity, which has also been found in other MF transporter(Kasahara and Kasahara, 2003). The most notable difference is that while both LacY and GlpT have an hydrophilic interior in the internal cavity, the internal cavity of EmrD comprises mostly hydrophobic residues, consistent with its function of transporting lipophilic compounds(Yin *et al.*, 2006a).

The best studied mechanistic model for an MF family transporter is that for H^+/Lactose symporter LacY. Several residues have been found to be irreplaceable for H^+/Lactose substrate translocation after mutating almost every position in the protein: they are Glu126 (helix 4) and Arg144 (helix 5), which are crucial for substrate binding and substrates specificity (Sahin-Toth *et al.*, 1999; Venkatesan and Kaback, 1998); Glu269 (helix 8) which is involved in both substrate and H^+ translocation(Weinglass *et al.*, 2005); Arg 302 (helix 9),His 322 (helix 10) and Glu325 (helix 10) which play an important role in H^+ translocation (Sahin-Toth and Kaback, 2001; Schlor *et al.*, 1997; Zhang *et al.*, 2007).

A model for the transport mechanism has been postulated based on the reported structure and biochemical analyses. Briefly, influx consists of seven steps:(1) starting from the outward-facing conformation; (2) protonation of LacY; (3) binding of lactose; (4) a conformational change that results in the reorientation of the substrate binding site to the inward-facing conformation; (5) release of substrate; (6) release of H^+ and (7) return to the outward facing conformation(Kaback, 2005). The outward-facing conformation of LacY is considered unstable and is immediately protonated. Before the binding of ligands, Arg144 is displaced from Glu 269 and forms a salt bridge with Glu126; Glu269 is located away from the hydrophilic cavity and H-bonded to Trp151, forming a platform for the initial recognition

of galactopyranosyl ring of lactose. Thus, the essential residues for substrate binding are not in the correct configuration to bind substrate immediately. After Glu269 binds H^+, the sugar initially recognizes Trp151 and this interaction leads to binding to Glu126 and Arg144. Then Glu269 moves out of the relatively hydrophobic environment and forms a new salt bridge and an H-bond with the sugar to complete ligand binding. Upon the binding of substrate, Glu269 transfers the H^+ to H322, causing the conformational change to the inward-facing conformation (Weinglass *et al.*, 2005). H322 may pass the H^+ to Glu325 afterwards(Schlor *et al.*, 1997). Substrate is then released to the cytoplasmic cavity and the salt bridge between Glu269 and Arg144 breaks and a new salt bridge is rebuilt between Arg144 and Glu126(Yin *et al.*, 2006b). Arg302, which is located in the C-terminal domain, and is charged-paired with Glu325, are considered to facilitate the deprotonation of Glu325 (Sahin-Toth and Kaback, 2001; Weinglass *et al.*, 2005). Finally, the H^+ is released to the same cavity as the substrate and the transporter returns to the out-ward facing conformation(Mirza *et al.*, 2006; Sahin-Toth *et al.*, 2000; Venkatesan and Kaback, 1998).

1.3.2.3 Resistance Nodulation Division (RND) transporters

RND transporters are larger ones than the other transporters previously described, being composed typically of approx. 1000 amino acids. They typically form 12 transmembrane helices and two large periplasmic loops, which contain more than 300 amino acid, between helice 1 and 2 and helice 7 and 8(Goldberg *et al.*, 1999; Gotoh *et al.*, 1999; Guan *et al.*, 1999; Hagman *et al.*, 1997). Similar to MF transporters, the sequence of the N-terminal half of these transporters resembles the C-terminal half, which again indicates these transporters have arisen by gene duplication. The two large periplasmic loops have been reported to form a periplasmic headpiece. Many studies have been done to define the importance of these periplasmic loops. After swapping the periplasmic loops between AcrB and AcrD, the substrate specificity of the transporter was found to have been interchanged(Elkins and Nikaido, 2002); some mutants in the central cavity and periplasmic domain have been reported to affect the substrate sensitivity and efflux activity (Hearn *et al.*, 2006; Mao *et al.*, 2002), therefore drawing the conclusion that these two periplasmic loops play an important role in substrate recognition in RND transporters.

The structure of AcrB (*Escherichia coli*) and its substrates translocation

Amongst all the RND transporters, the AcrB from *Escherichia coli* is the best studied one, its structure have been reported with and without bound substrates at 3.5Å resolution.

Figure 1.8 the crystal structure of AcrB (Murakami *et al.*, 2002)

A: Ribbon representation of AcrB side view, the protomers are colored to red, green and blue.

B: top view of AcrB

C: the arrangement of the transmembrane helices near the periplasmic side. The label numbers indicate the transmembrane helix numbers

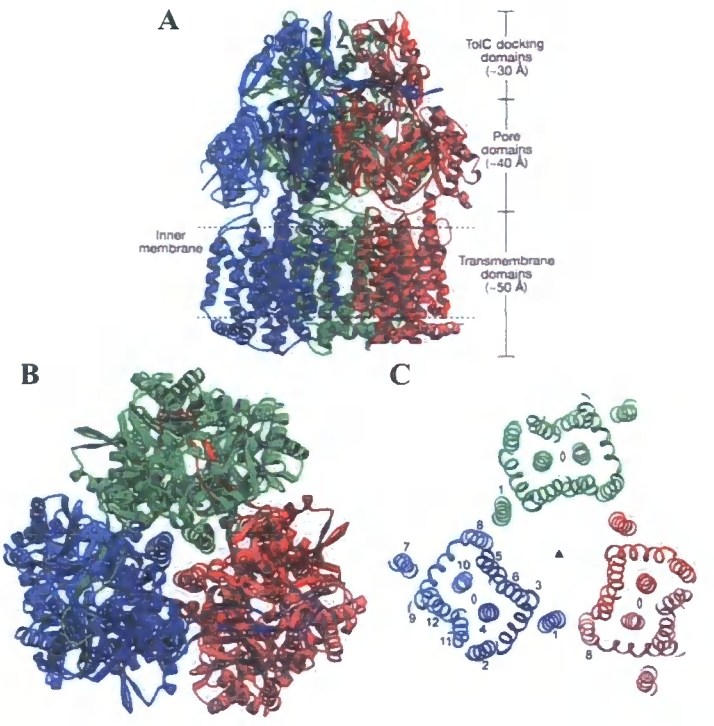

The overall AcrB structure is shown to be a trimer with "jellyfish" appearance. It comprises a periplasmic headpiece and a transmembrane region approximately 70Å and 50Å thick, with maximum diameters of 100Å and 80Å respectively. The headpiece is divided into two stacked parts: the upper part is 30 Å thick and the lower part is 40 Å thick, together they have a trapezoidal appearance when viewed from the side; this domain is about 70Å wide at the bottom and 40Å wide at the top.

The transmembrane domain of each protomer contains twelve transmembrane α-helices. A pseudo-two-fold symmetry axis exists in each transmembrane domain, that is, the six N-terminal helices are symmetrically arranged with the six C-termianl helices (Figure 1.8).

Viewed from the top, the upper part is open like a funnel. The internal diameter of the funnel opening is about 30Å. It is composed of two four-stranded mixed β-sheets. The headpiece is held together by a 35Å long hairpin structure that protrudes from the upper headpiece domain of each protomer and inserts into the next protomer. The six vertical hairpins at the top of AcrB trimer, are found to contact with the six α-helix-turn- α-helix structure at the bottom of TolC(Koronakis *et al.*, 2000) to form a tight seal by manual docking, therefore, the upper part of the headpiece is also called "TolC docking domain".

Three pore domains form a pore at the centre of the lower headpiece. Each protomer contributes one pore domain. The pore exists in the lower part of the headpiece and connects with the bottom of the funnel. The pore domain is composed of four subdomains: PN1, PN2, PC1 and PC2. PN1 and PN2 comprise the polypeptide segment between TM1 and TM2, and PC1 and PC2 comprise the segment between TM7 and TM8. All these subdomains contain a characteristic structural motif, that is, two β-strand-α-helix-β-strand motifs that are directly repeated and sandwiched with each other. Four subdomains in the pore domain are packed back to back in the centre, placing the α-helices on the outside. The pore forming helix is the second helix (Nα2) of PN1. A cleft exists between PC1 and PC2 at the periphery of each protomer. Vestibules are open at the side of the headpiece between PN2 and PC2, which lead to a cavity located at the bottom of the pore.

As a member of the secondary active transporter family, AcrB is energized by proton-motive force. It recognizes many structurally unrelated toxic compounds and actively engages in extruding them from cells. Many research studies have been done on transport mechanism; among them, the crystal structures of AcrB with four different bound ligands no doubt extend our understanding of the substrate binding sites in this transporter(Ward *et al.*, 2007).

Figure 1.10 AcrB with bound substrates (Borges-Walmsley *et al.*, 2003; Ward *et al.*, 2007)

The three protomers of AcrB are distinguished as red, blue and green respectively. Three distinct domains are formed by the trimer: the funnel, the pore and the central cavity, which are generalized by the black lines. The approximate binding positions of the drug dequalinium (Dq), ciprofloxacin (Cip), EtBr (Et) and R6G are indicated.

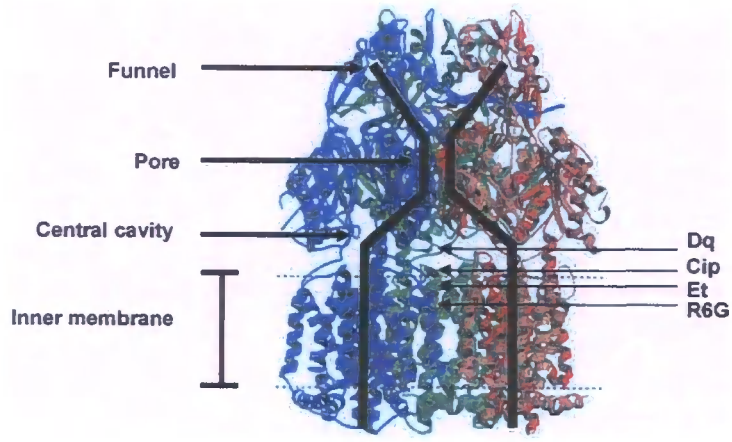

The central cavity that is formed by the three transmembrane domains of each AcrB protomer has been shown to play an important role in substrates binding. The crystal structure illustrates that all the four different ligands bind to various positions within the central cavity with the approximate positions shown in Figure 1.10. It has been reported that the interior surface of the upper part of the central cavity is surrounded by many hydrophobic residues, includes several phenylalanines. Most of them are highly conserved among the homologs of AcrB(Das *et al.*,2007), which also indicates that they may be involved in the function of these transporters. The four drugs, dequalinium (Dq), ciprofloxacin (Cip), EtBr (Et) and R6G, bind to sites that are not quite the same. All the residues close to the bound ligand are hydrophobic amino acids, suggesting the importance of hydrophobic and possible van der Waals interactions in drug binding. Moreover, the four drugs seem likely to bind close to the periplasmic surface of the inner membrane, which indicates the central cavity may be filled with the bilayer. Another notable feature is that after the binding of drugs, AcrB undergoes a conformational change compared to the drug-free structure. Each subunit is triggered to perform a 1° rigid-body rotation.The axis of rotation, passing through the side of each subunit,

is approximately parallel to the plane of the lipid-bilayer. Due to this rotation, the diameter of the periplasmic domain is enlarged by ~2.5Å(Ward *et al.*, 2007).

From the structure of AcrB with bound ligand, a mechanism for substrate efflux has been postulated: the drug entries the central cavity from either the vestibules or outer leaflet of the lipid bilayer(Aires and Nikaido, 2005), then it passes through the open pore domain to the funnel domain, and is eventually extrude into the external medium through the outer membrane protein TolC. This hypothesis is tentatively termed the "elevator mechanism". However, in 2006, a new model for the mechanism of substrates extrusion by AcrB was proposed as the "functional rotation mechanism", in which the efflux of the drugs is accomplished by a conformational change in each protomer(Dastidar *et al.*, 2007; Murakami *et al.*, 2006; Seeger *et al.*, 2006; Takatsuka and Nikaido, 2007).

Figure 1.11 Schematic representation of AcrB functional rotation mechanism(Seeger *et al.*, 2006)

A: Side view schematic representation of two of the three protomers of AcrB trimer. The accessory proteins of AcrB, AcrA and TolC are indicated by arrows. The three conformational states, loose (L), tight (T) and open (O) are colored blue, yellow and orange.

B: The lateral grooves in the L and T protomers indicate the drug binding sites. The different geometric forms represent low (triangle), high (rectangle) and no (circle) binding affinity for substrates.

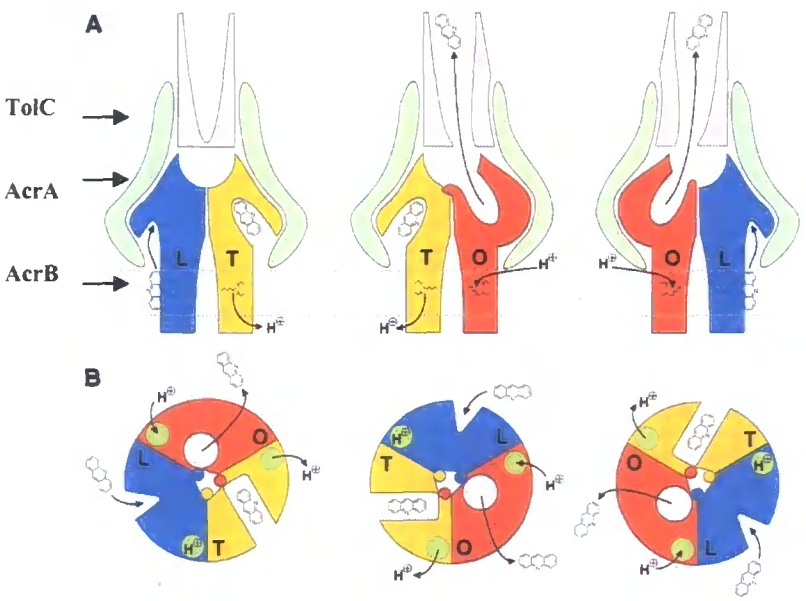

Two recently published papers reported the structure of AcrB at 2.8 and 3.0 angstrom resolution in a space group that allows asymmetry of the monomers. Both of the papers

reported a conformational difference in the pore domain between each protomer(Murakami *et al.*, 2006; Seeger *et al.*, 2006), which has led to the functional rotating pump mechanism.

Among the three protomers, one of them is found to have a substrate binding pocket, which is rich in aromatic amino-acid that connect to the vestibule, which is considered to be the drugs uptake pathway. In this state, exit from the binding site is blocked by the central helix. In the next state, the access to the vestibule is closed and the central helix that blocks the exit of drugs from the binding pocket is opened due to the movement of PN2 and PC1. The bound drug is then pushed out into the top funnel. After extruding the substrate, the binding pocket then shrinkes and the vestibule opens to the periplasm so that potential substrates can access to the vestibule, and another transport cycle starts.

After proposing the transport mechanism for AcrB, Seeger and colleagues undertook a biochemical study on AcrB, in which the interfaces of potential moving subdomains of AcrB were cross-linked. Its susceptibility of AcrB to noxious compounds increased and this effect could be reversed by adding the reducing reagent DTT, supporting the mechanism of functional rotation(Seeger *et al.*, 2008).

The transport of drugs by AcrB is driven by the proton motive force(Zgurskaya and Nikaido, 1999a). It has been found that energization of the transport machinery occurs in the transmembrane domain and is transmitted to the pore domain. Three charged residues in the transmembrane region are found to be functionally essential: Asp407, Asp480 and Lys940, which are located in the middle of TM4 and TM10, where they form an Asp-Lys-Asp ion-pair/hydrogen-bonding network in the TM segments. They are possible candidates for the proton-translocating pathway(Guan and Nakae, 2001; Murakami *et al.*, 2002). Recently, another residue, Thr978 in TM11, which in close to Asp407 has also been found to possibly be involved in the proton translocation pathway(Takatsuka and Nikaido, 2006). It has been shown that conversion of any of these residues to alanine produces a widespread conformational alteration, suggesting that the trigger for change is the disruption of the same salt bridge/H-bonding network(Borbat *et al.*, 2007). The conformational difference in this proton-translocation site in the TM domain is coupled to the closing and opening of the channel entrance and the exit to the funnel domain in each protomer. This indicates a

coordinated control in coupling drug export and proton-translocation(Sennhauser *et al.*, 2007).

Tripartite multidrug efflux pump

In gram negative bacteria, some transporters utilize a tripartite protein complex rather than a single transporter protein. These transporter systems consist of an inner membrane protein (IMP, such as an RND or MF transporter), a porin like outer membrane protein (OMP) and a membrane fusion protein (MFP), which is anchored to inner membrane by either a lipid moiety or a transmembrane α-helice. These three parts form a channel-like substrate translocation pathway that spans across both the inner membrane and outer membranes(Figure 1.1)(Borges-Walmsley *et al.*, 2003). Two well-studied pump systems are AcrAB/TolC from *Escherichia. coli* and MexAB/OprM from *Pseudomonas aeruginosa.* Among the three components, AcrB and MexB are IMPs belonging to the RND family; AcrA and MexA are MFP; TolC and OprM are OMP. In addition to transporters belonging to RND family, some MF transporters and ABC transporters also form tripartite efflux system, such as VceAB/VceC from *vibrio Cholerae* and MacAB/TolC from *Escherichia Coli.*

The structure and mechanism of the outer membrane protein

The outer membrane proteins of tripartite multidrug efflux pump play an important role in the translocation of diverse molecules, which include protein toxins and antibacterial drugs, from the cell. With the assistance of the membrane fusion protein, outer membrane proteins can perform these roles by the process of substrate-induced transient interaction with the inner membrane transporters. Some mutants of outer membrane proteins in bacteria can lead to heightened sensitivity to their substrates (Gil *et al.*, 2006; Li and Poole, 2001).

Figure 1.12 the crystal structures of TolC(Koronakis *et al.*, 2000)

A: A ribbon representation of TolC side view, the three protomers are colored red, yellow and blue respectively. The β-barrel is at the top (distal) end, and the α-helical domain is at the bottom (proximal) end.

B: A ribbon representation of coiled-coil closing the proximal end. Different protomers are colored as A.

C: A ribbon representation of open-state TolC from the proximal end. Different protomers are colored as A.

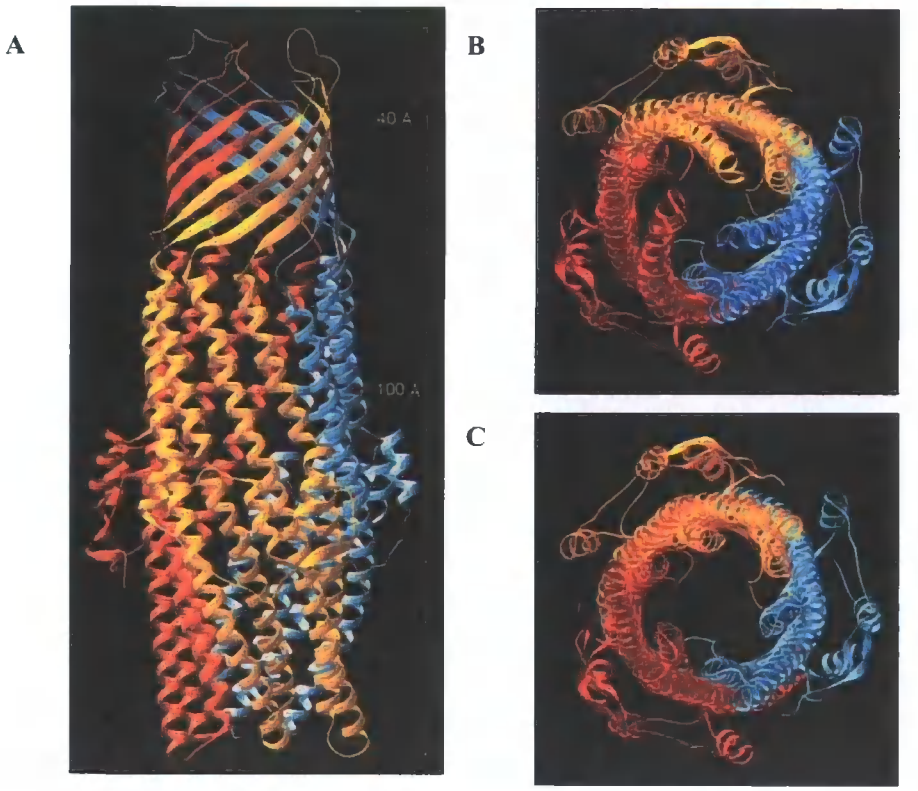

The overall structure of TolC is assembled as a trimer, with the appearance of a cannon that has a long axis measuring 140Å. For nearly 100 Å the body of TolC forms a uniform cylinder of about 35 Å internal diameter. The distal end of the structure is open and provides a wide solvent access, while the proximal end is tapered to a virtual close. The whole molecule can be divided into three parts: a β-barrel domain, a α-helical domain and a mixed α/β-equatorial-domain. In this trimer, the β strands associate in an antiparallel orientation to form a right-twisted 12-stranded β-barrel, to which each protomer contributes 4 strands. The β-barrel domain is located in the outer membrane with the top end widely open from this structure, but it may enable it to close the conformational movement of the loops between each β strand. The α -helical domain is formed by a 12-stranded antiparallel left-twisted α-helical barrel. Unlike the β-barrel domain, the helices that form the α -helical barrel are composed of long (H3 and H7) and short (H2 and H6, H4 and H8) helix. An inner pair of helices (H7 and H8) forms a conventional antiparallel coiled-coil, whilst an outer pair (H3 and H4) comprises a straight helix (H3) around its parterner (H4). The coiled-coils also contact each other. Coiled coils are stablized by an intermeshing of side chains that is call "knobs-into-holes" packing, which indicates the conformation of a small aliphatic side chain

of one helix fits into a small concavity formed by a ring of four small side chain on the second helix. The equatorial domain of TolC is formed by the loop between H4 and H7, which is composed of one short α-helix H5 and one short β-strand S3, and the C-terminal residues after H8 which was partly truncated to facilitate crystallisation of the protein(Koronakis *et al.*, 2000).

Apparently, to enable the transport, the tapered proximal end of the TolC must open and the present mechanism for the attainment of open state TolC is described by a "twist-to-open" model. In this model, the conformational change from the resting closed state of TolC to the modelled open state TolC is related to the circular network of intra- and intermonomer hydrogen bond and salt bridge(Koronakis *et al.*, 2000). This circular network is composed of six coiled coils, two from each protomer. The hydrogen bonds between inner and outer coiled coils in same monomer, links(fig1.13) Ⅰ and links Ⅱ by connect Asp153 with Tyr362 and Gln136 with Glu359. Links Ⅲconnect Arg367 of each inner coiled coil to the outer coiled coil of adjacent monomer, by a salt bridge to Asp153 and a hydrogen bond to Thr152(Andersen *et al.*, 2002).

Figure 1.13 the structure of the TolC periplasmic entrance(Andersen *et al.*, 2002)

A: the resting closed state of TolC viewed from the periplasmic side. Four helices in one monomer are highlighted as yellow (H7), red (H8), green (H3) and blue (H4). The hydrogen bond and salt bridge between intra- and intermonomer are numbered and indicated by dotted lines.

B: the presentation of periplasmic circular network, showing the residues involved in intra- and intermonomer links. The helices are colored like A.

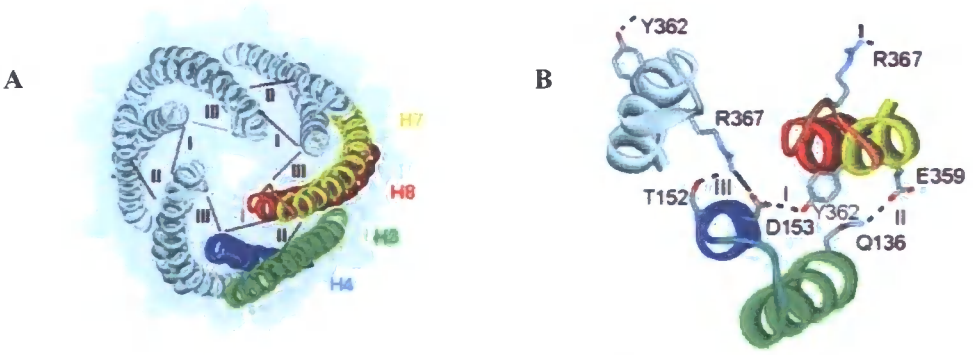

This mechanism is supported by some structural and biochemical data, after disrupting the above hydrogen bond and salt bridge by replacing the relative residues, the conductance

of TolC increases, which is also prominent after substituting the residues Y362 and R367, indicating that these residues are involved in determining the entrance diameter(Andersen *et al.*, 2002). Similar work demonstrated an increased sensitivity to the large antibiotic, vancomycin, which also indicates the importance of these residues in opening the periplasmic entrance of TolC(Augustus *et al.*, 2004). A chemical cross-linker was used to constrain the movement of the coiled-coils by forming disulphide bonds, TolC-dependant export was then found to be abolished(Eswaran *et al.*, 2003). Very recently, the published structure of a TolC double mutant of Y362 and R367 was shown a partially open state, again prove the importance of the coiled-coil interaction in the conformational change between the closed and open states(Bavro *et al.*, 2008).

In 2004 and 2005, the structures two other β-barrel outer membrane proteins, which are also components of tripartite multidrug efflux pumps, were reported, OprM from *pseudomonas aeruginosa* and VceC from *Vibrio cholera*. OprM is the outer membrane accessory protein of the RND transporter MexB and VceC belongs to the MF tripartite transporter VceAB/VceC(Akama *et al.*, 2004a; Federici *et al.*, 2005).

The overall structures of both OprM and VceC resembled TolC, but VceC is structurally closer to OprM than TolC. Although the sequence identity between structurally aligned segments is very low (OprM is 21% identity with TolC and VceC is 8.3% identity with TolC), most of these residues are hydrophobic and play a structural role. The major differences between OprM and VceC with TolC are the size of the pore that is formed by the loops between the β-strands and the electrostatic surface potential inside the channel. The top end of the β-barrel is widely open in TolC, while three short loops of OprM protrude toward the inside of the pore forming a constriction. In the case of VceC, the pore is formed by the loops between strands S1 and S2 of each protomer. These loops are five residues longer than in TolC and OprM and are oriented so as to rest upon the porin-like domain, providing only a small passage with a diameter of ~6Å. After comparing the electrostatic surface potential of these proteins, it has been found that all the channel interiors are generally electronegative. However, in VceC, two rings of clustered negative charge are found, which are partly conserved in OprM but barely in TolC. It has been proposed that the difference in charged residues may facilitate substrate movement across the channel. Beside these striking

differences, the secondary structures of the equatorial domains have also been found to vary in these three outer membrane proteins. Because this part is proposed to interact with the corresponding membrane fusion proteins, the differences in these domains may indicate the different requirement of binding their partner membrane fusion protein(Akama *et al.*, 2004a; Federici *et al.*, 2005).

The structure of the membrane fusion protein

The membrane fusion protein is another important component of tripartite antibiotic efflux pumps. They are anchored to the inner membrane by either an N-terminal lipid modification or a transmembrane helix. However, it has been shown that membrane fusion proteins are fully functional as expressed in the periplasmic without attaching to inner membrane(Yoneyama *et al.*, 2000). Some biochemical experimental results indicate that the interaction between the membrane fusion protein and their cognate partner plays an important role in the drug efflux process(Mokhonov *et al.*, 2004; Stegmeier *et al.*, 2006).

Two structures of the membrane fusion proteins that are accessory proteins of RND transporters have been reported: MexA of the MexAB/OprM system from *pseudomonas aeruginosa* and AcrA of the AcrAB/TolC system from *Escherichia coli*.

Figure 1.14 the structure of MexA from *pseudomonas aeruginosa*(Higgins et al., 2004)

A: The ribbon representations of MexA, different domains are indicated.

B: Top view of the MexA molecule.

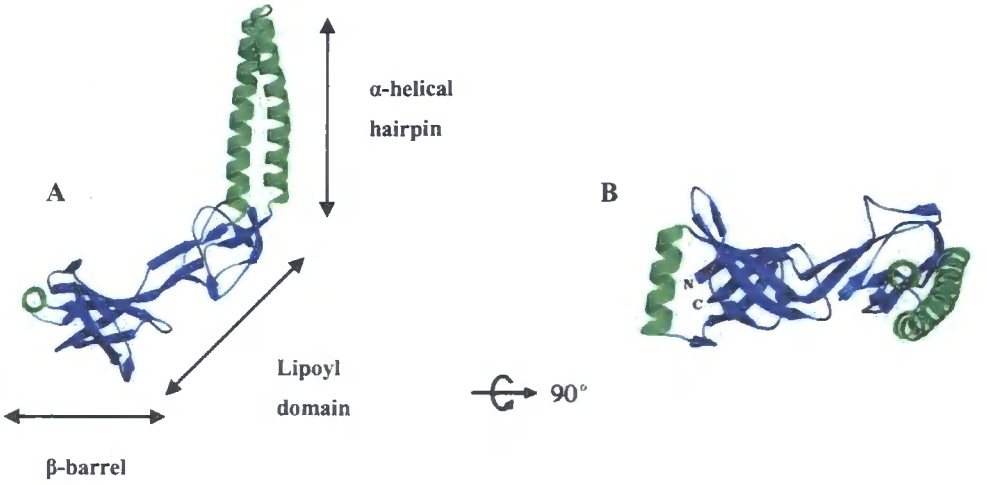

The MexA monomer incorporates three domains: a β-barrel domain, a Lipoyl domain and an α-helical hairpin. The β-barrel domain is composed of six anti-parallel β-strands with a

single α-helix located at one entrance to the barrel. The lipoyl domain comprises of two interlocking lipoyl motifs of four β-strands. The α-helical hairpin is 47Å long, it forms an intervening sequence between the two lipoyl motifs. Some highly conserved residues through the family are found in certain positions of heptad repeat: position a and d contains many large hydrophobic side chains, which form the core of the hairpin; alanine is found predominantly in the f position whereas the c position contains mainly hydrophilic residues. These conserved residues form strips along the exposed sides of the hairpin with a large hydrophilic residues that lie in either end, which are probably involved in hydrogen bond formation and in interactions with its cognate inner and outer membrane proteins(Akama *et al.*, 2004b; Higgins *et al.*, 2004).

After the publication of the MexA structure, another structure for a membrane fusion protein, the stable core of AcrA was reported. The overall structure of AcrA strongly resembles MexA, except the α-helical hairpin which is 11 Å longer. Notably, AcrA was found in four conformations in the crystal. The biggest difference is a 15° reorientation of the α-helical hairpin. These conformations provide evidence for "hinge-like" conformational flexibility between the α-helical hairpin and the lipoyl domain and that this structural change is reversible(Ip *et al.*, 2003). Although this flexibility wasn't been shown in the crystal structure of MexA, similar conformational changes were found in MexA by using molecular dynamics(MD) simulations(Vaccaro *et al.*, 2006). Interestingly, the magnitude of this conformational flexibility is remarkably congruent with the conformational changes implicated in opening of TolC channel(Mikolosko *et al.*, 2006), which indicates the importance of the hairpin domain(Stegmeier *et al.*, 2006) and its conformation flexibility is some how related to the interaction with inner and outer membrane proteins.

The interaction between each component in the RND tripartite efflux pump

As we mentioned previously, in gram negative bacteria, the tripartite efflux pumps which composed of three types of protein have been found to play an important role in exporting a wide variety of drugs and toxic compounds. Although several crystal structures of OMP, IMP and MFP have been reported, the question remains as to how these three proteins assemble to form a functional pump and how channel opening occurs.

Among all the RND tripartite antibiotic efflux pumps, the two best studied models are the AcrAB/TolC and MexAB/OprM systems. These two pumps are homologous and share similarity in structure. Although there is still no definitive experimental data for the stoichiometric composition of an engaged tripartite system, some research has been undertaken to study how these components collaborate with each other.

Cross-linking and isothermal titration calorimetry studies have shown that AcrAB/TolC can form a stable complex that can be stabilized by the presence of substrates(Tikhonova and Zgurskaya, 2004; Touze *et al.*, 2004). Among these three components, the membrane fusion protein is considered to span the periplasmic space, where it acts as a very important part in maintaining the ternary structure of the pumps(Zgurskaya and Nikaido, 1999b). Apart from the evidence that the MFP can interact with both the IMP and OMP directly, failure to co-purify the IMP and OMP in the absence of the MFP(Mokhonov *et al.*, 2004), also indicates the importance of the MFP in the whole system.

The MFP and its cognate OMP have been reported to interact independently of the presence of any externally added substrate or the IMP(Husain *et al.*, 2004). This interaction is consistent with genetic studies in which extragenic supressors of a mutant TolC strain were found in the AcrA gene(Gerken and Misra, 2004). As mentioned before, the MFP, in the cases of AcrA and MexA, is composed of three domains, which are an α-helical domain, a β-barrel domain and a lipoyl domain. From these domains, it is the α-helical domain that is thought to functionally interact with its cognate OMP(Stegmeier *et al.*, 2006). After changing the α-helical domain of AcrA for this part of MexA, the function of the AcrAB/OprM complex was restored. To find out the exact residues interacting in both the OMP and MFP, cross-link was carried out on both wild type AcrA with site-specific TolC cysteine variants and wild type TolC with AcrA cysteine variants. These studies identified the intramolecular groove proximal to the TolC entrance as the interaction surface, highlighting the exposed residues along the TolC α-helices H3 and H7 from tip and up to just below the equatorial domain, and reciprocally, the N-terminal α-helix of the MFP coiled-coil(Lobedanz *et al.*, 2007). Although in this study, the one mutant that locates at the equatorial domain of TolC didn't interact with AcrA, two hydrophobic residues located at the equatorial domain have

been reported to be involved in the transport activity of TolC(Yamanaka *et al.*, 2004). The possibility is that the equatorial domain of TolC also is involved in the interaction with AcrA.

Despite the fact that a lot of work has been done to show the interaction between the MFP and IMP, none of them elucidated the precise interaction between the MFP and IMP yet. It has been shown that the MFP and IMP can interact specifically and independently of either the substrate or OMP(Kawabe *et al.*, 2000; Zgurskaya and Nikaido, 1999a, , 2000). Mutagenesis and cross-link studies indicate that the N-terminal periplasmic domain of the IMP is presumably involved in determining the specificity of interaction with the cognate MFP, with residues 60-612 apparently of particular importance(Tikhonova *et al.*, 2002). These residues are located on the outward-facing surface of a large groove in each monomer that was previously predicted to be involved in binding to its partner MFP(Murakami *et al.*, 2002). Interestingly, in antibiotic resistant *pseudomonas aeruginosa*, Jocelyn et al found that several mutants in MexB occured in this region, corresponds to the MexA binding part of MexB(Middlemiss and Poole, 2004). As to the interacting part of AcrA, its C-terminus is reported to be involved in the interaction with its cognate IMP, AcrB(Elkins and Nikaido, 2003; Touze *et al.*, 2004). Also consistent with the studies of HlyD, which indicate that the C-terminal regions of the MFPs is responsible for the binding(Schlor *et al.*, 1997). Furthermore, it has also been found that the residues involved in this binding are poorly conserved in the MFP family and these unique residues may be important for and define the MFPs interaction with their IMP partner(Nehme *et al.*, 2004).However, in other reports, the β-barrel of the MFP is considered to interact with the IMP (Gerken and Misra, 2004; Krishnamoorthy *et al.*, 2008).

Whether or not there is direct interaction between IMP and OMP hasn't drawn to a conclusion yet. More people believe IMP and OMP can not form a stable complex without the assistance of MFP(Mokhonov *et al.*, 2004; Tikhonova and Zgurskaya, 2004; Touze *et al.*, 2004), while some others think the IMP can interact with OMP directly. Norihisa *et al* has shown the interaction between TolC and AcrB via site-directed disulfide cross-linking. They found the residues that involved in most contact between AcrB and TolC are located at the tip of the vertical hairpin of AcrB and the tip of coiled-coil of TolC, moreover, there are still some residues apart from the tip of TolC involved in second-most contact. These finding have

led to a two-step contact mechanism which accompanies a conformational change on both AcrB and TolC. Because the cross-linking is independent of AcrA, they propose that AcrB first interacts with TolC and then the complex is stablized by AcrA(Tamura *et al.*, 2005).

Several models of how the tripartite complex is assembled have been proposed.

Figure 1.15 Models of the proposed assembling of the tripartite complex(Akama *et al.*, 2004b; Fernandez-Recio *et al.*, 2004).

A1: Side view of the 1:1:1 model, the IMP, OMP and MFP are colored green, blue and red respectively.

A2: View is along the vertical axis

B1: Side view of the 1:2:1 model, the IMP and OMP are colored purple and blue, two MFP bind to one protomer are coloered dark blue and red.

B2: View is along the vertical axis

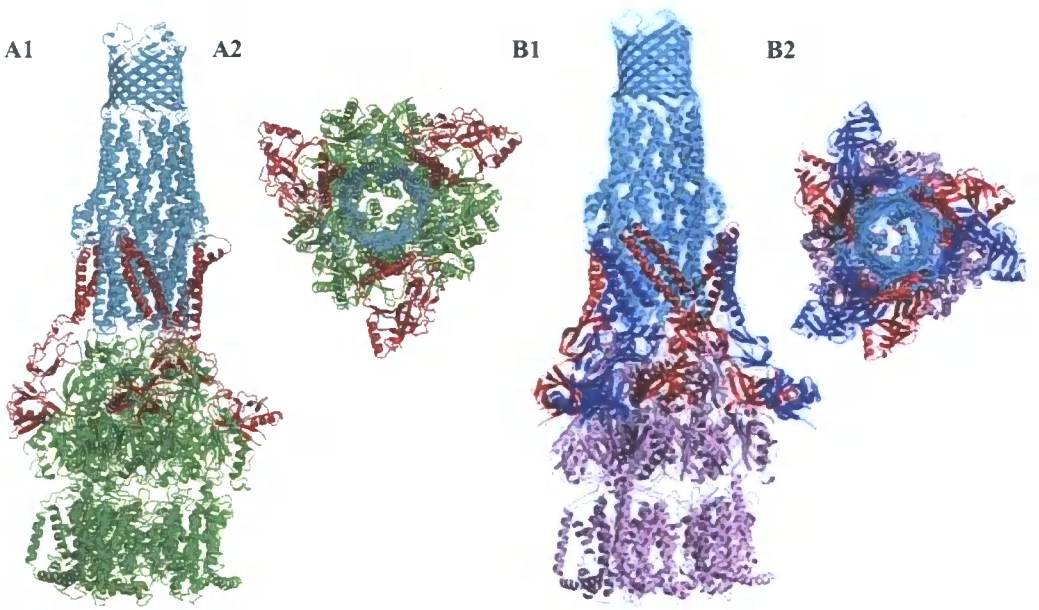

Beside these two models, there are still other alternative models have also been proposed. One of them is based on the compositional ratio of 1:3:1 and another suggest a tridecamer. Because there is no definitive experimental data for the stoichiometric composition of an engaged pump yet, it is hard to decide which model reflects the pump composition in native condition. More work is still needed to elucidate this.

The Mtr (multiply transferable resistance) system of *Neisseria gonorrhoeae*

Strain of *Neisseria gonorrhoeae* started to emerge with clinically significant levels of resistance to penicillin just after the introduction of penicillin to treat gonorrhoea. These gonococcal clinical isolates display hypersusceptibility to penicillin and structural diverse hydrophobic agents (HAs), such as drugs, dyes, detergents and host-derived compounds (fatty acids and bile salts), as well as some cationic antimicrobial peptides(Shafer *et al.*, 1998; Tzeng *et al.*, 2005). The Mtr system was found to confer resistance to these antibacteria compounds. Genetic and physiological studies demonstrated that the Mtr system functions as an energy-depend efflux pump by a mechanism requiring the proton motive force(Hagman *et al.*, 1995; Lucas *et al.*, 1995). The Mtr system is composed of the *mtrCDE* genes and the *mtrR* gene encodes a transcriptional repressor that appears to regulate expression of the upstream and divergent *mtrCDE* operon(Hagman and Shafer, 1995). The *mtrCDE* genes encode membrane proteins analogous to the MexAB/OprM of *Pseudomonas aeruginosa* and AcrAB/TolC of *Escherichia coli* that mediate export of structural diverse antimicrobial agents. Hagman *et al* has reported that the *mtrD* gene encodes a membrane protein with mass of nearly 114kDa and displays a significant similarity to RND family proteins(Hagman *et al.*, 1997). The *mtrE* gene encodes an outer membrane protein with mass of 48.3KDa, which is associated with the Mtr phenotype, and is identified as a homologue of export-associated outer-membrane proteins, such as OprM and TolC. Insertional inactivation of the *mtrE* gene can result in hypersusceptibility of mutant strains to a range of HAs(Delahay *et al.*, 1997). The expression of MtrCDE are considered to be modulate by two transcriptional regulators, MtrA and MtrR, which can activate and repress the expression respectively (Rouquette *et al.*, 1999). A lot of works has been done on MtrR to establish that the insertional or deletional mutants of MtrR can lead strains that are hypersusceptibile or have decreased susceptibility to the substrates of the Mtr system, due to the overexpression or defective expression of MtrCDE(Johnson *et al.*, 2003; Veal *et al.*, 1998; Veal *et al.*, 2002; Zarantonelli *et al.*, 2001).

1.4 Regulation of bacterial multidrug efflux pumps

Because bacteria in the environment are exposed to lots of noxious compounds, such as antibiotics and deleterious molecules that originate from their own metabolism, their MDR genes need to be expressed at a low level before significant efflux of clinically relevant antimicrobial compounds occurs. This lead to a proposal that MDR pumps are pre-existing and protect bacteria against the low level of toxic compounds they encounter in the environment. Therefore, to survive in the unstable surrounding they require rapid, adaptive responses to toxic molecules, which are normally mediated by regulatory proteins(Cases *et al.*, 2003), such as the TetR, repressor of the tetracycline-specific pump TetA(B) from *Escherichia coli* and QacR of the multidrug transporter QacA from *Staphylococcus aureus*(Grkovic *et al.*, 1998) . Analysis of the pumps and their regulatory controls indicates that the efflux of medically relevant antimicrobial compounds is the primary function of these systems(Grkovic *et al.*, 2002; Ramos *et al.*, 2005).

Regulators involved in transcriptional control can be classified into families on the basis of sequence similarity and structural and functional criteria. Among them, the TetR family is an important one that play a role in MDR regulation. Members of the TetR family are two domains proteins with a DNA-binding domain and a regulatory domain that recognises the signals *via* the binding ligand. They show high sequence similarity in the DNA-binding domain, which contains a helix-turn-helix (HTH) motif, and no significant similarity in the regulatory domains corresponding to their various signalling molecules(Dover *et al.*, 2004; Frenois *et al.*, 2004; Jeng *et al.*, 2008; Okada *et al.*, 2008; Orth *et al.*, 2000; Schumacher *et al.*, 2001).

TetR and QacR are two members of the TetR family that have been well characterized genetically and biochemically. A series of publications about TetR and QacR revealed the structures of these two proteins both with their operators and substrates, and proposed a mechanism for transcriptional control of MDR by the TetR family of regulatory proteins. It has been shown that although these two protein share similarity in structure, they have distinct differences in many aspects.

1.4.1 The structures of TetR and QacR with bound to their corresponding operators

The crystal structure of TetR revealed a protein consisting of 10 α-helices, which forms a homodimer in the native state, α1 to α10 form the first monomer and α1′ to α10′ form the other monomer. The dimerization of TetR is accomplished by the interaction between helices α8 and α10 with helices α8′ and α10′, which forms a four-helix bundle(Hinrichs *et al.*, 1994). This four –helix bundle is also reported to involve in the central part of the regulatory domain, which will be elucidated in the following section.

Figure 1.16 structure of TetR-operator complex(Orth *et al.*, 2000)

A: A ribbon representation of the overall structure of the TetR-DNA complex. α-helices of one monomer are labelled. The helices that form the DNA binding domain are colored blue; the helices that form the rigid scaffold are colored yellow, the rest of the helices undergo conformational change after the binding of inducer are colored green.

B: schematic representation of interaction between one monomer of TetR and its half-15bp operator. Hydrogen bonds are represented as arrows and van der Waals interaction as dotted lines.

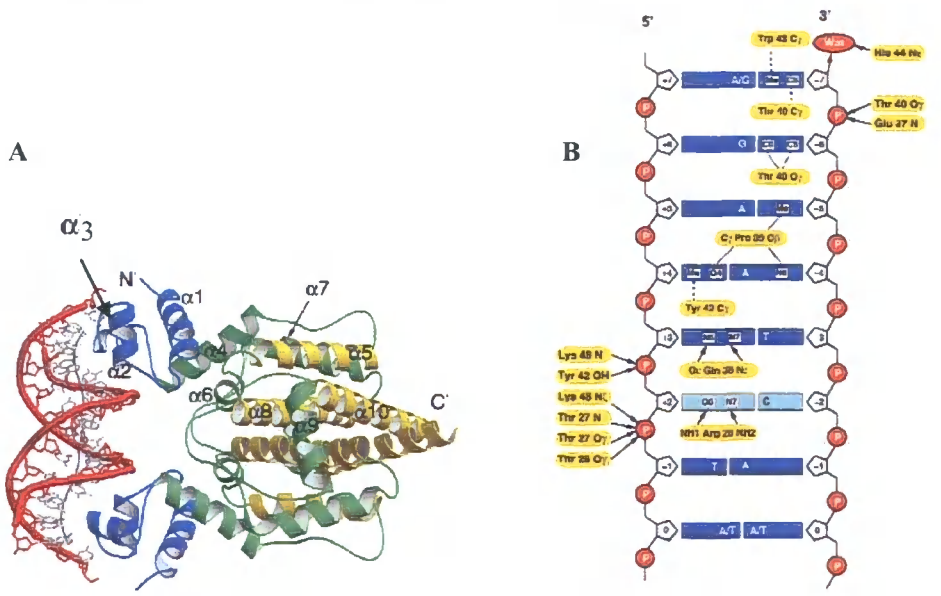

The DNA binding domains are formed by a three-helix bundle (α1-α3), within which α2 and α3 constitute the helix-turn-helix (HTH) motif, which are typical structures involved in protein-DNA interactions. These HTH motifs are found in most of the reported TetR repressors, such as AcrR from *Escherichia coli*, EthR from *Mycobacterium tuberculosis* (Dover *et al.*, 2004; Frenois *et al.*, 2004), SCO0332 from *Streptomyces coelicolor* (Okada *et*

al., 2008) and IcaR from *staphylococcus epidermidis*(Jeng *et al.*, 2008). However, it is also been found that there is a TetR repressor, CmeR of *Campylobacter jejuni*, that has a random coil in the DNA-binding domain instead of a α3 helix(Guan *et al.*, 2007). In TetR, each HTH motif binds to the major groove of the palindromic operator and the minor groove is not recognized. All base pairs of 15-mer operator fragment, except the central three pairs, are engaged in TetR binding. At the recognition sites, the major grooves are widened to 14-14.5Å, while the major groove at the opposite site of the central base pair is narrowed to 9.5Å. With the corresponding change in the minor grooves, the helical repeat of DNA is increased to 38Å due to the partial unwinding of the DNA duplex. In the bent half-operator, all residues of helix 3 are involved in recognition, except Leu41, which is part of the hydrophobic core stabilizing the three-helix bundle. Other residues that are involved in DNA contacts are located in the first helix of HTH, the turn of the HTH and both of the interhelical loops connect the HTH to the adjacent helices(Aramaki *et al.*, 1995). Because there are no water molecules incorporated into the protein-DNA interface, Pro39 is employed to contribute to this close fit. Moreover, Pro39 switches TetR binding from one DNA strand to the other by forming van der Waals interaction with each of the nucleotides at positions +4 and -5. (Orth *et al.*, 2000)

Figure 1.17 structure of QacR-operator complex(Schumacher *et al.*, 2002)

A: Overall structure of the QacR-DNA complex. The subunit of one dimer is shown in blue (distal) and cyan (proximal), whilst other is purple (distal) and green (proximal). The helices in one monomer are numbered. DNA is shown with phosphate, oxygen, carbon and nitrogen colored yellow, orange, gray and blue respectively.

B: Schematic showing QacR-DNA half site contacts. Hydrogen bonds are indicated by arrows, van der Waal contacts are shown as diamonds.

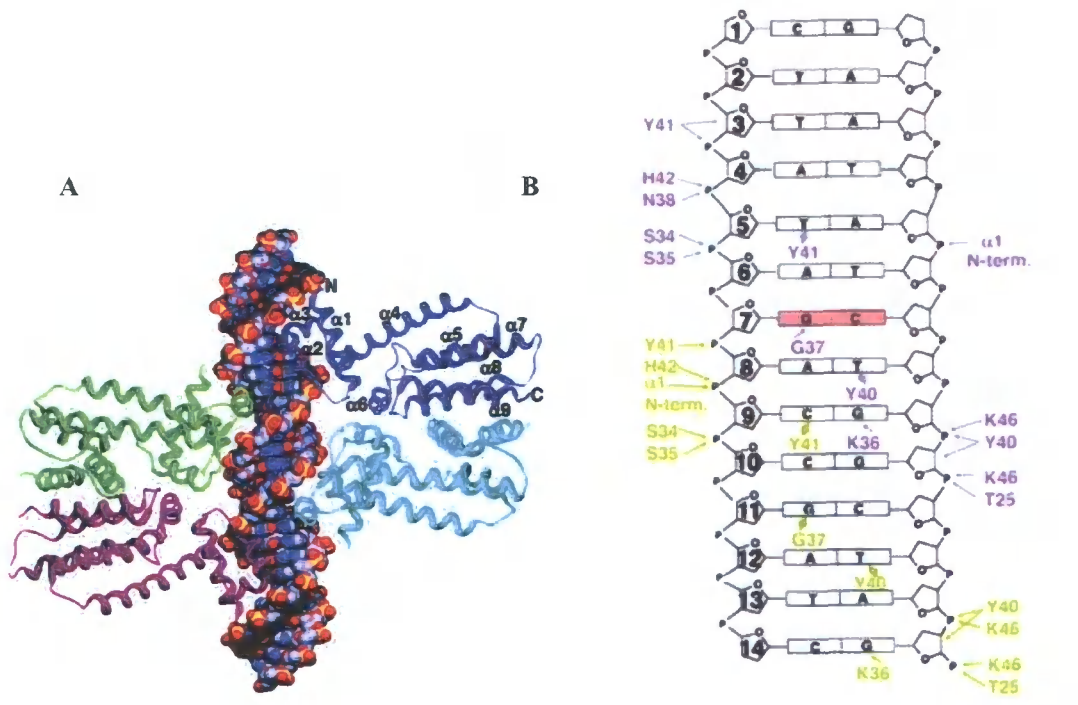

The structure of the complex revealed that a pair of QacR dimers bind to one DNA (Grkovic *et al.*, 2001). Each QacR monomer consists of nine helices, the first three helices α1-α3 form DNA-binding domain that contains a HTH motif, while the α4-α9 form the regulatory/dimerization domain. Unlike its homologue TetR, the four-helix dimerization motif is formed by α8 and α9 of each monomer, but in case of TetR, it is α8 and α10. One dimer binds to each side of the DNA, with two HTH motifs in contact with the major grooves of the DNA. The minor grooves are not recognized as in TetR. Although the distal monomers make the majority of the base-specific interactions, the proximal monomer makes several base and phosphate contacts; both interactions show a distinguishing feature of DNA recognition by QacR(Schumacher *et al.*, 2002).

The binding between duplex DNA and QacR dimer is reported to be cooperative (Grkovic *et al.*, 1998; Grkovic *et al.*, 2001). However, it has been shown that such binding is not mediated by protein-protein interactions because QacR does not self-assemble into a tetramer without the presence of the DNA(Grkovic *et al.*, 2001). Structural analyses have shown that features of the DNA and protein conformation are keys to bind cooperatively. The center-to-center distance between the recognition helices of each QacR dimer was found to be extended, as a result of DNA unwinding and expansion of the major grooves. It leads to a

postulate that binding of the first dimer, produces an induced fit to the protein and DNA to make an optimal major groove for the second dimer to bind.

As homologues of the same family, QacR and TetR and other members share some similarities in binding their corresponding operators; such as their DNA-binding domains all consist of α1-α3, with a HTH that contacts with the major grooves, while the minor grooves are not recognized; their recognition helix interacts deeply with the DNA so that no water molecules exist in the interface between the protein and DNA. However, they still have distinct differences in the mode of DNA recognition. TetR employs only one dimer to bind the duplex DNA operator, while QacR uses two cooperative binding dimers to increase the binding affinity and specificity. This cooperative binding are found in most of other members, such as AcrR, EthR, IcaR, TtgR, TtgV, VceR and CmeR(Chen *et al.*, 2007; Federici *et al.*, 2005; Guan *et al.*, 2007; Jeng *et al.*, 2008; Krell *et al.*, 2007), while EthR is proposed to bind one operator with four dimers(Dover *et al.*, 2004). When TetR binds to the operator, it widens the major grooves at the recognition sites to create a optimized position for binding, whilst narrows the minor grooves and other major grooves. In the case of QacR, the entire IR1-binding site is widened, causing a longer center-to-center distance. The contacts between DNA and the TetR HTH motif from each monomer are nearly identical, while the HTH motif of QacR from each monomer in one homodimer makes a different set of contacts, each with a non-palindromic site(Orth *et al.*, 2000; Schumacher *et al.*, 2002).

1.4.2 The structures of TetR and QacR binding their corresponding substrates

The Tetracycline (Tc) binding pocket is composed of the COOH-termini of α4 and α6 and the helices α5, α7, α8, α8' and α9' (prime refers to the second monomer of the homodimer). The entrance of the drug binding tunnel has been proposed to be the opening next to the C-terminus; the docking of $[Mg\ Tc]^+$ suggested a lateral motion of α9'comparable to a "sliding door"(Orth *et al.*, 1998).

Figure 1.18 Chemical structure of tetracycline and schematic description of the interaction between tetracycline and TetR.

Hydrogen bonds are represented by dashed lines; hydrophobic interactions are shown by hatched lines. W1, W2 and W3 are water molecules in the octahedral coordination shell of Mg^{2+} and Me

represent methyl. Charges are marked (+) and (-). The residues involved are labelled with the corresponding helix. (Hinrichs *et al.*, 1994)

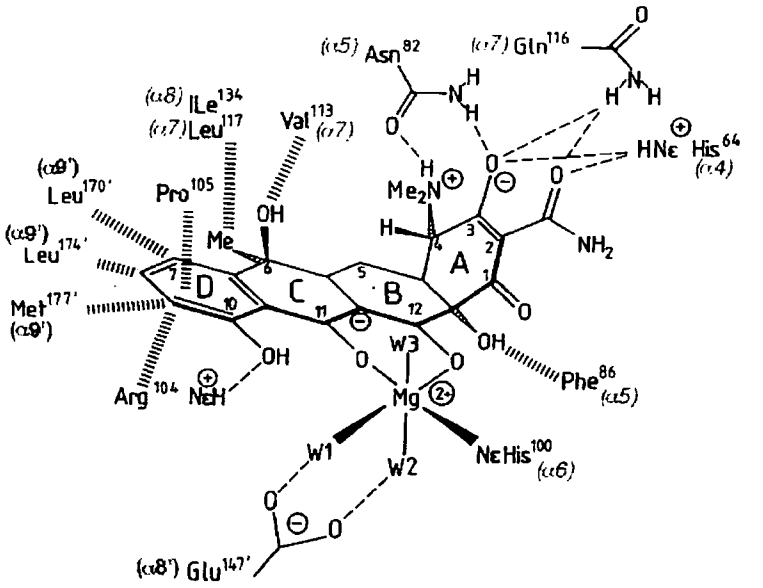

The drug binding in TetR binding cavity is mediated by Mg^{2+}, which is octahedrally coordinated by the group O11/O12 of Tc, His100 (α6) and three water molecules W1, W2 and W3. W1 and W2 also interact with Glu147'(α8') via hydrogen bonds. The highly conserved Phe86 (α5) form a aromatic hydrogen bond with the hydroxyl group O-121. Gln116 (α7) and His64 (α4) form hydrogen bonds to the Tc amide oxygen in position 2 and to O-3. The interaction with His64 is quite important because after its substitution to Lysine, the affinity to Tc is reduced and the substrate specificity can be changed(Scholz *et al.*, 2003). The O-3 and N-4 of Tc are bridged to Asn82 (α5) by hydrogen bonds(Hinrichs *et al.*, 1994). It has been reported that modifications of the functional groups of Tc involved in forming hydrogen bonds and Mg^{2+} coordination, like ring A and hydrophilic positions O^{10}, O^{11}, O^{12}, $O^{12|}$, can abolish the bacteriostatic interaction with the ribosome, thereby losing antibiotic activity (Hlavka & Boothe, 1985).Variations of those groups that are only in hydrophobic contact (presents in hatched lines) with the protein are permissible (Sum *et al*, 1994). This explains why the 9-(N,N-dimethylglycylamido)-6-demethyl-6-deoxy-tetracycline, which has modifications at position 6 and 7, leads to a reduced but still significant induction of TetR (Orth *et al.*, 1999). However, it has been proposed that the Tc variants bind slightly different positions in the TetR Tc binding pocket(Henssler *et al.*, 2004; Scholz *et al.*, 2003).

Figure 1.19 The structure of the ternary QacR-proflavin(pf)-ethidium(Et)(Schumacher *et al.*, 2004).

A: The ribbon diagram of the QacR-pf-Et ternary complex, the nine helices are numbered and the Pf and Et molecules are presented as yellow and red sticks respectively.

B: The key residues involved in the binding of pf and Et, acidic residues are colored red.

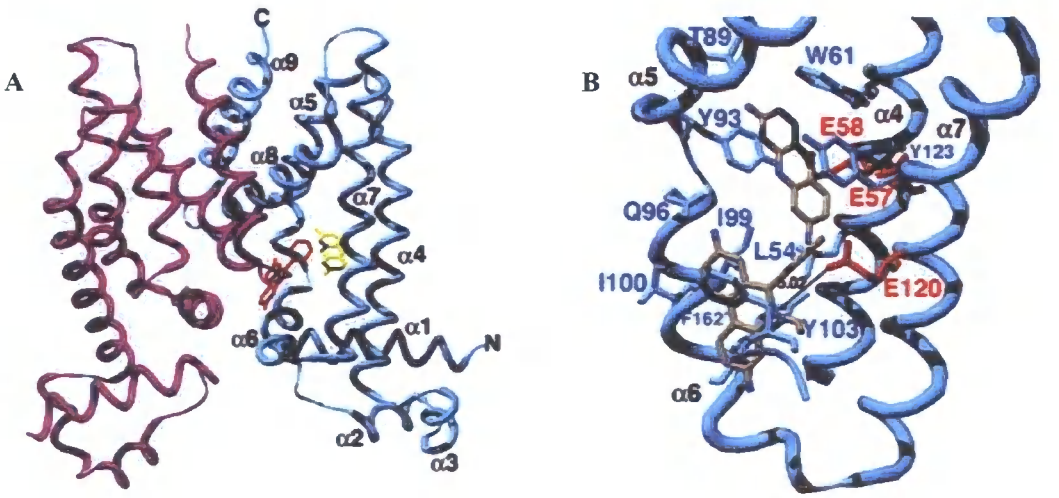

Unlike TetR, QacR is a multidrug binding protein and its drug binding mechanism is rather different to that for TetR. Several binary and ternary structures of QacR with drugs have shown the common and distinct features of QacR when it binds to drugs with different structures.

All the reports so far agree with the presence of separate but linked drug-binding sites in QacR, which means QacR contains a large multidrug binding pocket composed of lots of overlapping mini binding pockets. The large drug-binding pocket is composed of residues from all the helices of the inducer-binding domain except α9, as well as the residues from α8'. The entrance to the aromatic drug-binding site is formed by divergence of α6, α7, α8 and α8'. Different drugs bind to different binding pockets by making hydrophobic interactions, hydrogen bonds and van der waal interactions with the corresponding residues. In 2001, the report of the structures of six QacR complexes with different drugs, including Rhodamine 6G (R6G), Ethidium (Et), Dequalinium (Dq), crystal violet (CV), Malachite Green (MG) and Berberine (Be), revealed that there are different drug-binding pockets for each inducer. Among them, the binding pockets of R6G, Et and CV are distinct but partially overlapped,

while MG and Be bind within the pockets of CV and R6G respectively. Because Dq is a bivalent cationic lipophilic compounds, it binds the same pocket as that defined for R6G and Et (Schumacher et al., 2001). The structures of QacR with the other three drugs, proflavin (Pf) and the two bivalent diamidines, pentamidine and hexamidine, indicates the presence of individual drug-binding pockets. Pf has been shown to bind in the R6G pocket, while hexamidine spans the multidrug-binding pockets like Dq, pentamidine twists about its central linker and is therefore bent into the core of the protein, creating a noval drug-binding pocket(Murray et al., 2004; Schumacher et al., 2004). Another distinguishing feature of multidrug binding proteins that recognize cationic drugs is the need for the presence of negatively charged glutamate or aspartate residues. In QacR, five glutamate residues have so far been found that can neutralizes the positive charge of drugs; they are Glu57, Glu58 and Glu63 from a4, Glu90 from a5 and Glu120 from a7(Murray *et al.*, 2004; Schumacher *et al.*, 2001; Schumacher *et al.*, 2004). In 2004, Schumacher *et al* reported a ternary structure of QacR with two drugs bound, pf and Et, which shows how the drug-binding pocket adjusts to permit binding of more than one drug. In the QacR-Pf-Et ternary structure, Pf remains in the R6G pocket, with the protein-drug contacts nearly identical to those observed in QacR-Pf binary structure, while the Et molecule has shifted considerably, with the side chain of Tyr123 moved to a position that is identical to that which it assumes in the QacR-binary structure, in which there is a 1Å increase in the distance from the side chain carboxylate of the drug-neutralizing residue Glu120 to the positive charged Et. However, the key contacts between Et and QacR are still maintained. This conformational change after the binding of the first drug may facilitate binding of the second drug(Schumacher *et al.*, 2004).

The C-termial multidrug-binding pocket has also been found in other reported structural and functional studies of TetR family members. Although they may have a variable size and entrance, the overall structure and features resemble one-another. For example, the inner wall of the ligand-binding pocket is composed mainly of hydrophobic residues, with the exception of TetR, other members can accommodate different drugs in the binding cavity, with different drugs bound to distinct binding site(Borbat *et al.*, 2007; Chen *et al.*, 2007; Guan *et al.*, 2007).

1.4.3 Induction mechanism of TetR and QacR

The TetR repressor mediates an important mechanism of bacterial resistance against the antibiotic tetracycline. It controls the expression of TetA, a membrane associated protein that export the antibiotic out of the cell, by tightly binding, its operator DNA in the absence of Tc; upon binding of Tc with an associated Mg^{2+} ion, it dissociates from the DNA and allows the expression of TetA. Several models have been proposed for the induction mechanism(Lanig *et al.*, 2006; Orth *et al.*, 1998). Among all the mechanisms, the one that deduces from the TetR, TetR:Tc and TetR:DNA crystal structures is supported by most structural and biochemical studies.

Figure 1.20 the conformational change of TetR upon binding of $[Mg\ Tc]^+$ (Grkovic *et al.*, 2002)

The TetR:DNA is colored blue and TetR:Tc is yellow. The DNA phosphate-ribose backbone is shown in red, bases in grey, Tc in orange and Mg^{2+} in red, the water molecules that constitute the water zipper in the induced conformation as blue spheres, which locks the DNA binding domain in a conformation unable to bind to the operator.

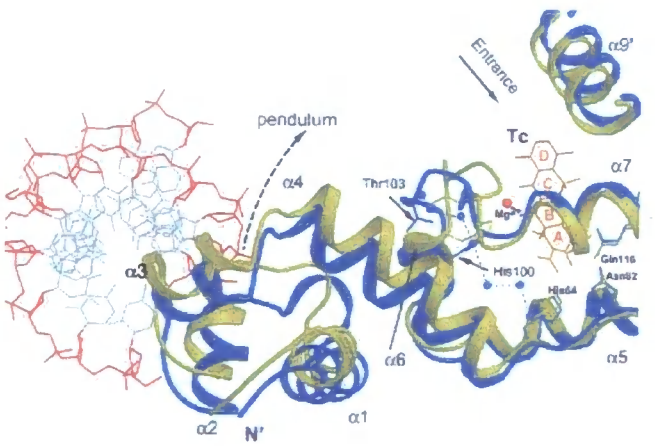

The subsequent events that are triggered by the entry of $[Mg\ Tc]^+$ into the binding site are listed below. (a) Functional groups of Tc-ring A form tight hydrogen bonds to His64 (α4), Asn82 (α5) and Gln116 (α7). (b) Mg^{2+} binding to His100 (α6) triggers the formation of a type II β-turn, His100 to Thr103, at the expense of the C-terminal turn of, produces a partial unwinding of α6. The importance of Mg^{2+} also been established because when Tc binds in the absence of Mg^{2+}, TetR remains in the non-induced state and can bind to DNA

(Kedracka-Krok *et al.*, 2005). (c) Next to this β-turn, the loop, incorporating residues Arg104 to Pro105, is reoriented to form a part of the hydrophobic pocket surrounding the Tc ring D. (d) by rotating 90°, the Glu147' (α8') can hydrogen bond to Gly102 of new β-turn and also to the remaining two Mg^{2+} coordinated water molecules, W1 and W2. (e) Formation of a salt bridge between Asp178' (α9') and Arg104 draws α9' closer and completes the "sliding door" movement of α9' residues, closing the entrance to the binding pocket. It has also been shown that the loop separating α8 and α9, which only has weak electron density in the TetR-[Mg Tc]$^{+}$ complex structure, is important for induction by interfering with the initial closure of the Tc-binding pocket(Berens *et al.*, 1995; Berens *et al.*, 1997; Hecht *et al.*, 1993). (f) α4 is in contact with the unwinding part of α6 and the resulting void is filled by α4 moving in the same direction, like a pendulum. (g) the movement of α4 is associated with a displacement of the DNA-binding domain α1 to α3 into a position where the homodimer TetR no longer fits into the adjacent major grooves of the operator DNA, thereby inducing the expression of TetA(B)(Aleksandrov *et al.*, 2008; Orth *et al.*, 1998).

Figure 1.21 conformational changes between DNA-bound QacR and drug (R6G)-bound QacR

A: superimposition of the DNA-bound conformation (yellow) and the drug-bound conformation (blue) of the QacR drug binding domain.R6G is colored red.

B: Details of the conformational changes upon the binding of R6G. The expulsion of Tyr92 and Tyr93 elongates α5 by one turn.

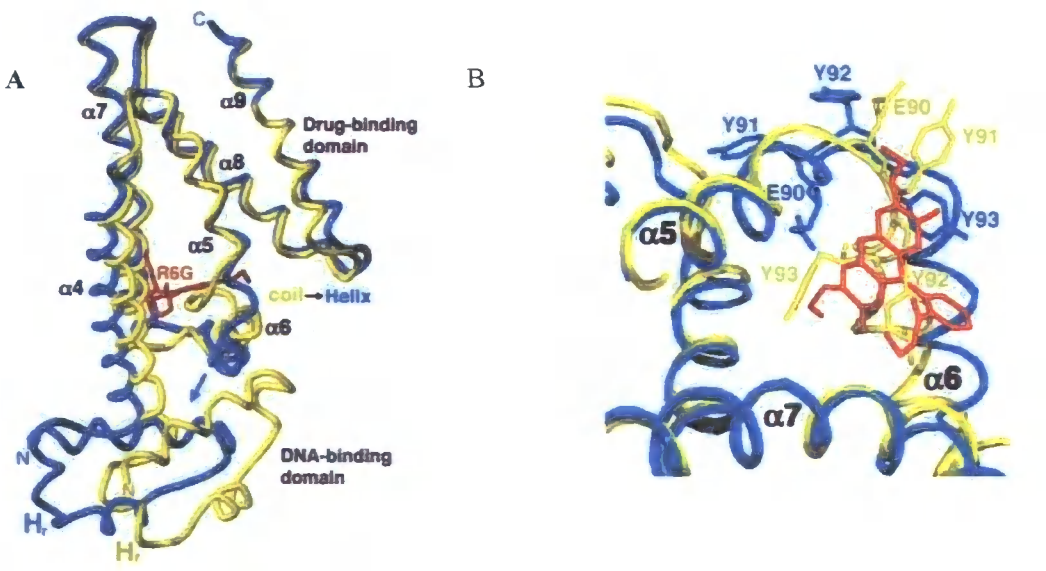

As a repressor that belongs to the same family as TetR, QacR shares similarities in its induction mechanism. In analogy with TetR, the binding of drugs triggers a conformational change that starts from helix α5 and α6, which leads to a pendulum motion of α4, finally producing a translation and rotation of the DNA-binding domain (α1-α3), causing QacR to dissociate from the DNA. However, QacR still displays distinct features in the events after binding to drugs. First of all, QacR binds to its ligands with a stoichiometry of 2:1, compared with 1:1 in TetR; in drug-bound subunit, the binding of drugs triggers a coil-to-helix transition of the C-terminus of α5, which is facilitated by expulsion of Tyr92 and Tyr93; the drug-free subunit of the dimer also undergoes a translation and rotation, although not as obvious as for the drug-bound subunit, which makes a large increase in the center-to-center distance as described before(Schumacher *et al.*, 2001).

The conformational changes due to the binding of ligands to TetR and QacR reflect the common induction mechanism of TetR family reprssors. These structural analyses resemble the functional analysis on some levels: for example, it has been shown in biochemical studies that upon the binding of ligand, the interaction between the repressor and their corresponding operator can be dissociated (Federici *et al.*, 2005; Krell *et al.*, 2007; Teran *et al.*, 2006).

1.4.4 Regulation by the MtrR repressor of Mtr efflux system of *Neisseria gonorrhoea*

As described before in section 1.3.2.3, the MtrCDE efflux pump of *Neisseria gonorrhoea* is associated with increased resistance to inhibitory hydrophobic agents (HAs) (Hagman *et al.*, 1995; Tanaka *et al.*, 2006; Veal *et al.*, 1998). It has been characterized as an active efflux pump that is driven by the proton gradient(Rouquette-Loughlin *et al.*, 2004; Tanaka *et al.*, 2006). Noticeably, this system has also been reported to confer resistance to antimicrobial polypeptides, such as a procine Protegrin-1(PG-1) and a linear synthetic protegrin variant(PC-8), as well as a human cathelicidin peptide(LL-37)(Shafer *et al.*, 1998). Genetic studies have shown that the expression of the Mtr system is negatively controlled by the transcriptional repressor MtrR, which belongs to the TetR family; deletion or inactive mutation of MtrR can lead to overexpression of the Mtr system and

hypersusceptibility to HAs(Hagman and Shafer, 1995; Pan and Spratt, 1994; Veal *et al.*, 1998; Veal *et al.*, 2002; Zarantonelli *et al.*, 2001). It has been reported that the Mtr system is positively controlled by a transcriptional activator, MtrA, which belong to the AcrC/Xyls family(Rouquette *et al.*, 1999). A recent report indicated that MtrA can mutate spontaneously to compensate for the mutant MtrR during infection(Warner *et al.*, 2007), however, the detailed mechanism of this protein is still unknown.

Figure 1.22 organization of the *mtrCDE* region of *N.gonorrhoea*(Delahay *et al.*, 1997)

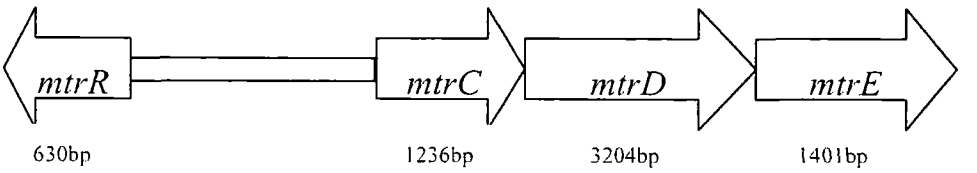

The *mtrR* gene is divergently transcribed with respect to the *mtrCDE* operon and it has been shown be capable of specifically binding the DNA sequence between the *mtrR* and *mtrC* genes. This binding site is located at 27-nucleotides (5'-TTTTTATCCGTGCAATCGTGTATGTAT-3') on the *mtrC* coding sequence that includes the promoter for *mtrCDE* transcription and the complementary 22-nucleotides (5'-ATCCGTGCAATCGTGTATGTAT-3') contains the -35 region of the *mtrR* promoter, with an inverted repeat that is underlined(Hagman *et al.*, 1997). Biophysical and biochemical studies has shown a stoichiometry of two dimers binding to one DNA site in MtrR(Hoffmann *et al.*, 2005), in analogy to QacR that we mentioned before.

In conclusion, although some work has been done to elucidate the characteristies of MtrR, additional studies are still needed to better understand the mechanism of transcriptional control in the Mtr system.

Chapter 2 Materials and Methods

2.1 Laboratory Apparatus

2.1.1 Centrifugation

The following table is a list of all the centrifuges that were used in this study; whilst further detailes on usage is outlined in the subsequent chapter.

Table 2.1 Centrifugation apparatus

Centrifuge	Rotor	Max speed(rpm)	Capacity	Temperature
Progen GenFuge 24D		13,300	24 x1.5ml	Room Tem
Beckman Coulter Avanti JE	JA 10 JA20	10,000 20,000	6 x500ml 8 x40ml	4°C
Beckman Coulter Avanti J20 XP	JLA8.1000	8,000	6 x1 L	4°C
Beckman L8-70M	Type 50.2 Ti	50,000	12 x25ml	4°C
Beckman Coulter Optima L-90K	Type 50.2 Ti	50,000	12 x25ml	4°C
Sigma 3-16K		4,500	12 x50ml	4°C
Jouan CR3i		4,100	8 x50ml	4°C

2.1.2 Cell disruption

The cell disruption system from Constant system (UK) was used in this work. All disruptions were performed at 4°C with a pressure of 15KPSI and passed two or three times through the equipment according to the type of sample. Generally, in order to break the cells completely to provide as much cell membrane as possible, the membrane protein expressing cells were passed through disrupter 3 times and the soluble protein expressing cells were passed through two times.

2.1.3 ÄKTA purifiers

All the purification steps were conducted on ÄKTA purifier CU950 from Amersham.

2.2 The media for bacterial growth

All the media were sourced from Melford Laboratories Ltd or Sigma-Aldrich.

2.2.1 Preparation of the media

The quantity of the media or reagents was measured on a digital scale and the required volume of the deionsed water, from Purlte Prestige Analyst HP purifier, was used to make up the media solution.

2.2.2 Sterilization

Sterilization of the media was performed by autoclaving in a Priorclave Tactrol 2 at 121°C , 4 atmosphere pressure, for 15 minutes, whilst plastic and glass wares were autoclaved for 30 minutes at 121°C.

2.2.3 Media were used in this study

Luria-Bertani (LB) Medium

NaCl	10g/litre
Tryptone	10g/litre
Yeast extract	5g/litre

LB Agar

NaCl	10g/litre
Tryptone	10g/litre
Yeast extract	5g/litre
Agar	15g/litre

2 xYT Broth

NaCl	5g/litre

Tryptone	16g/litre
Yeast extract	10g/litre

SOC Medium

NaCl	0.585g/litre
KCl	0.1865g/litre
Tryptone	20g/litre
Yeast extract	5g/litre

The above were autoclaved and the following filter sterilised components were added:

1M $MgCl_2 \cdot 6H_2O$	10ml
1M $MgSO_4$	10ml

2.3 Antibiotic

The stocks of antibiotics that were used in this study were made at 1000× the working concentration, using deionsed water or ethanol as required. In order to avoid inactivation due to the heat in the autoclave, a 0.22μm filter was chosen to sterilize the antibiotic stock that was dissolved in water. All the stocks were stored at -20°C.

The working concentration of the antibiotics was Carbenicillin 100μg/ml (water), Chloramphenicol 34μg/ml (ethanol) and Kanamycin 50μg/ml (water).

2.4 Other reagents

Table 2.2 reagents

Name	Supplier	Stock Conc	Working Conc
IPTG*	MELFORD	1M	0.2-1mM
X-gal		20mg/ml in N,N' –dimethylformamide (DMF)	80μg/ml
L-Arabinose*	Sigma	20%(w/v)	0.04%
DTT	MELFORD	1M	1mM

THP solution	Novagen	0.5M	0.1-0.5mM
dNTP	Promega	10mM each	0.1mM
DNAase	Sigma	1,500u	100u/ml

* The stock was sterilized by passing through 0.22μm syringe filter.

2.5 The strains and vectors

The strains and vectors that were used in this study are listed in table 2.3 and table 2.4.

Table 2.3 Strains

Strain	Description	Reference or source
Nova-blue	*endA1 hsdR17(r_{K12}^- m_{K12}^+)supE44 thi-1 recA1 gyrA96 relA1 lac* F' [*proA+B+ lacIqZΔM15* ::Tn*10*(TetR)]	Novagen
BL21 (DE3)	*F*, ompT, hsd*Sß(rß-mß-)*, dcm, gal, *(DE3) ton*	Stratagene
BL21-AI	*F- ompT hsdSB(rB- mB-) gal dcm araB::T7RNAP-tetA.*	Invitrogen
C41	*The strain C41(DE3) was derived from BL21(DE3) [E. coli F- ompT hsdSB (rB- mB-) gal dcm (DE3)], it has at least one uncharacterized mutation, which prevents the cell death associated with the expression of toxic recombinant proteins.*	Miroux and Walker, 1996
C43	*The strain C43(DE3) was further derived from C41(DE3) transformed with the F-ATPase subunit gene and cured, therefore it contains no plasmid*	(Miroux and Walker, 1996)
Kam3 (DE3)	*ΔacrAB*	Morita *et al.*, 1998

Table 2.4 Vectors

Vector	Description	Antibiotic Resistance	Reference or source
PGEM-T easy	*The pGEM -T Easy Vector Systems is convenient systems for the cloning of PCR products. This vector has a 3'terminal thymidine to both ends. These single 3'-T overhangs at the insertion site greatly improve the efficiency of ligation of a PCR product into the plasmids by preventing recircularization of the vector and providing a compatible overhang for PCR products generated by certain thermostable polymerases.*	Ampicillin	Promega
PET21a(+)	*pET-21(a) is a transcription vector designed for expression from bacterial translation signals carried within a cloned insert. A C-terminal His•Tag® sequence is available.*	Ampicillin	Novagen
pACYCDuet™-1	*pACYCDuet™-1 is designed for the coexpression of two target genes. The vector contains two multiple cloning sites (MCS). each of which is preceded by a T7 promoter/lac operator and ribosome binding site (rbs).*	Chloramphenicol	Novagen
pET24a	*These vectors differ from pET-21a only by their selectable marker (kanamycin vs. ampicillin resistance).*	Kanamycin	Novagen

2.6 Polymerase Chain Reaction (PCR)

All the PCRs were conducted in a Eppendorf Mastercycler Gradient 5331 thermal cycler. Two polymerases used in this study, HotstarTag and Proofstart polymerases, both from Qiagen, are described in the following table.

Table 2.5 Hotstart and proofstart Thermostable DNA Polymerase

Characteristic	Resulting DNA ends	5′-3′ exonuclease activity	3′-5′ exonuclease activity
Hotstar Tag	3′ A	Yes	No
Proofstart	Blunt	No	Yes

2.6.1 Oligonucleotide primers

All the oligonucleotide primers in this study were synthesized by Invitrogen and Fisher, at a scale of 25nmol or 50nmol, desalted. Appropriate amount of deionized water was added to resuspend the primers to final concentration of 50pmol/μl. All the primers stocks were kept at -20°C.

The following table is a list of the oligonucleotides that were used in this study:

Table 2.7 primers were used in this thesis

Name	Squence (5′-3′) Bolded sequences indicate restriction endonuclease sites. Underlined sequences indicate start and stop codons.
MtrD NdeI F	**CATATG**GCTAAATTCTTTATCGACCGCCCCATTTTCG
MtrD XhoI R	**CTCGAG**ATATTGTTTATCGTCCGAACCGGTTATACCCG
MtrD BamHI F	**GGATCC**GGCTAAATTCTTTATCGACCGCCCCATTTTCG
MtrD SalI R	**GTCGAC**ATATTGTTTATCGTCCGAACCGGTTATACCCG
MtrD KpnI R	**GGTACC**ATATTGTTTATCGTCCGAACCG
MtrC NdeI F	**CATATG**GGCTTTTTATGCTTCTAAGGCGATGCGTGCG
MtrC XhoI R	**CTCGAG**TTTCGCTTCAGAAGCAGGTTTGGCTTCAG
MtrC BamHI F	**GGATCC**GGCTTTTTATGCTTCTAAGGCGATGCGTGCG
MtrC SalI R	**GTCGAC**TTTCGCTTCAGAAGCAGGTTTGGCTTCAG
MtrC truncate NdeI F	**CATATG**GGCGGGCAGCCTGCGGGTCGG

MtrC hairpin NdeI F	**CATATG**ATCGACAGTTCCACTTATGAAGC
MtrC hairpin XhoI R	**CTCGAG**AATGCGCGAACGGTTCAGATTG
MtrE NdeI F	**CATATG**AATACTACATTGAAAACTACCTTGACCTCTGTTG
MtrE HindIII R	**AAGCTT**TTTGCCGGTTTGGGTATCCCGTTTCAATCCGC
MtrE BamHI F	**GGATCC**GAATACTACATTGAAAACTACCTTG
MtrE KpnI R	**GGTACC**TTTGCCGGTTTGGGTATCCCGTTTCAATCCGC
MtrC SD-link EcoRI R	**GAATTC**TAATAATTCCTCTTATTTCGCTTCAGAAGCAGG
MtrE ATG EcoRI F	**GAATTC**ATGAATACTACATTGAAAACT
MtrC hairpin NcoI F	**CCATGG**AGATCGACAGTTCCACTTATGAAGG
gIII NdeI F	**CATATG**AAAAAACTGCTGTTCGCGATTCCG
MtrR NdeI F	**CATATG**AGAAAAACCCAAAACCGAAGCCTTG
MtrR XhoI R	**CACGTG**TTTCCGGCGCAGGCAGGGATGG

2.6.2 DNA analysis techniques

2.6.2.1 Agarose gel electrophoresis

Molecular grade agarose powder (VWR) and 1x TAE (Tris-acetate-EDTA) buffer were mixed to the desired concentration (1-2%), according to the size of DNA fragments that needed to be analysized, and the mixture was microwaved to totally dissolve the ingrediants. Ethidium Bromide was added to a final concentration of 0.1μg/ml to facilitate visualisation of the DNA following electrophoresis. The molten gel was poured into a casting tray, a comb was fitted into one end of the gel, and the gel left at room temperature to solidify. The comb was removed before running and the gel, which was submerged into 1 x TAE buffer within a running chamber. Each sample was mixed with 6 x DNA loading buffer, which includes glycerol to make the sample deposit in the wells and dye to make the migration of the sample easy to be tracked. A 1kb plus DNA marker (Invitrogen) was loaded into at least one well a lane. A voltage of 6V/cm was applied to the electrophoresis chamber, promoting the migration of the DNA in the sample towards the positive electrode (anode) of the electrophoresis tank. Adequate migration of the DNA can be assessed visually by monitoring the migration of the tracking dye from the loading buffer.

The DNA samples were visualised by placing the gel on an ultraviolet transilluminator and photography was taken of the relevant area of the gel using a gel dock (GENE Genius Bioimaging System, Syngene).

6x DNA Loading buffer

Bromophenol Blue	2.5g/litre
Glycerol	30%

2.6.2.2 Quantification of DNA

The concentration of oligonucleotide DNA was determined by spectrophotomeric analysis in preparation for Isothermal Titration Calorimetry (ITC).

Oligonucleotides, like double-stranded DNA, are most commonly quantified by measuring their absorbance of ultraviolet light at 260 nm. Single-stranded oligonucleotides (ssDNA) dissolved in neutral aqueous solution at a concentration of 33 µg/ml will have an absorbance at 260 nm (in a 1 cm cuvette) of approximately 1.0 unit. An OD value of 1.0 corresponds to approximately 50µg/ml for double-stranded DNA (dsDNA). To determine the concentration of an oligonucleotide (e.g. primer) stock solution, make one to a few dilutions of the stock solution (e.g., 100 - 500 fold) in distilled water or dilute TE buffer [10 mM Tris-HCl, 0.1 mM EDTA (pH 7.0)], measure its (their) absorbance at 260 nm and calculate the concentration using the formula below:

µg/ml of nucleic acid= OD260 x conversion factor

1 OD260 Unit = 50µg/ml for dsDNA

1 OD260 Unit = 35µg/ml ssDNA

$$\text{P mol DNA} = \mu\text{g DNA} \times \frac{pmol}{330\ pg} \times \frac{10^6\ pg}{1\mu g} \times \frac{1}{N}$$

N is the number of nucleotides and 660pg/pmol is the average molecular weight of a ssDNA

$$\text{P mol DNA} = \mu\text{g DNA} \times \frac{pmol}{660\ pg} \times \frac{10^6\ pg}{1\mu g} \times \frac{1}{N}$$

N is the number of nucleotides and 660pg/pmol is the average molecular weight of a dsDNA

2.6.2.3 DNA sequencing

All DNA sequencing was all carried by DBS Genomics, School of Biological and Biomedical Sciences, Durham University on an Applied Biosystems 3730 DNA Analyser.

DNA sequencing is the determination of the precise sequence of nucleotides in a sample of DNA. The most popular method for doing this is called the dideoxy method or Sanger method. To perform the sequencing, the single-strand template DNA is supplied with a mixture of all four normal (deoxy) nucleotides, in ample quantities, and DNA polymerase I.

Because all four normal nucleotides are present, chain elongation proceeds normally until, by chance, DNA polymerase inserts a dideoxy nucleotide (shown as colored letters) instead of the normal deoxynucleotide (shown as vertical lines). If the ratio of normal nucleotide to the dideoxy versions is high enough, some DNA strands will succeed in adding several hundred nucleotides before insertion of the dideoxy version halts the process.

At the end of the incubation period, the fragments are separated by length from longest to shortest. The resolution is so good that a difference of one nucleotide is enough to separate that strand from the next shorter and next longer strand. Each of the four dideoxynucleotides fluoresce a different color when illuminated by a laser beam and an automatic scanner provides a printout of the sequence.

2.6.3 PCR amplification

Various size reactions were conducted in thin wall 0.5ml PCR tubes. 10×buffer, dNTP, primer forward, primer reverse, Q solution, water, polymerase, template were added according to the table below.

Table 2.8 Hotstar Tag

Components	Amount (µl)/reaction	Stock Concentration	Final concentration
10×Hotstar Tag buffer	10	10×	1×
dNTP	2	10mM	0.2mM
Primer Forward	1	50pmol/µl	0.5µM

Primer reverse	1	50pmol/μl	0.5μM
Q solution	20	5×	1×
Hotstar Tag polymerase	0.5	5u/μl	-
Template DNA	Variable	-	100ng-1μg genomic DNA, 1-50μg plasmid DNA
Add water to	100		

Table 2.9 Proofstart polymerase

Component	Amount (μl)/reaction	Stock Concentration	Final concentration
10×proof Start buffer	5	10×	1×
dNTP	1.5	10mM	0.3mM
Primer Forward	1	50pmol/l	1μM
Primer reverse	1	50pmol/μl	1μM
Q solution	10	5×	1×
Proofstart polymerase	1	5u/μl	2.5u/reaction
Template DNA	Variable	-	100ng-1μg genomic DNA, 1-50μg plasmid DNA
Add water to	50		

After mixing all the components according to the above recipes, the tubes were centrifuged for short time and put in the thermal cycler. The program was set according to the different type of polymerases, melting temperature of the primers and the length of the fragments. In general, the annealing temperature should be about 5°C blow the melting temperature and 1 minute of extension time for amplification of a 1kb DNA fragment.

Table 2.10 PCR program for Hotstar Tag polymerase

Initial activation step	**15min**	**95°C**
3-step cycling		
Denaturation	1min	94°C
Annealing	1min	50-63°C
		according to the Tm of primers
Extension	1min/kb	72°C
Number of cycles	30	
Final extension	10min	72°C
End of PCR cycling	-	4°C

Table 2.11 PCR program for Proofstart polymerase

Initial activation step	**5min**	**95°C**
3-step cycling		
Denaturation	1min	94°C
Annealing	1min	50-63°C
		According to the Tm of primers
Extension	1min/kb	72°C
Number of cycles	30	
End of PCR cycling	-	4°C

2.6.4 Purifying the PCR product by Gel Extraction Kit (Qiagen)

After mixing with 6×loading buffer, the PCR product was loaded on a 1-2% electrophoresis agarose gel. When the samples had ran to the appropriate position, the gel was analysised under a UV lamp.

The DNA bands were excised from the gel with a scalpel and put in 1.5 eppendorf tubes. QG buffer from the kit (100µl/100mg) was added, then the tubes were incubated in a 50°C water bath until the gel had totally melted. The mixture was applied to spin column and centrifuged at 13,000rpm for 1 minute. The flow-through was discarded and the collector was

put back to column again. To clean up the unmelted gel, 0.5ml of QG was added to the column, followed by centrifugation for 1 minute. After this, 0.75ml of PE washing buffer was applied to the column and centrifuged to remove the buffer. In order to get ride of the residual ethanol in the membrane, an extra one minute centrifugation was made after discarding the flow-through in the collector. Finally, the column was transferred to a clean 1.5ml eppendorf tube and 35 µl of nucleotidase free water was applied to the membrane of the column to elute the DNA. The DNA was collected by centrifugation for 1 minute at 13,000rpm.

2.7 competent cells

Two types of competent cells were used in this study, according to the requirement of the competency.

Magnesium chloride and Calcium Chloride protocol was used to make fresh competent cell of variant host strains for expression. A single colony was used to incubate 10ml of LB broth. When the OD600 reached 0.5-0.6, the cells were put on ice for 10 minutes, and then harvested at 2000rpm for 5 minutes. After draining the rest of the medium, the cells were re-suspended with 1ml of ice-cold 0.1M magnesium chloride, then transferred to a 1.5ml eppendorf tube. The next step was to collect the cells by centrifugation at 4,000rpm for 30 seconds, which were then resuspended with 1ml 0.1M Calcium Chloride. After the centrifugation, the cells were suspended in 250µl 0.1M $CaCL_2$ and 150µl was used for a single transformation.

Another more complicated method was chosen to make chemically competent cells for cloning. This rubidium chloride protocol gives better transformation efficiencies than calcium chloride procedures for most strains. A single colony was picked to inoculate 5ml of LB broth, which was shaken at 37°C overnight, and 2.5 ml was used to inoculate 250 ml of LB. The cells were grown in 1L flask until A600 was 0.4 to 0.6 (approx. 5-6 hours). The cells were pelletted by centrifugation at 2500rpm for 5 minutes at 4 degrees, and then were gently resuspended in 0.4 volumes (of original culture volume) of ice cold TFB1. For a 250 ml culture, 100 ml of TFB1 was used. The cell suspension was then incubated on ice for 5 minutes at 4 degrees followed by centrifugation at 2,500rpm for 5 minutes at 4 degrees to

collect. The cells were gently resuspended in 1/25 volume of ice cold TFB2. For 250 ml culture, 10 ml of TFB2 was used. The cells were incubated on ice for 15-60 minutes and then aliquoted as 50 µl /tube. Finally, the tubes were frozen in liquid Nitrogen for storage at -80 degrees.

TFB1 Buffer – 100mM rubidium chloride, 50mM manganese chloride, 30mM potassium acetate, 10mM calcium chloride, 15% glycerol, pH 5.8.

TFB2 Buffer- 10mM MOPS, 10mM rubidium chloride, 75mM calcium chloride, 15% glycerol, pH 6.8.

2.8 Cloning the DNA fragment by pGEMT easy vector

The pGEMT easy vector was chosen for cloning of PCR products in this study because it has a 3'terminal thymidine at both ends. These single 3'-T overhangs at the insertion site greatly improve the efficiency of ligation of a PCR product into the plasmid by preventing recircularization of the vector and providing a compatible overhang for PCR products generated by certain thermostable polymerases.

Hotstar Tag polymerase can produce 3'-A overhangs at the each end of the PCR product, however, Proofstart polymerase can only generate blunt ends to a PCR product, so a following 'adding 3'-A overhangs' step was done before ligating in pGEMT vector.

Table 2.12 Adding 3'-A overhangs

Component	Amount (µl)/reaction	Stock concentration	Final concentration
5X GoTaq® Reaction Buffer	4	5X	1 X
PCR product	1-7		
dATP	0.2mM	20mM	0.2mM
GoTaq polymerase	1		
Add water to	20		

After mixing all the components above, the reaction was put in a thermal cycler at 72°C for 30 minutes. Then it was used for ligation with the pGEMT vector.

The PCR product and pGEMT easy vector ligation reaction was mixed as the following table.

Table 2.13 pGEMT easy vector ligation reaction

component	Amount (μl)	Stock concentration	Final concentration
2 X ligation buffer	5	2 X	1X
PCR product	3		
pGEMT easy vector	1	50ng/μl	2.5 ng/μl
T4 ligase	1	5u/μl	5u/reaction

The ligation reaction was mixed well by short centrifugation and then was put at 4°C to ligate overnight.

The transformation of the ligation was performed by transferring the cloning pGEMT vector to Nova-blue competent cell.

5μl of ligation was gently added into 50μl competent cells on ice, incubated on ice for 30 minutes followed by a 30 seconds heat shock at 42°C. The tube was put back to ice for 2 minutes after heat shock, then 250μl SOC stock was added to the tube and the tube was shaken for 1 hour at 37°C. Finally various amount of the reaction was spreaded on the plates that contained 100μg/ml carbenicillin. After 16 hours incubation at 37°C, the positive colonies were checked by PCR.

Because the insertion of the PCR product interrupts the coding sequence of β-galactosidase, recombinant clones can be identified by color screening on indicator plates. White colonies are always produced by clones containing PCR products and blue ones can result from no insertion or PCR fragments that are cloned in-frame with the lacZ gene.

To achieve the blue-white screen, 10μl of 1M IPTG and 50μl 20mg/ml X-gal were spreaded onto the carbenicillin plate. Before transformation reaction was applied, the plate was incubated in 37°C for 1 hour, in order to reduce the number of false positive colonies.

2.9 Restriction Endonucleases digestion

After cloning the PCR fragment into the cloning vector pGEMT, for proper expression, it needs to be ligated into expression vector. First of all, both of the pGEMT plasmid and the expression vector have to be digested with the restriction endonucleases, and digested expression vector and the PCR fragment were connected together by T4 ligase.

The restriction endonucleases digestion was performed according to the following reaction

Table 2.14 Digestion reaction

components	Various volume(μl)		
10 X buffer	2	5	8
BSA	0.2	0.5	0.8
Enzyme 1	1	2	3
Enzyme2	1	2	3
Recombinant plasmid or expressing Vector	10	20	30
ddH_2O	5.8	20.5	35.2
Total volume(μl)	20	50	80

After mixing all the components by high speed centrifugation for a short time, the reaction was put in a 37°C incubator or thermal cycler for 3-5 hours, followed by incubation at 65°C for 15minutes to inactivate the enzymes. The digestion reactions were analysed by 1% or 2% agarose gel Electrophoresis.

2.10 ligate the PCR fragment to expressing vector

Before ligating the PCR fragment into the correspondent vector, both of them were purified using a gel extraction kit. All the components were mixed in PCR tube according to the following table.

Table 2.15 T4 ligase reaction

Components	Amount (μl)
5 X buffer (Invitrogen)	2
PCR product (after digested and purified)	4-5*
Vector (after digested and purified)	2-3*
45°C 5 minutes, then add	
T4 ligase (Invitrogen)	1
16°C 1.5 hours, followed by 4°C overnight	

* According to the concentration of the fragments. In general, the PCR fragment should be 3 times of vector to increase the efficiency of ligation..

2.11 Transfer the ligation to competent cells

In order to get highly efficient transformation, Nova-blue competent cells that were prepared by the rubidium chloride protocol were normally used at this step. 5μl of the ligation was used for transfermation of 50μl of competent cell, after incubating on ice for 30 minutes; a 45 second heat shock was performed at exact 42°C without shaking. The tube was put on ice for 2 minutes and 250μl of SOC medium was added in. after shaked at 37°C incubator for 1 hour, various amount of the transformation reaction was spreaded on the LB-agarose plates contain appropriate antibiotic. The plates were put in a 37°C incubator and the result was checked after 16 hours.

The positive colonies were analysed by PCR or restriction endonuclease digestion.

The plasmid with correct insertion was abstracted from overnight culture of the cells by using Miniprep Kit (Qiagen or Promega). Then it was transferred into the competent cells of the host strain used for protein expression. The positive colonies were tested again by PCR.

The recombinant strain was then ready for protein expression and purification.

2.12 Recombinant protein expression methods

2.12.1 Overexpression of the recombinant protein

A single colony of the *E.coli* strain containing the desired recombinant plasmid was used to inoculate various amounts of LB broth, with appropriate antibiotic, and shaken at 37°C overnight. 3-5 ml of overnight culture was used to inoculate 1 litre of YT Broth containing antibiotics. Cultures were grown in flasks at 37°C, with 180rpm rotary agitation, until the optical density at 600nm reached middle log phase, for about 0.5-0.6. Then IPTG at various concentrations, ranged from 0.1-0.5mM was added to the culture. According to the genotype of expressing host, 0.2% (w/v) of L-arabinose needs to be added in some cases.

After addition of the inducer, the temperature was adjusted to 25-28°C according to the toxicity of the host. At meantime, and the rotary speed was reduced to 160-180rpm. In the case of soluble proteins, the cells were harvested 3-4 hours after induction. For membrane proteins, at least 5 hours is needed before harvesting, 16 hours of overnight agitation is geenerally applicable.

2.12.2 Preparing the soluble protein Homogenate and cell membrane by centrifugation

2.12.2.1 Extraction of the soluble protein homogenate

The cells were harvested by centrifugation at 6,300rpm for 8 minutes. The cell lysis buffer was used to resuspend and homogenized the cell pellet. A typical lysis buffer was Tris 20mM NaCl 300mM Glycerol 10% pH 7.5, the details of which will be mentioned in the Chapter 4 an 5. Appropriate amount of DNAse I (Sigma, 100u/litre culture) and proteinase cocktail inhibitor tablet (Roche, 1 tablet/12 litre) were added to the cells, which were put on ice for 15 minutes before disruption.

The cells were homogenized by passing the resuspended cells 3 times through the constant cell disruptor, operated at pressure of 15 KPSI, at 4°C. An enriched supernatant fraction containing cytosolic proteins from bacterial cell components was obtained by ultracentrifugation at 43,000rpm for 1 hour. The supernatant from the centrifugation was kept for the subsequent purification.

2.12.2.2 Extraction of the cell membrane

The cells were harvested and disrupted by the same procedure above. The cell homogenate was centrifuged at 18,500rpm for 1 hour to spin down the cell debris and the supernatant that contains cell membrane and cytosolic protein was ultracentrifuged at 43,000rpm for 2 hours to deposit the cell membrane.

The cell membrane from ultracentrifugation was homogenized in membrane resuspension buffer (Tris 20mM NaCl 100-300mM Glycerol 20% pH 7.6-7.8 THP 0.5mM) by passing through thin syringe needle. Finally, the extracted membrane was stored at -70°C, ready for protein purification.

2.13 Recombinant protein purification methods

2.13.1 Immobilized metal affinity chromatography

Immobilized metal affinity chromatography (IMAC) was used primarily in this work to purify polyhistidine tagged recombinant proteins. This is achieved by using the natural tendency of histidine to chelate divalent metals. Chelating Sepharose, when charged with Ni^{2+} ions, selectively binds proteins if complex forming amino acid residues, in particular histidine, are exposed on the protein surface. $(His)_6$ fusion proteins can be easily bound and then eluted with buffers containing imidazole.The basis of the seperation is the different affinity with resin between the 6-Histidine proteins and the proteins from host strain.

The 6×Histidines that cognated to the recombinant proteins were generated by expressing vectors.

A typical purification was done in three steps: binding, washing and elution.

For soluble protein, the Imidazole concentration of the supernatant from the cell homogenate was adjusted to 10mM, loaded into pre-equilibrated nickel chelating columns by peristaltic pumps at a speed of 0.8ml/minute at 4°C. The loaded columns were connected to an AKTA purifier for washing and elution. The washing buffer was normally Tris 20mM NaCl 300mM Glycerol 10% pH7.5-8.0, with various concentrations of Imidazole, ranging from 50mM to 115mM. In this step, a peak at 280nm could be detected due to the contaminant protein from the host. In order to get pure fusion protein, the column would be

washed by washing buffer until the trace returned to the baseline. The elution step was undertaken by high concentration of Imidazole in the elution buffer, usually the washing buffer with 300mM Imidazole. Because of the high affinity binding of both Nickel and Imidazole to the His-tag, the protein bound to resin can be replaced and eluted.

In the case of membrane proteins, a detergent needs to be used to solubilize the cell membrane. The non-ionic detergent Dodecyl-β-D-maltoside (DDM) was adopted for MtrD and MtrE in this work. The cell membrane stock was thawed and the total volume was made up to 50ml/6 liters of culture in membrane resuspending buffer. Then 2% (w/v) of DDM was added and the mixture was gently rotated at 4°C for 1-2 hours until the membrane homogenate was totally clear. After ultracentrifugation for 1 hour at 43,000rpm, and 4°C, the supernatant was loaded on to a pre-equilibrated column via a peristaltic pump. Then the columns were connected to an AKTA purifier and washed with the washing buffer, Tris 20mM NaCl 300mM Glycerol 20% DDM 0.2% pH 7.5-7.8 THP 0.5mM, until the trace at 280nm returned to the baseline. To elute the protein, an Imidazole concentration of 500mM in the washing buffer was used. Protein fractions were collected manually.

2.13.2 Desalting of the protein sample

A HiTrap Desalting column packed with the size exclusion medium Sephadex G-25 superfine was used to perform the buffer exchang procedures in this study. This was accomplished by group separation between high and low molecular weight, that buffer exchange was accompanied by removal of the low molecular weight contaminants.

For buffer exchange, the columns were equilibrated with the ideal (elution) buffer on the AKTA purifier until the salt concentration reached to a stable level. Then 1.5ml/column of protein sample was applied to the column using a syringe (if the volumn was less than 1.5ml, buffer was added to a total volume of 1.5ml), and the flowthough was discarded. Finally, 2ml/colmn of ideal buffer was injected into the coumn to elute. The protein in elution buffer was collected, ready for the next step.

Normally, a desalting step was applied before the ion exchange of protein or the dialysis before setting crystallization trials.

2.13.3 Ion exchange chromatography

Ion exchange chromatography is based on adsorption and reversible binding of the charged sample molecules to oppositely charged groups attached to an insoluble matrix. The pH value at which a protein molecule carries no net charge is called the isoelectric point (pI). When the buffer pH is higher than the pI of the protein molecule, it will carry a negative charge and will bind to an anion exchange column; otherwise, the protein will carry a positive charge and will bind to a cation exchange column. In addition to the pH of the buffer, the ionic strength is also critical for binding and elution of both target and contaminant molecules in ion exchange chromatography. Ion exchange chromatography (IEX) separates biomolecules according to differences in their net surface charge.

A typical Ion Exchange Chromatography includes the following steps: equilibration, sample application, elution and final wash. Before loading the sample, the column is equilibrated with start buffer. Ideally, samples should be in the same conditions as the start buffer. After all the sample has been loaded, the column is washed so that all non-binding proteins have passed through the column (i.e. the UV signal has returned to baseline), conditions are altered in order to elute the bound proteins. Most frequently, proteins are eluted by increasing the ionic strength (salt concentration) of the buffer or, occasionally, by changing the pH. As ionic strength increases, the salt ions (typically Na+ or Cl-) compete with the bound components for charges on the surface of the medium and one or more of the bound species begin to elute and move down the column. The proteins with the lowest net charge at the selected pH will be the first ones eluted from the column as ionic strength increases. Similarly, the proteins with the highest charge at a certain pH will be most strongly retained and will be eluted last. The higher the net charge of the protein, the higher the ionic strength that is needed for elution. By controlling changes in ionic strength using different forms of gradient, proteins are eluted differentially in a purified, concentrated form.

A wash step in very high ionic strength buffer removes most tightly bound proteins at the end of an elution.

In this study, Hi trap Desalting columns were adopted for the buffer exchang of samples before they were loaded to an ion exchange column. The start buffer was normally Tris (or

phosphate) 20mM NaCl 50mM Glycerol 10% with variable pH, detergent was needed when it was membrane protein. After applying the sample to the column, 2 column volumes of start buffer were used to wash the column. The protein elution was started by using a gradient concentration of NaCl in 10–20 column volumes with an up to 0.5 M NaCl in the start buffer. At this step, the elution fractions were collected for analysis. Finally, the coumns were washed with 5 column volumes of 1 M NaCl to elute any remaining ionically bound material.

In this study, ion exchange chromatography was also employed to perform the protein concentration. To achieve this, the protein sample was desalted and loaded on to an ion exchange column, and then it was eluted with a high ionic strength buffer, such as that containing 0.4M NaCl. Because of the sudden increase in the ion strength, the protein was eluted very fast. This technique is especially suitable for concentrating membrane proteins because it doesn't cause detergent accumulation like ultrafiltration spin column do. Ion exchange chromatography can also be used to change the detergent of membrane protein for crystallography studies. After binding the protein to column, wash the column with at least 2 column volume of buffer with ideal detergent first, then elute the protein. This is considered to be the best way to change the detergent of a membrane protein (Bergfors, 2002).

2.13.4 Gel Filtration Chromatography

Gel filtration separates molecules according to differences in their size as they pass through a gel filtration medium packed into a column. Unlike ion exchange or affinity chromatography, molecules don't bind to the chromatography medium so buffer composition does not directly affect the resolution. Consequently, a significant advantage of gel filtration is that conditions can be varied to suit the type of sample or the requirements for further purification, analysis or storage without altering the separation.

To perform a separation, the packed bed is equilibrated with buffer which fills the pores of the matrix and the space in between the particles. Then the sample is applied to the column. When buffer and sample move through the column, molecules diffuse in and out of the pores of the matrix. Smaller molecules move further into the matrix and so stay longer on the column.

Hiload 16/60 superdex 75 prep grade and Hiload 16/60 superdex 200 prep grade were adopted in this study according to the size of molecules that needed to be separated. A typical gel filtration run was to equilibrate the column with more than 3 column volumes of buffer, which had been filtered and degassed right before use. According to the manufactural user manual, no more than 5 ml of sample was loaded onto the column using a superloop, and then the run was started with the same buffer, at a constant flow rate. The fractions of each peak were collected and analysized by SDS-PAGE electrophoresis.

Because of the need to apply a huge volume of washing buffer, gel filtration chromatography was only used during the soluble protein purification in this study. The detailed buffer conditions of each protein will be discussed in the following chapters.

Gel filtration chromatography had also been used in this study to determine the size of the protein molecules. Unlike electrophoretic techniques, gel filtration provides a means of determining the molecular weight or size of native proteins under a wide variety of conditions of pH, ionic strength and temperature, free from the constraints imposed by the charge state of the molecules. Molecular weight determination by gel filtration can be made by comparing an elution volume parameter, such as Kav (Kav= $\frac{Ve-Vo}{Vt-Vo}$) of the substance of interest, with the values obtained for several known calibration standards. Vo, void volume, is the interstitial space of the gel particle, which is the elution volume of a very large or excluded molecules (Dextran blue in this study) that do not enter the gel pore; Ve is the elution volume of the sample and Vt represents the sum of the internal and external volume within the beads. A calibration curve is prepared by measuring the elution volumes of several standards, calculating their corresponding Kav values (or similar parameter), and plotting their Kav values versus the logarithm of their molecular weight. After the standard curve is made, apply the sample by exact the same condition to determine the elution volume (Ve). Calculate the corresponding Kav for the component of interest and determine its molecular weight from the calibration curve.

2.14 Recombinant protein analysis

2.14.1 SDS-PAGE

In this study, SDS-PAGE (sodium dodecyl sulfate polyacrylamide gel electrophoresis) was used to test the expression and purification of the protein. The commercial resources of pre-cast gels from Invitrogen were adopted to perform the electrophoresis. Depending on the size of the protein of interest and the degree of separation, 12% NuPage Bis-Tris gel or 4%-12% NuPage Bis-Tris gel were chosen.

The gels were clamped vertically into a running tank. MOPS running buffer was added in until the both anode and cathode were submerged, as well as all the wells of the gel. Before loading the samples were mixed with 4x LDS loading buffer (NuPage, Invitrogen), then they were loaded into the wells carefully, together with 10μl of SeeBlue marker (from Invitrogen) to one lane. A voltage of 200v was applied to the tank until the dye from the loading buffer had shifted to the bottom of the gel.

The protein bands were visualised by staining in Coomassie blue for 20 minutes and destained with destained buffer via several washes.

For separation of some smaller proteins, such as the hairpin domain of MtrC, a home made 18% gel was used. The gels were made by using glass slides and the stand from BIO-RAD.

10x MOPS Running Buffer

MOPS	104g
Tris base	61g
SDS	10g
EDTA	3g
dH_2O	up to 1 litre

Coomassie Blue stain

Methanol	40% v/v
Acetic acid	10% v/v
Coomassie Brilliant Blue R-250	0.1% w/v
dH_2O	50% v/v

Coomassie blue destain

Methanol	40% v/v
Acetic acid	10% v/v
dH_2O	50% v/v

2.14.2 Blue Native Electrophoresis

BN-PAGE has been developed for the separation of membrane proteins and multiprotein complexes in the molecular mass range from about 10kDa to 10,000kDa. The basic principles of BN-PAGE is that Coomassie blue G250 is added to the membrane protein and this dye seems to bind to surface of all membrane protein but not to all water-soluble proteins. Binding of a large number of anionic dye molecules is the basis for the Blue Native Electrophoresis.

Table 2.16 buffers and stock solution for BN-PAGE

solution	composition
Deep Blue Cathode buffer	50mM Tricine, 7.5mM Imidazole, 0.02% Coomassie blue G250
Slightly blue cathode buffer	50mM Tricine, 7.5mM Imidazole, 0.002% Coomassie blue G250
Gel buffer (3×)	75mM Imidazole/HCl, 1.5M 6-aminocaproic acid
Anode buffer	25mM Imidazole
AB-mix (30%)	Commercial product from Sigma
5% Coomassie blue G250	Suspended in 500mM 6-aminocaproic acid

Table 2.17 Gradient gel preparation

	Sample gel	Gradient separation gel	
	4%	6%	15%
AB-mix	0.5ml	4ml	8.5ml
Gel buffer (3×)	2ml	6.7ml	5.6ml

Glycerol	-	-	4.25ml (80%)
Water	3.5ml	9.2ml	-
APS (10%)	50µl	110µl	100µl
TEMED	5 µl	12µl	10µl
Total volume	6ml	20ml	18ml

The separation gel was casted at 4°C but then was left at room temperature to polymerize. The gradient was accomplished by a gradient mixer. The sample gel was casted at room temperature.

BN-PAGE was performed at 4°C. The deep blue cathode buffer B was used to fill the electrophoresis tank after clamping the gel vertically. The samples were centrifuged at 10,000g for 15 minutes avoid them to sedimentation; then glycerol, to a final concentration of 15% was added to them to increase the density and to facilitate the application of the samples. After loading the samples, a voltage of 100V was maintained until the samples had moved into the sample gel; then the voltage was increased to 200V. After about one-third of the running distance, the cathode buffer was changed to slightly blue cathode buffer. This optional buffer exchange improves detection of faint bands. After the samples ran to the desired distance, the run was stopped and the gel was dehydrated and analysized.

2.14.3 Mass Spectrum

All the mass spectrum analyses were performed in the department of Chemistry, University of Durham, by Mr Matthew Burton, in a Thermo Finnigan LTQ FT in ES+in ES+mode spectrometer. The following experimental parameters were used to record mass spectra, 0.1mg/ml MtrR was dialysized to 10mM ammonium bicarbonate buffer.

2.14.4 Protein concentrating

Several methods of concentrating protein were employed according to the requirement of the experiments. The ultrafiltration spin column (Vivascience) was the commonest way to concentrate the protein, if it was a soluble protein or membrane protein that did not require a low detergent concentration.

Ultrafiltration is a convective process that uses anisotropic semi-permeable membranes to separate macromolecular species and solvents primarily on the basis of size. It is particularly appropriate for the concentration of macromolecules and can also be used to purify molecular species or for solvent exchange. Ultrafiltration is a gentle, none denaturing method that is more efficient and flexible than alternative processes.

In order to maximize the recovery of the protein, the size of the membrane needs to be around two-thirds of the size of the protein. A 30kDa membrane was used for MtrE (MW 30kDa) and a 100kDa membrane for MtrD (MW 114kDa).

Because, in membrane protein solutions, there is always a lot of detergent molecules that bind to the protein, which are difficult to remove, the use of ultrafiltration columns can cause the accumulation of the detergent in the liquor. Ion exchange was used to concentrate the protein when there was a requirement for the detergent concentration to be maintained or lowered, and when very high concentrations of the protein was not necessary. The protein was desalted and loaded onto a pre-equilibrated ion exchange column, 2 column volumes of buffer with the desired concentration of detergent was applied to the column. Finally, the protein was eluted at a high salt concentration buffer. This enabled the protein to be concentrated at same time without increasing the detergent concentration.

2.14.5 Bradford protein assay

The Coomassie Plus - The Better Bradford™ Assay Kit from Pierce was adopted throughout this study for determining the concentration of proteins. The Coomassie Plus Kit is a quick and ready-to-use coomassie-binding, colorimetric method for total protein quantitation. This modification of the well-known Bradford method greatly reduces the tendency of coomassie reagents to give nonlinear response curves by a formulation that substantially improves linearity for a defined range of protein concentration. In addition, the Coomassie Plus Reagent results in significantly less protein-to-protein variation than is observed with other Bradford-type coomassie formulations.

To perform the test, combine a small amount of protein sample with the assay reagent, mix well, incubate briefly and measure the absorbance at 595 nm. Protein concentrations are

estimated by reference to the absorbances obtained for a series of standard protein dilutions, which are assayed alongside the unknown samples.

2.14.6 Western blot

The western blot is an analytical technique used to detect specific proteins in a given sample. It uses gel electrophoresis to separate native or denatured proteins by the length of the polypeptide. And then the proteins are transferred to a membrane, where they are detected using probed specific antibody.

2.14.6.1 Buffer used in this study

Table 2.18

A.	**Transfer buffer**	
	(fresh made)	
	Glycine	2.9g (≈39mM)
	Trizma base	5.8g (≈48mM)
	SDS	0.37g
	Methanol	200ml
	Add water to	1000ml
B.	**ELISA washing buffer**	
	Phosphate stock	30ml
	NaCl	4.38g
	Tween 20	250ul
	Add water to	500ml
C.	**Phosphate stock(PH≈7.4)**	
	KH_2PO4	2.586g
	K_2HPO4	14.12g
	Add water to	400ml

2.14.6.2 Western blot procedure

Firstly, a SDS-PAGE gel of the protein samples was ran, and then the gel was soaked in transfer buffer for 15 to 30 minutes. At same time, a piece of PVDF membrane that was slightly bigger than the gel was cut and a marker was made at the corner. The membrane was soaked in methanol for 30 seconds followed by proper wash by deionized water. Finally the membrane was soaked in transfer buffer for 15 minutes, as well as the nylon sponges and the filter paper that were used for the transfer.

The apparatus was assembled as the following order from Anode to Cathode: nylon sponge, filter paper, gel, PVDF membrane, filter paper, nylon sponge. The bubbles between the layers need to be gently removed.

The transformation was performed by using a potential of 180mA for 1.5 hours.

After the transformation finished, the membrane was washed with washing buffer for 15 minutes, then the washing buffer was carefully Pipetted out and blocking buffer (washing buffer with 3% of Bovine Serum Albumin) was added in. The blocking was done by gently shaking at room temperature for one hour and overnight at 4°C

The blocked membrane was washed with washing buffer 3 times at room temperature, for 5 minutes each. The first antibody, mouse anti 6His monoclonal antibody (sigma, 1:3000 diluted with washing buffer) or mouse anti S-tag (a fusion peptide tag derived from pancreatic RNase A that is widely used in protein expression applications) monoclonal antibody (novagen, 1:5000 diluted with washing buffer) was added to the membrane and shaked at room temperature for 1 hour. Followed by three times 10 minute washes with washing buffer, the second antibody was added to the membrane. The goat anti mouse IgG (Sigma), conjugated with an Alkaline phosphatase, was diluted to 1:5000 before use. After allowing the reaction to proceed for one hour with the second antibody, the membrane was washed 3 times with washing buffer.

Finally, the chemiluminesence detection method was used: 1ml of Immune-star substrate (Bio-Rad) was added to a clean square Petri dish onto which the membrane was put, then another 1 ml was added on the top surface of the membrane, so that the substrate could react with the membrane properly. The reaction was left for 5 minutes, and then the membrane was

placed between 2 pieces of Saran film, and safely attached to the autoradiographic cassette. Finally, the blot was exposed to a X-ray film in the dark room for different times until optimal signals were produced.

2.15 Biochemical Assay

2.15.1 Antimicrobial susceptibility assays

The Minimum Inhibitory Concentration (MIC) of drugs was determined using 96 well microplates with various drugs (Penicillin G, Tetracycline, erythromycin, nafcillin) at different concentrations.

The fresh plates containing chlorampenicol (34mg/ml) were made for growth of the strains to be tested. A single colony was picked and used to inoculate LB broth supplemented chlorampenicol and shaken overnight at 37°C.

A 0.3 ml overnight culture was used to inoculate 30ml of LB broth with supplemented chlorampenicol, which was shaken at 37°C until the optical density at 600nm(OD_{600}) had reached to 0.3-0.5, then Isopropyl β- D -1-thiogalactopyranoside (IPTG) was added to final concentration of 1mM. After induction, shaking was continued for 2 to 3 hours.

The cell was adjusted to 3×10^6 cfu/ml (when A_{600}=0.1, the colony forming units is 1×10^8/ml).

The 96 well MIC microplates were prepared by adding each antibiotic in triplicated to three rows. To the first column, 40ul antibiotic solution of the highest concentration was added, and then the rest of the wells each were filled with 20ul LB broth containing chlorampenicol. A 20ul from the first well was pipetted and mixed with second one, then a 20ul from second well was taken and mixed with the third well, continue diluting all the wells were continued diluting like these to make 1/2 serial dilution.

100ul cells of 3×10^6 cfu/ml was added to each well and mixed well with the antibiotic solution. The final colony forming unit of each well was 5×10^5 cfu/ml.

All the plates were checked after incubated at 37°C for 20 hours. The smallest concentration of antibiotic that could inhibit the growth of the cells is the minimum inhibitory concentration.

2.15.2 Growth curve

The recombinant strains of Kam3(DE3)[pACYC], Kam3(DE3)[pACYC/MtrD], Kam3(DE3)[pACYC/MtrC,MtrD], Kam3(DE3)[pACYC/MtrC,MtrD,MtrE], Kam3(DE3)[pACYC/MtrD,gIII MtrC hairpin], Kam3(DE3)[pACYC/MtrE,gIII MtrC hairpin] of table 4.1 were used in this study.

Fresh plates and overnight cultures were prepared in the same manner as for MIC tests. A 0.3ml of each overnight culture was used to inoculate 30ml of 2×YT broth (containing 34mg/ml of chlorampenicol), and then was shaken at 37°C until optical density at 600nm had reached to 0.3-0.5, and then Isopropyl β- D -1-thiogalactopyranoside (IPTG) was add to final concentration of 1mM. After induction, shaking was continued for 3 hours.

Each recombinant strain was diluted with 2×YT broth, containing 34μg/ml chlorampenicol, to an OD_{600} 0.1. Four test tubes were set for each strain, three of them were added appropriate amounts of the test drugs, while the last one was without test drug and served as a control of normal growth.

All the tubes were shaken violently at 37°C. The OD_{600} was determined by spectrometer every 30 minutes.

2.16 *in vitro* protein interaction analysis

2.16.1 Pull-down assay

2.16.1.1 How does the pull-down assay work?

According to the schematic diagram blow, the pull-down assay is performed by two kinds of proteins, one is the bait protein, which fuses with a 6-histidine tag that can be trapped by Nickel-NTA sepharose, the other one is the prey protein, it fuses with a fusion tag (eg. an S-tag, which is a 15aa peptide with the sequence of KETAAAKFERQHMDS) that can be detected by a specific monoclonal antibody.

After mixing these two kinds of protein together for some time, Nickel-NTA sepharose is added in the mixture. Because of the strong affinity of resin-bound Ni for the 6 consecutive

histidine (his) residues of the tag on recombinant proteins, the bait protein binds to the Nickel agarose. If the prey protein can interact with the bait protein specifically, it will not be washed away from the bait protein easily, so there will be a certain amount of bait-pray protein complex that exists in the mixture. When the poly-histidine tag of the bait protein is trapped by nickel agarose and after washing properly, the recombinant protein is eluted and analyzed. If the fusion tag of the prey protein can be detected, that means the prey protein does from a stable complex with the bait protein.

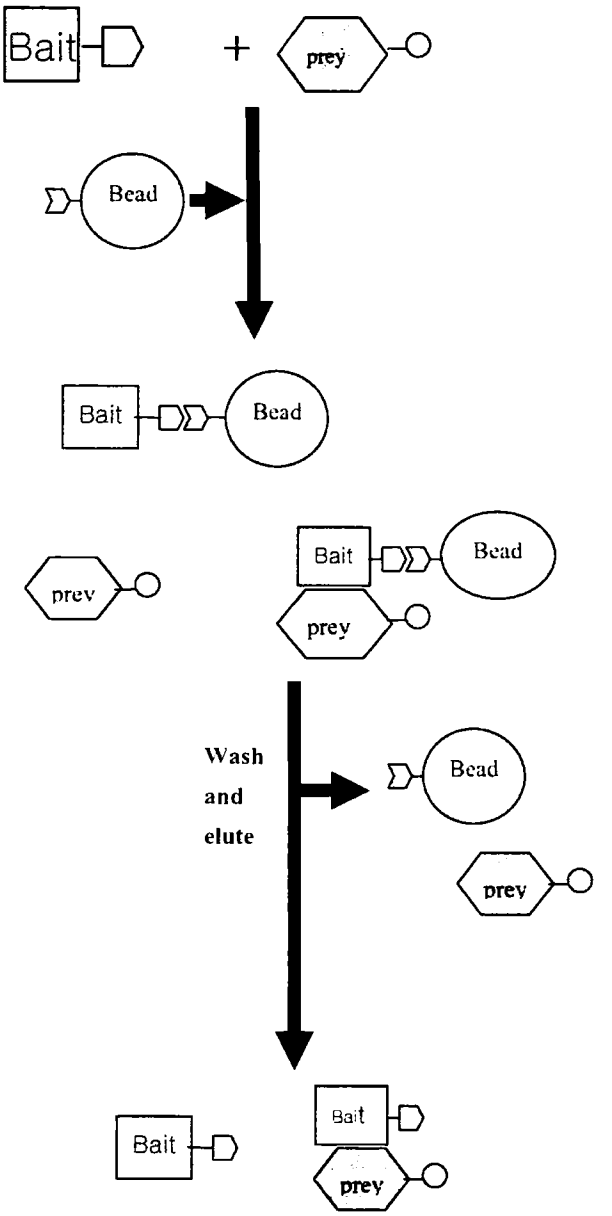

2.16.1.2 Construction of the proteins that were used in pull-down assay

The strains that were used in pull-down assay.

Table 2.19

The interaction between	Bait protein	Prey protein	Constructs were used to produce pray protein
MtrD(IMP) and MtrC(MFP)	MtrD-Histidine$_6$	MtrC-S·tag	Bl21(DE3)[pACYCDuet-MtrC(NdeI +XhoI)]
MtrE(OMP) and MtrC(MFP)	MtrE-Histidine$_6$	MtrC-S·tag	Bl21(DE3)[pACYCDuet-MtrC(NdeI +XhoI)]
MtrD(IMP) and MtrE(OMP)	MtrD-Histidine$_6$	MtrE-S·tag	Bl21(DE3)[pACYCDuet-MtrE(NdeI +KpnI)]

2.16.1.3 Detect the interaction between the proteins by Pull-down assay

The Pull-down assay was performed according to the following procedure.

Pure proteins with a C-teminal histidine tag, which eluted from the Nickel chelating columns in the previous description, were used as bait protein in this study. In order to reduce the effect of the high concentration of imidazole in the protein samples, desalting was performed by Hitrap desalting columns, by which proteins were exchanged into buffer, Tris 20mM NaCl 300mM Glycerol 10% DDM 0.1% pH 7.5.

The crude membrane fraction of the prey protein, was extracted according to the 2.12.2.2. They were divided into separate tubes that contain the membrane from 2-liter cell cultures each.

The membrane of the prey protein was made up to 20ml with buffer above and solubilised with 0.2g DDM (1%, w/v) for 1 hour. Then 2ml of purified 6-Histidine fusion bait

protein from above was added to the prey protein solution and mixed with gently rotation at 4°C for 1 hour.

After adjusting the Imidazole concentration of the bait and prey protein mixture to 10mM, it was loaded onto 1ml Ni-chelating HP column with a peristaltic pump at 4°C.

To get ride of the non-specific binding of the prey protein with Nickel agarose beads, a negative control was set at the same time. One tube of the prey protein was solubilised by exactly the same procedure as above, except 2 ml of buffer was added instead of bait protein.

Both the test and negative control columns were connected to an AKTA purifier and washed with 30ml of washing buffer (Tris 20mM NaCL 300mM Glycerol 10% Imidazole 115mM DDM 0.1% pH 7.5), then eluted with the same buffer with 300mM Imidazole.

The elutions of both the test and the negative control were analysed by SDS-PAGE electrophoresis and Western-blotting using antibodies against the different fusion tags.

2.16.2 Protein-Protein cross-link analysis

Cross-linking is the process of chemically joining two molecules by a covalent bond. Cross-linking reagents contain reactive ends to specific functional groups (primary amines, sulfhydryls, etc.) on proteins or other molecules. Several chemical groups that may be targets for reactions in proteins and peptides are readily available, allowing them to be easily conjugated and studied using cross-linking methods.

In this study, two different crosslinkers were employed in analysing the interaction of all the components of Mtr system, DMA (Dimethyl adipimidate•2 HCl) and EGS (Ethylene glycolbis (succinimidylsuccinate)). The spacer arms of DMA are 8.6Å and EGS are 16.1 Å. Because both of them are reactive towards amines, there is a requirement that there are no primary amines in the buffer. Before the cross-linking analysis, all the protein samples were exchanged into phosphate buffer by dialysis or ion exchange chromatography. The DMA and EGS stock solution were made freshly before use, with water and DMSO respectively to concentration of 50mM and 100mM. The concentration of the proteins was determined and a 20 fold molar excess of the cross-linker was added to them. The reactions were left at room temperature for 60 minutes.

At last, the reactions were mixed with loading buffer; DTT, to a final concentration of 10mM, was added in the reactions, which were boiled for 5 minutes before applying to a 4-12% Bis-Tris Nu-PAGE gel (Invitrogen) for electrophoresis.

2.16.3 Isothermal Titration Calorimetry (ITC)

ITC measurements were carried out at 25°C using a VP-ITC MicroCalorimeter (MicroCal). This instrument is equipped with a 1.437-ml cell and a 300μl syringe.

Because MtrD and MtrE were in Tris 20mM NaCl 300mM Glycerol 10% pH 7.5 containing 0.1% DDM, it was necessary to add DDM to N-terminal truncated MtrC and MtrC hairpin proteins, and then to dialyse in different dialysis cassettes at same time with MtrD or MtrE respectively against the same buffer above. After dialysis, the concentration of each protein was determined using Bradford Protein assay kit.

In the experiments for the interactions of the MtrR with peptides and Penicillin G, MtrR was dialysed against the buffer, which was then used to dissolve the peptides. In the case of Penicillin G, MtrR was dialysed against the buffer Na_2HPO_4 20mM NaCl 300mM Glycerol 10% pH8.0. The buffer outside the dialysis cassette was used to dissolve the substrates to the appropriate concentration, and they were used to titrate into the protein. When testing the interaction of MtrR with its operator DNA, the annealing was carried out by mixing equimolar amounts (100μM) of each oligonucleotide in annealing buffer (Tris-HCl 10mM, $MgCl_2$ 0.5mM pH8.0). The mixture was incubated at 95°C for 5 minutes, followed by slow cooling to room temperature. Both DNA and MtrR were subsequently dialyzed in buffer Tris 20mM NaCl 300mM Glycerol 10% pH8.0. The MtrR was placed in the cell and titrated with the DNA fragment.

Because MtrD and MtrE normally have a lower concentration than the soluble N-terminal truncated MtrC and MtrC hairpin proteins, the MtrD and E were placed in the sample cell whilst the soluble proteins were placed in the syringe for the titration. In the case of MtrD and MtrE, MtrE was used to titrate into MtrD.

Typically, all the proteins and substrates samples were degassed prior to ITC measurements. An experiment generally involved using a single 2μl and a series of 8μl injections of protein or substrates into the protein solution. All data were corrected by using

the heat changes arising from injection of proteins into buffer before data analysis with ORIGIN software (MicroCal).

2.17 Structural study

2.17.1 Circular Dichroism

Circular Dichroism (CD) is observed when optically active matter absorbs left and right hand circular polarized light slightly differently. It can be used to help determine the structure of macromolecules (including the secondary structure of proteins and the handedness of DNA).

Because the measurement of CD is complicated by the fact that typical aqueous buffer systems often absorb in the range where structural features exhibit differential absorption of circularly polarized light, the proteins buffer needs to be changed to appropriate one. The protein concentrations required for performing CD spectroscopy was 1-6μM and the protein samples were dialyzed against Tris-sulfate NaF 300mM pH7.5 overnight. The same NaF buffer was used to dilute the protein samples, because this has low absorbance. CD spectra were recorded using a Jasco J-810 spectropolarimeter from 180 to 260nm with a 0.2cm path length quartz cuvette. Each scan is the mean of three accumulations. The data were analysised by on-line software, DICHROWEB for Line Circular Dichroism Analysis, which is based at the School of Crystallography, Birkbeck College, University of London.

2.17.2 Protein crystallography

Crystallography is an important experimental science for determining the arrangement of atoms in solids. Obtaining crystals is currently the bottleneck in determining the structure of macromolecules by crystallography, especially in the crystallization of membrane proteins, which have distinct biochemical and biophysical properties from soluble proteins.

Because membrane proteins are embedded within the lipid bilayer and contain both a hydrophilic surface exposed to the solvent and a hydrophobic region buried within the lipid bilayer. A suitable detergent, such as deodecyl-β-D maltoside (DDM), is needed to obtain membrane protein from lipid bilayer,

Obtaining sufficient quantities of a membrane protein is a basic requirement to proceed with crystallization trials, a condition that allows the protein to be concentrated is also needed. As described previously, Immobilized Metal Affinity Chromatography (IMAC) and Ion Exchange chromatography were used to purify the two proteins, MtrD and MtrE, which were tried in crysatllization trials in this study. Basically, the preparation of the protein samples for crystallography was accomplished by overexpression; membrane extraction; membeane solubilisation; initial purification by Immobilized Metal Affinity Chromatography (IMAC); concentrating by ion exchange chromatography; dialysis overnight; and finally, concentrating using ultrafiltration spin columns. At last the protein concentration was checked using a Bradford Protein Assay kit and precessed to crystallization trials.

Two kinds of crystallization methods were adapted in this study, hanging drops and sitting drops. The hanging drops were set mainly for sparse matrix screens and additive screens for the purpose of saving protein samples. Normally, 1ml of precipitant solution was transferred to each reservoir, then 1μl of protein sample and 1μl of precipitant solution from the reservoir was mixed on the siliconized glass cover lid, at last the lid was screwed on the reservoir. The sitting drops were used in the optimizing screens. After transferring 1ml of precipitant solution to a reservoir, a plastic microbridge was put in reservoir. 5μl of protein sample was then mixed with 5μl of precipitant solution from the reservoir. A glass cover was then applied to seal the reservoir.

To check the diffraction of the crystals, the crystals were picked up by loops and frozen in liquid nitrogen. The diffraction of the crystals was checked at the European Synchrotron Radiation facility (ESRF) by Dr Xueyuan Pei, University of Cambridge.

Chapter 3 Crystallography study of the IMP MtrD and the OMP MtrE

3.1 Cloning, expression, purification and crystallization of the outer membrane protein MtrE

3.1.1 Cloning the *mtrE* in pET21a expression vector

A pair of primers, MtrE forward and MtrE reverse, which ware designed according to the multi-cloning site of the pET21a vector and the 5' and 3' ends of the *mtrE* sequence, were used to amplify the *mtrE* fragment. The start codon was supplied by the 5' *NdeI* restriction site and the stop codon was supplied by pET21a vector, in stead of by the reverse primer.

The following Hotstar polymerase PCR programme was used to amplify the gene fragment of *mtrE*. after 15mintues of initial activation, the annealing temperature was 60°C and run for 30 cycles. Because Hotstar polymerase has terminal transferase activity, which means it can add a 3' hanging A tag, there is no special step needed except a 10 minutes final extension at 72°C.

Figure 3.1 PCR amplification of *mtrE*

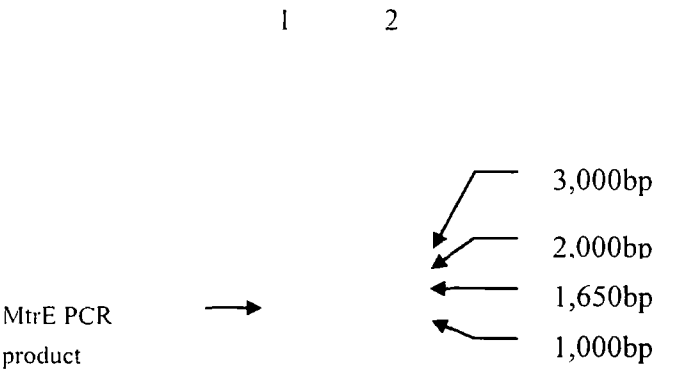

Lane1: Amplified *mtrE* gene

Lane2: 1kb DNA ladder (Invitrogen)

The PCR product was purified from the gel using a Gel Extraction Kit, then it was ligated into the pGEM-T easy vector by T4 ligase at 4°C overnight. The whole reaction was transferred to Nova-blue competent cell afterwards and white colonies were picked and tested by PCR. The positive ones were used to inoculate an overnight culture. The plasmid was extracted the next morning from the overnight culture and was digested with *NdeI* and *HindIII* for 5 hours at 37°C.

Figure 3.2 pGEM-T easy-*mtrE* digested by *NdeI* and *HindIII*

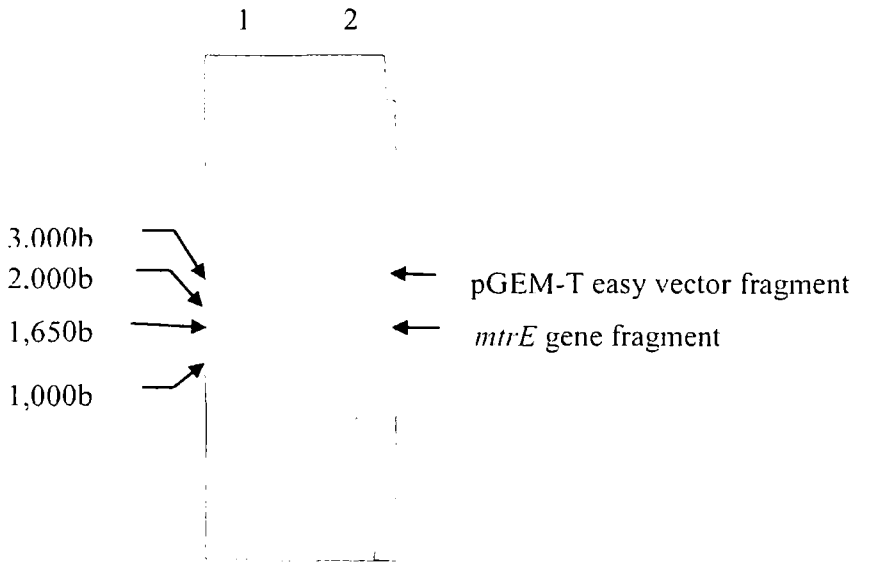

Lane1: 1Kb DNA ladder (Invitrogen)

Lane2: pGEM-T easy-MtrE digested by NdeI and HindIII

After being purified with a Gel Extraction Kit, the 1.5 Kb *mtrE* gene fragment was ligated into pET21a vector, which had been digested with *NdeI* and *HindIII* with T4 ligase. The ligase reaction was transformed to Nova-blue competent cell. White colonies were picked and were tested by PCR. The positive plasmid was extracted from the overnight culture and confirmed by DNA sequencing; at last was transferred to C43(DE3) competent cells. One colony was picked express MtrE.

3.1.2 Overexpression of MtrE

One colony of C43/pET21a-mtrE (NdeI+HindIII) was used to inoculate 50ml of LB broth with 100μg/ml Carbenicillin (final concentration), which was cultured overnight. 3ml of overnight culture was used to inoculate 1 litre of YT broth with 100μg/ml carbenicillin. 12 litres of culture were usually made for purifying the protein. The culture was induced by 0.5mM IPTG (final concentration) when the OD reached 0.6-0.7. Then the temperature was decreased to 25°C and the rotatation speed was changed from 200rpm to 180rpm. The cells were harvested 5 hours after induction.

3.1.3 Purification of MtrE by IMAC

The cell membrane was extracted as described before and then homogenized in the membrane resuspension buffer (Tris 20mM NaCl 200mM Glycerol 20% THP 0.5mM pH7.8). Before solublizing the membrane with DDM, one tablet of proteinase inhibitor was added for the membrane from every 6 liters cells. After solublization with DDM and being ultracentrifuged, the soluble fraction was loaded onto a pre-charged Ni-chelating column (1column/fraction from 6 liters of cells).

The column was connected to an AKTA purifier and washed with washing buffer 1 (Tris 20mM NaCl 300mM Imidazole 50mM Glycerol 20% DDM 0.2% THP 0.5mM pH 7.8) first, followed by washing buffer 2 (Tris 20mM NaCl 300mM Imidazole 100mM Glycerol 20% DDM 0.2% THP 0.5mM pH7.8), then washing buffer 3 (buffer 2 with higher salt concentration), finally, the MtrE was eluted with elution buffer (buffer 1 with 500mM Imidazole).

Figure 3.3 SDS-PAGE gel of MtrE after purified by Ni-chelating coumn

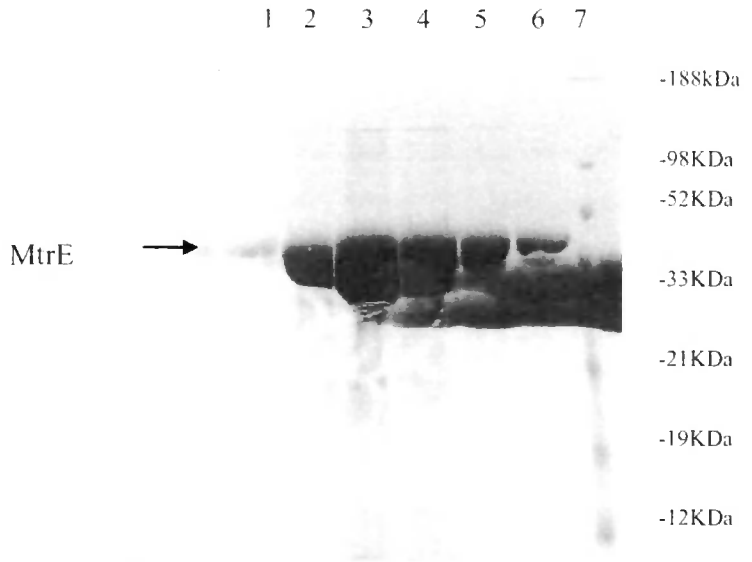

Lane1-6: MtrE fractions from IMAC (20μl/lane)

Lane7: Seeblue marker (Invitrogen)

3.1.4 Crystallization of MtrE

X-ray crystallography enables us to visualize protein structures at the atomic level and enhances our understanding of protein function. Specifically we can study how proteins interact with other molecules, how they undergo conformational changes. Because the diffraction from a single protein molecule is too weak to measure, we use an ordered three-dimensional array of molecules, in other words a crystal, to magnify the signal.

3.1.4.1 Protein preparation

Before setting up crystallization trials, the buffer condition for MtrE was changed and then the protein was concentrated by cation exchange chromatography.

Table 3.1 Buffers for concentrating the MtrE by Ion exchange chromatography

	BufferA1	BufferB1
Tris	10mM	10mM
NaCl	50mM	500mM
Glycerol	10%	10%
DDM	0.1%	0.1%
THP	0.5mM	0.5mM

PH 7.8 7.8

Figure 3.4 SDS-PAGE gel of MtrE after being concentrated by Cation exchange chromatography

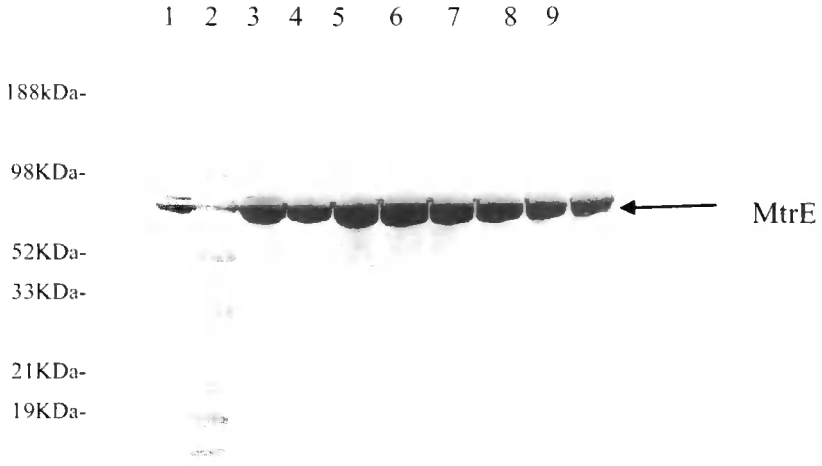

Lane1: Seeblue Marker (Invitrgen)

Lane2-8: MtrE after being concentrated (5μl/lane)

The protein fractions corresponding to Lane2-9 of the above gel were desalted, and the buffer was changed to Tris 10mM NaCl 100mM Glycerol 10% DDM 0.1% THP 0.5mM pH7.8. Then protein sample was dialysized against the same buffer above by dialysis cassette (Pierce). Finally, the protein was concentrated to 5mg/ml using a 30KDa ultrafiltration spin column. After determining the protein concentration with Bradford protein assay kit, the protein sample was used for crystallization trials.

The protein was run on a Blue-Native gel to check the homogeneity of MtrE;. from the Blue-Native gel figure 3.5, MtrE forms Trimer in the native state.

Figure 3.5 blue-Native Gel Electrophoresis of MtrD and MtrE

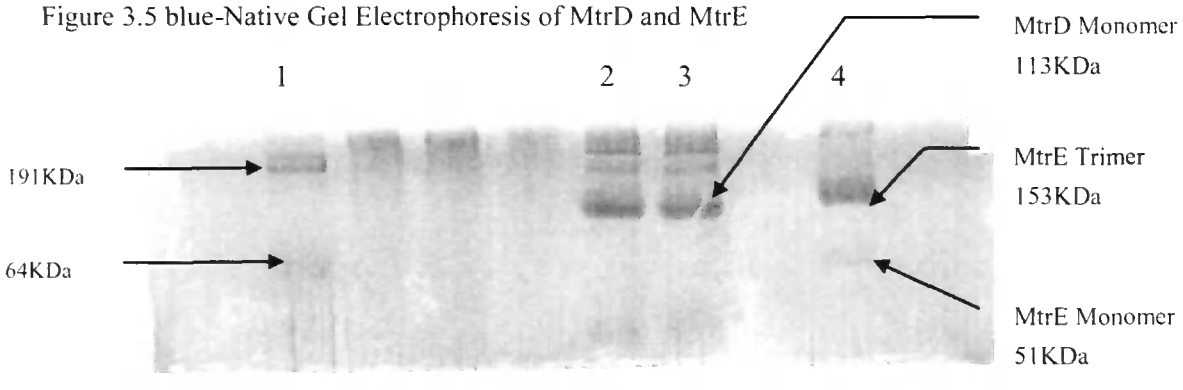

Lane1: SeeBlue Marker (Invitrogen)

Lane2, 3: MtrD

Lane4: MtrE

3.1.4.2 Sparse matrix screen

For the identification of initial crystallization conditions, a flexible sparse matrix screen is used. In the initial screen we examine the roles of pH, precipitant, additives, and temperature.

The MbClass and MbClass II Suites from Nextal, MemStart™ and MemSys™ from Molecular Dimensions were employed in this study to provide an effective initial screening set of crystallization conditions for the membrane proteins MtrE.

The hanging drop method was used for the sparse matrix screen because of the small volumes used, ease of set-up that can be quickly checked. 1ml of solution containing precipitant or another dehydrate agent, from each initial screening kit, was transfer to the 24 wells plates respectively. 1μl of protein sample was dropped onto the cover lid, then mixed with 1μl of the solution from each reservoir, being careful to avoid bubbles and pervasion. Then the lid was screwed onto the correspondence well tightly. After all the wells were done, the plates were moved to the incubator at a temperature of 18°C.

Two weeks after all the trials had been set, one condition was found to produce microcrystals and one small crystal, which is condition No.26 of the MemStart™ kit from Molecular Dimensions. The formulation is 0.2 M tri-sodium citrate 0.1 M Tris 30 % v/v PEG 400 pH 8.5.

This condition was used as a base for optimization of the crystallization conditions.

3.1.4.3 Optimization screen

3.1.4.3.1 Initial optimization

The condition above that favoured nucleation was used in the initial optimisation. For each condition, a new tray was set up in which one parameter was varied and the others kept constant in according with the following table.

Table 3.2 Formulation of initial optimization

Formula varied in						
precipitant 1 concentrations varied, with precipitant 2	A1 0.1M Tris 0.2M Na Citrate pH 8.5 PEG 400 v/v 15%	A2 0.1M Tris 0.2M Na Citrate pH 8.5 PEG 400 v/v 20%	A3 0.1M Tris 0.2M Na Citrate pH 8.5 PEG 400 v/v 25%	A4 0.1M Tris 0.2M Na Citrate pH 8.5 PEG 400 v/v 30%	A5 0.1M Tris 0.2M Na Citrate pH 8.5 PEG 400 v/v 35%	
precipitant 1 concentrations varied, without precipitant 2	B1 0.1M Tris pH 8.5 PEG 400 v/v 15%	B2 0.1M Tris pH 8.5 PEG 400 v/v 20%	B3 0.1M Tris pH 8.5 PEG 400 v/v 25%	B4 0.1M Tris pH 8.5 PEG 400 v/v 30%	B5 0.1M Tris pH 8.5 PEG 400 v/v 35%	
buffer and pH varied	C1 0.1M MES 0.2M Na Citrate pH 6.5 PEG 400 v/v 30%	C2 0.1M Na HEPES 0.2M Na Citrate pH 7.0 PEG 400 v/v 30%	C3 0.1M Na HEPEs 0.2M Na Citrate pH 7.5 PEG 400 v/v 30%	C4 0.1M Tris 0.2M Na Citrate pH 8.0 PEG 400 v/v 30%	C5 0.1M Tris 0.2M Na Citrate pH 8.5 PEG 400 v/v 30%	
protein concentration varied	D1 2.5mg/ml	D2 3mg/ml	D3 3.5mg/ml	D4 4 mg/ml	D5 4.5mg/ml	D6 5mg/ml

The trials were checked after 2 weeks, the best crystals were produced in C1, which is 0.1M MES 0.2M Na Citrate PEG400 v/v 30% pH6.5, with a protein concentration of 5mg/ml. This condition was used for further optimization.

Figure 3.6 MtrE crystals after optimized

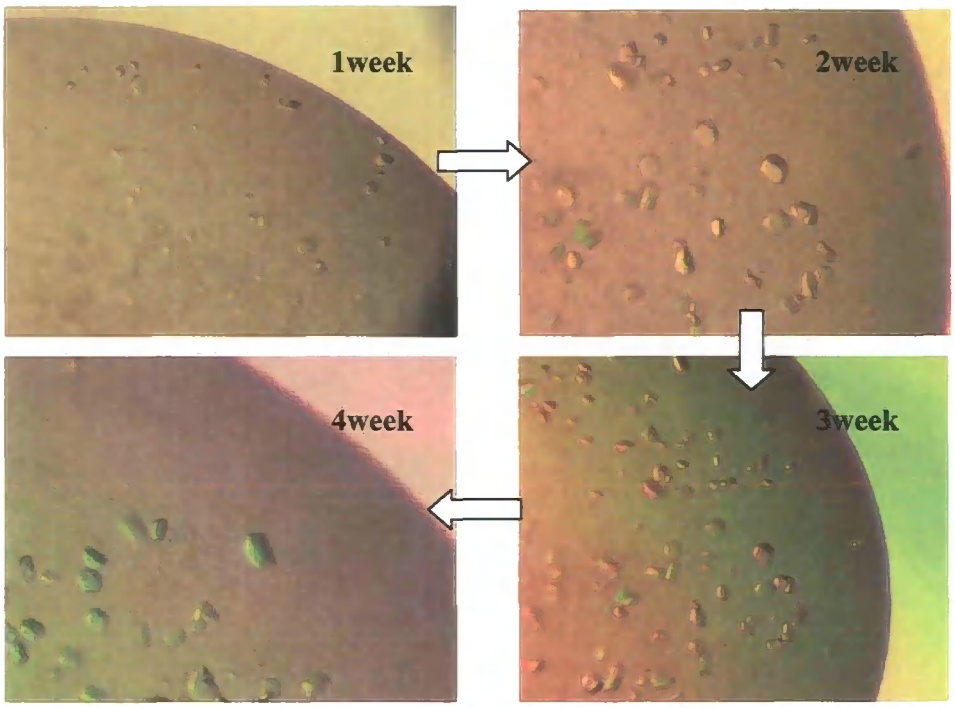

These four photos are for the crystals after different time, which were produced by the conditions above. Obviously, the crystals are too many and small, aound only 50-80μm long, so further optimizations were still be needed to be done to get high quality crystals for the crystallography.

3.1.4.3.2 Additive and detergent screen

The additive screen is a complete reagent kit designed to provide a rapid screening method for the manipulation of the sample-sample and sample-solvent interactions to enhance or alter sample solubility. The additive screen evaluates the effect of such factors as multivalent cations, salts, amino acid, dissociating agents, linkers, polyamines, chaotropes, co-factors, reducing agents, polymers, chelating agent, carbohydrates, polyols, non-detergents, amphiphiles, detergents, osmolyte, organic (non-volatile) and organic (volatile) reagents. The additive screening was performed again using the hanging drop method for the benefit of effective cost and setting multidrops with a single reservoir. 1ml of

crystallization reagent (0.1M MES 0.2M Na Citrate 30v/v PEG 400 pH 6.5) was pipetted into the reservoirs first, then 1 μl of MtrE sample was pipetted onto the cover lid. 0.22 μ l of additive was carefully pipetted into the sample and mixed, 1 μl of precipitate solution from the reservoir was added to the drop and mixed well. The cover lid was sealed tightly on the reservoir and the plates were moved to 18°C incubator.

Figure 3.7 MtrE crystals after Additive screen

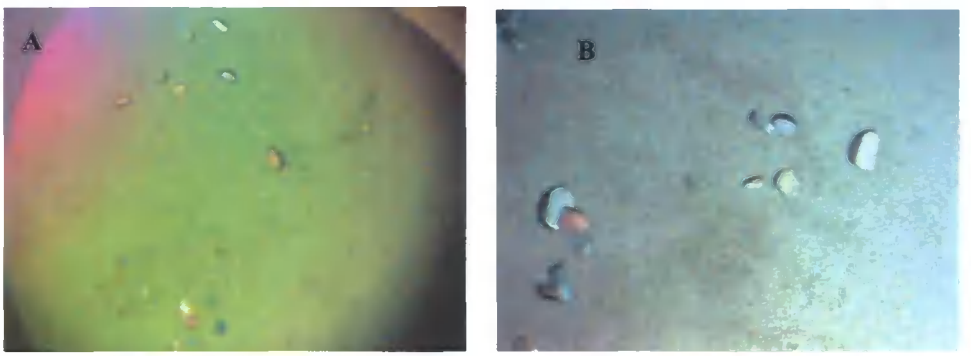

A: The crystals were produced in condition No.14 (0.1 M Praseodymium(III) acetate hydrate) of Additive screen (Hampton research)

B: The crystals were produced in condition No.24 (1.0 M Cesium chloride) of Additive screen (Hampton research)

The crstals from drop A and B in the above graph were frozen and sent to the ESRF. The diffraction was checked by Dr Xueyuan Pei, University of Cambridge. The best one diffracted to 8Å.

Figure 3.8 diffraction pattern of MtrE

Detergent screens are designed to be capable of manipulating hydrophobic sample-sample interactions which can lead to non-specific aggregation that prevents or interferes with sample crystallization. The detergents also perturb water structure which may play a role in sample crystallization.

The detergent screens from Hampton Research include 72 unique detergents for their ability to influence the solubility and crystallization of the sample. According to the user guide, the recommend final concentration is 1-3×CMC. To obtain a 1×CMC final concentration, 1μl of protein was pipetted onto the cover lid and then mixed with 0.22μl detergent solution(10×CMC), 1μl of precipitant solution(0.1M MES 0.2M Na Citrate 30v/v PEG 400 pH 6.5) from the well was mixed well in the drop. To get 2×CMC detergent concentration, 1μl of protein was mixed with 0.5μl detergent solution and then 1μl of crystallization reagent. Mixing 1μl of protein with 1μl of detergent solution and 1μl of precipitant solution was used to a 3×CMC of final detergent concentration. After the drops had been set, the cover lids were screwed onto the wells and the plates were moved to an 18°C incubator.

The plates were checked after three days, bigger crystals were found in the drop which has N-Decanoyl-Sucrose at a concentration of 3×CMC. No better crystals were found in the detergent screen of 1×CMC and 2×CMC.

Figure 3.9 MtrE crystals with N-Decanoyl-Sucrose from the detergent screen

The biggest crystal in this drop was about 150μm long and 30μm wide. Unfortunately, because the drop was destroyed during the delivery, the diffraction of the crystals weren't tested. The same condition was set several times but we never manage to produce the similar crystals again.

3.1.4.3.3 Cation exchange chromatography for MtrE

In order to improve the diffraction of the crystals, further purification of MtrE was adopted to increase the purity of the protein, which was accomplished by Ion exchange chromatography. Because the pI (Isoelectric Point) of MtrE is 9.5; a Hi-trap SP (5ml column volume, Amersham) Cation exchange column was used in this study.

Before undertaking the Cation exchange of MtrE, the column was pre-equilibrate with 5 column volume of buffer B2 (table 3.3) followed by 5 column volume of buffer A2 (table 3.3). The eluted MtrE from 3.3.3 was desalted into buffer A2 using a Hi-trap desalting column. The desalted MtrE was then loaded onto a Cation exchange column on an AKTA purifier. MtrE was eluted from the column using a gradient of 0%−100% buffer B2.

Table 3.3 Buffers for concentrating the MtrE by Ion exchange chromatography

	BufferA2	BufferB2
Tris	10mM	10mM
NaCl	50mM	500mM
Glycerol	10%	10%
DDM	0.1%	0.1%
THP	0.5mM	0.5mM
PH	7.6	7.6

Because the B2 buffer has a higher concentration of salt, the gradient of B2 can produce a constantly increase of ionic strength in the column. The molecules in the column are eluted separately according to their net charge.

Figure 3.10 Cation exchange chromatography of MtrE

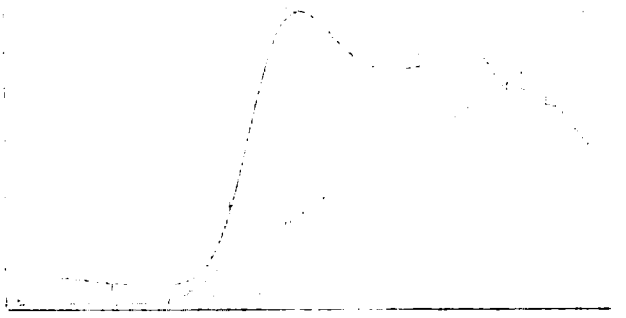

The above graph is the cation exchange chromatography of MtrE. The fractions from the first peak were used for crystallization.

After being eluted from the cation exchange column, the protein was diluted and consequently needed to be concentrated again for setting the trials. In order to avoid accumulating detergent in the liquor, cation exchange chromatography was used again for concentrating the MtrE, as described in 3.3.4.1.

The MtrE was desalted into the crystallization buffer, Tris 10mM NaCl 100mM Glycerol 10% DDM 0.1% THP 0.5mM pH7.8, for the purpose of decreasing the salt concentration, followed by dialysis against the buffer for 3 hours. The protein was then concentrated to 5mg/ml (Bradford Protein Assay Kit, Pierce) using a 30KDa vivaspin centrifugal concentrator.

The same trials as before were set up using both hanging drop and sitting drop methods. The drops were checked after 2 weeks. The sitting drops were set by mixing 5µl of protein, 4µl of crystallization reagent and 1µl of additive.The plates were checked 2 weeks after being set.

Figure 3.11 Crystals of MtrE after further purification

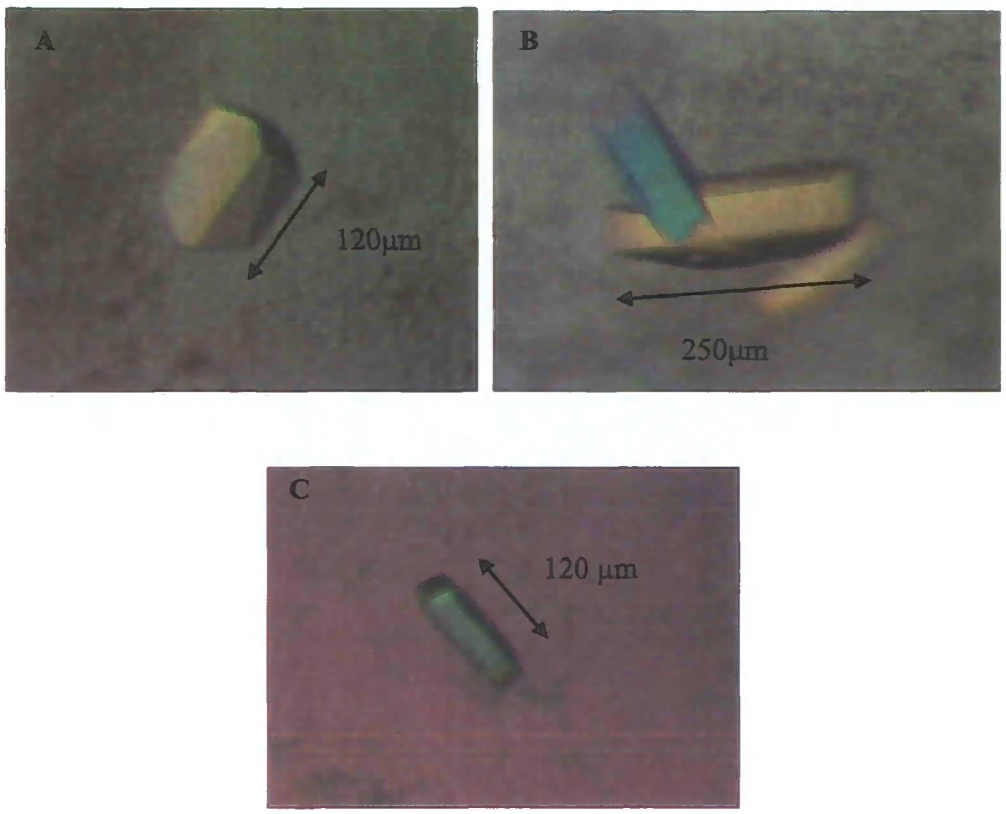

A, C: crystals from hanging drops

B: crystals from sitting drops

:

From the above figures, we can see the improvement in both size and shape of the crystals. Maybe it means that after further purification by cation exchange chromatography, both the purity and homogeneity were better than before. These crystals were sent to ESRF to check the diffraction, unfortunately, none of them diffracted better than 8Å.

3.2 Cloning, expression, purification and crstallization of the Inner membrane protein MtrD

3.2.1 Cloning of *mtrD* in pET21a vector

3.2.1.1 PCR amplification of *mtrD*

A pair of primers, which were designed according to the multi-cloning site of pET21a vector and 5' and 3' end of the *mtrD* sequence, MtrD forward and MtrD reverse were used to

amplify the *mtrD* fragment. The start codon was supplied by 5' *NdeI* restriction site and the stop codon was supplied by pET21a vector, instead of in the reverse primer.

Due to the size of the fragment, which was more than 3kb, the proofstart polymerase was employed to amplify the *mtrD* fragment. The amplification was performed with an annealing temperature of 55°C and extension time of 3 minutes 20 seconds for 30 cycles. Because Proofstart polymerase can only generate blunt ends on PCR products, it was necessary to incorporate a step of 'adding 3'-A overhangs' before ligate to pGEMT vector.

Figure 3.12 PCR amplification of *mtrD*

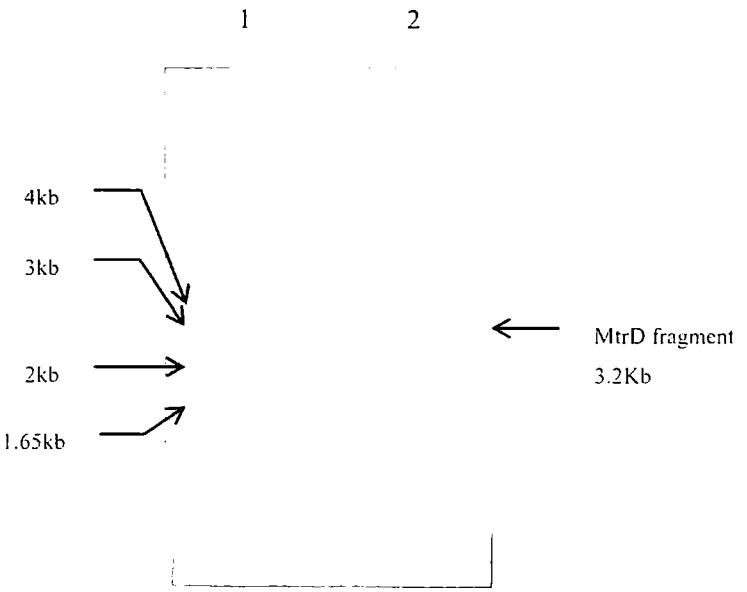

Lane 1: 1kb DNA ladder

Lane 2: amplified *mtrD* gene

3.2.1.2 Sub-cloning the *mtrD* gene fragment into the expression vector pET21a

After purifying the fragment from the agarose gel using a Gel Extraction Kit (Chapter 2.6.3?), then followed by adding 3' –A overhangs, the gene fragment was ligated overnight at 4°C into pGEM-T easy vector. The ligation mixture was transformed to nova-blue competent cells and after incubating these at 37°C overnight, the white colonies were picked and tested by PCR with the primers MtrD forward and MtrD reverse. The positive colonies were used to inoculate an overnight culture and the plasmid was extracted and digested by endonuclease *HeaII*; then the whole digestion reaction was purified using a QIAquick Nucleotide Removal

Kit, followed by digestion with *NdeI* and *XhoI*. The pET21a expression vector was digested with *NdeI* and *XhoI* simultaneously.

Figure 3.13 the expression vector pET21a and pGEMT easy-MtrD after digesting with *NdeI* and *XhoI*

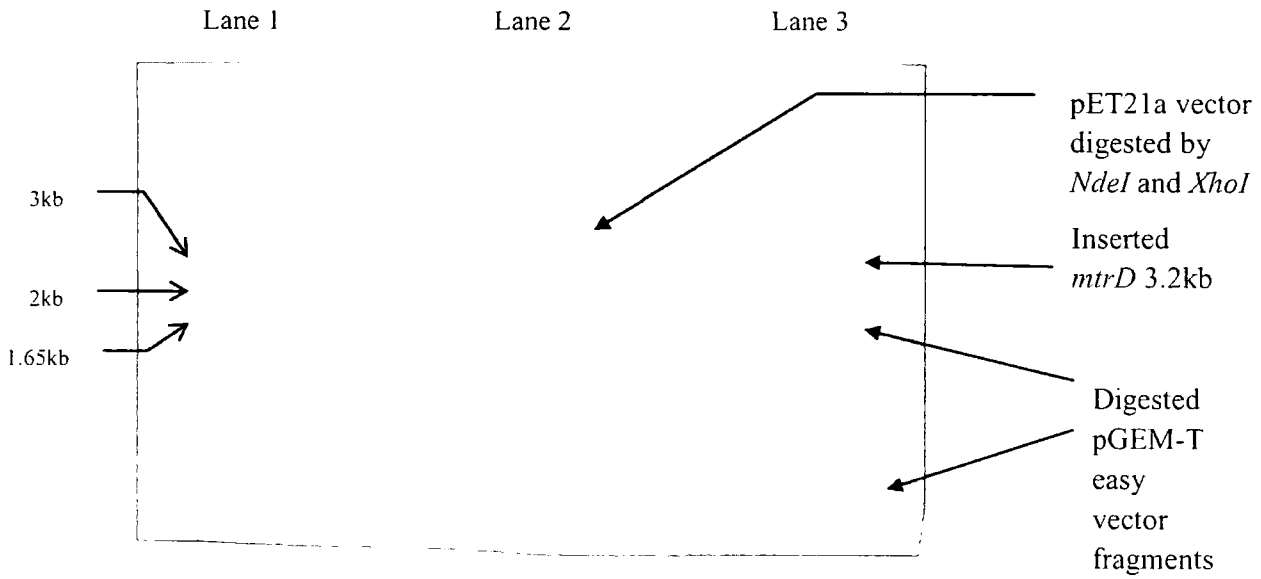

Lane 1: 1kb DNA ladder

Lane 2: pET21a expression vector digested by *NdeI* and *XhoI*

Lane 3: pGEM-T easy/*mtrD* digested by *HeaII* followed by *NdeI* and *xhoI*

The digested pET21a vector and the *mtrD* fragment were purified using a Gel extraction kit, then ligated with T4 DNA ligase. The ligation reaction was transformed to Nova-blue competent cells. Several colonies were picked from the plates and tested by PCR. The one with the right orientation of insertion was used to inoculate the overnight culture and the plasmid was extracted. Finally, the pET21a-MtrD(NdeI+XhoI) construct was used for transformation of C43 competent cells. A positive colony was accepted for expression od MtrD.

3.2.2 Overexpression of MtrD

The recombinant construct, pET21a-MtrD was used to produce the inner membrane protein MtrD with a fused C-terminal 6 Histidine tag. The overexpress strain C43 was selected to express the MtrD due to the characteristic of high toxicity of membrane protein.

C43(DE3) (Miroux and Walker, 1996)was derived from C41(DE3) by selecting for resistance to a different toxic protein and can express a different set of toxic proteins to C41(DE3) , the strain C41(DE3) was derived from BL21(DE3) and it has at least one uncharacterized mutation, which prevents cell death associated with expression of many recombinant toxic proteins.

As described in Chapter 2.12, one colony was picked to inoculate 100ml of LB broth with of 100μg/ml carbencillin. 3ml of overnight culture was used to inoculate 1 liter of YT broth with 100μg/ml carbenicillin in. Normally, one batch of protein (5mg) was obtained from 24 liters of medium. After being induced with a final concentration of 0.5mM IPTG, the temperature was decreased to 25°C and the cells were harvested 5 hours later.

3.2.3 Purification of MtrD by Immobilized Metal Affinity Chromatography

The cell membrane was extracted and homogenized in the membrane resuspension buffer (Tris 20mM NaCl 100mM Glycerol 20% THP 0.5mM). pH 7.5 Before being solublized with DDM, one tablet of proteinase inhibitor was added for the membrane from 6 liters cells. After solublization with DDM and being ultracentrifuged, the soluble fraction was loaded onto a pre-charged Ni-chelating column (1column/fraction from 6 liters of cells). The column was connected onto AKTA purifier and washed with the washing buffer 1 (Tris 20mM NaCl 300mM Imidazole 50mM Glycerol 10% THP 0.5mM DDM 0.2% pH7.5), followed by washing buffer 2 (Tris 20mM NaCl 300mM Imidazole 100mM Glycerol 10% THP 0.5mM DDM 0.2% pH7.5). The protein was eluted with the same buffer as above but with 300mM Imidazole. The eluted fractions were checked by SDS-PAGE electrophoresis.

Figure 3.14 SDS-PAGE of MtrD after being purified by Ni-chelating chromatography

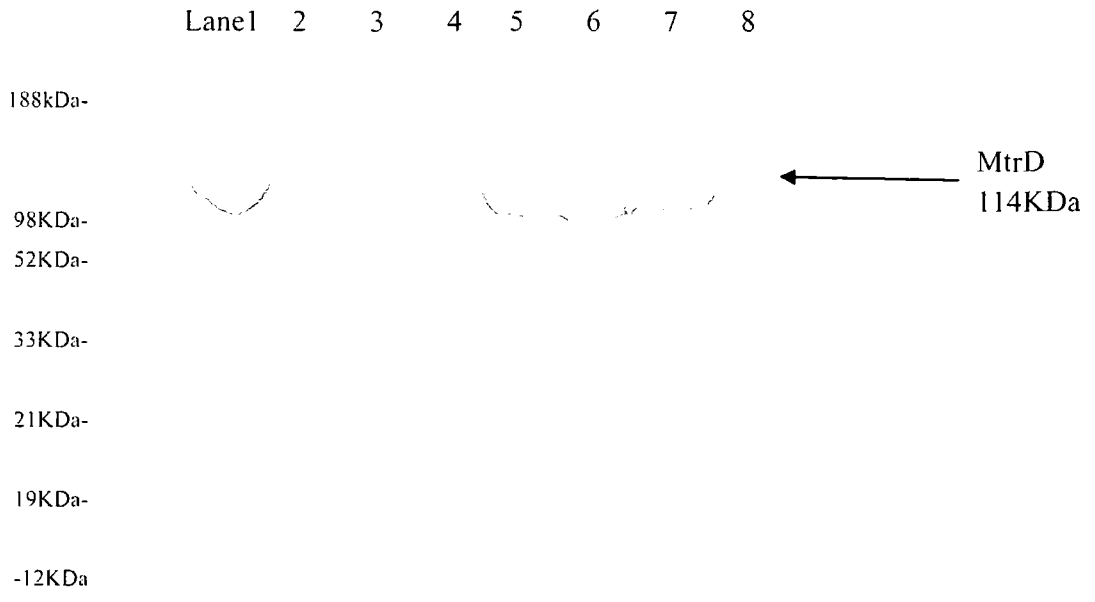

Lane 2; SeeBlue protein marker(Invitrogen)

Lane 3-7: The elution fractions from Ni-Chelating column (20μl/lane)

3.2.4 Desalting and Concentrating the MtrD by anion exchange chromatography

Due to the high concentration of the Imidazole and low amount of protein in the eluted fraction, a desalting and concentrating step was performed after MtrD had been purified.

The desalting of the protein was accomplished using a prepacked HItrap desalting column as described before. One 5ml column can be used to desalt 1.5ml of protein, so the number of columns can be determined from the total amount of protein sample. If the sample amount was not a multiple of 1.5ml, it had to be made up to an exact multiple with buffer.

The Hitrap desalting column was connected onto AKTA, which was then pre-equilibrated by the ideal buffer, Tris 20mM NaCl 50mM Glycerol 10% DDM 0.1% THP 0.5mM pH7.5. The protein sample was loaded onto the column by a syringe. 2ml per column of ideal buffer was used to elute the protein. After this desalting step, 95% of buffer could be changed to the ideal buffer.

In order to get the higher concentration of MtrD for setting the crystallization trials, anion exchange chromatography was adopted to concentrate the protein without accumulating the detergent.

A pre-packed RESOURCE™ Q (6ml) column was used for this step; it was connected to an AKTA purifier and then equilibrated with 30ml (5 column volume) of Buffer B followed by 30ml (5 column volume) of Buffer A. The desalted MtrD was loaded onto the Resource Q column at a flow rate of 1ml/minute. Then the protein was eluted with a high salt buffer.

Table 3.4 Buffers for concentrating the MtrD by Ion exchange

	BufferA	BufferB
Tris	10mM	10mM
NaCl	50mM	500mM
Glycerol	10%	10%
DDM	0.1%	0.1%
THP	0.5mM	0.5mM
PH	7.5	7.5

Figure 3.15 SDS-PAGE of MtrD after concentrated by Anion exchange chromatography

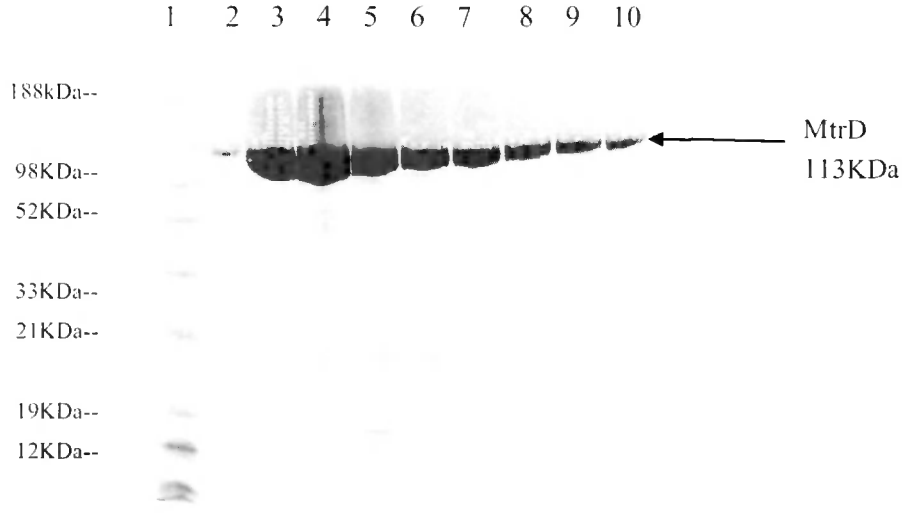

Lane 1: Seeblue marker (Invitrogen)

Lane 2-10: MtrD after concentrated (5μl/lane)

3.2.5 Crystallization of MtrD

3.2.6 Protein preparation

Before setting up the crystallization trials, the buffer was changed to Tris 10mM NaCl 100mM Glycerol 10% DDM 0.1% THP 0.5mM. Then the protein sample was dialysized against the same buffer using a dialysis cassette (Pierce). Finally, the protein was concentrated to 15mg/ml using 100KDa ultrafiltration spin column.

Figure 3.16 SDS-PAGE of MtrD before applying to crystallization trials

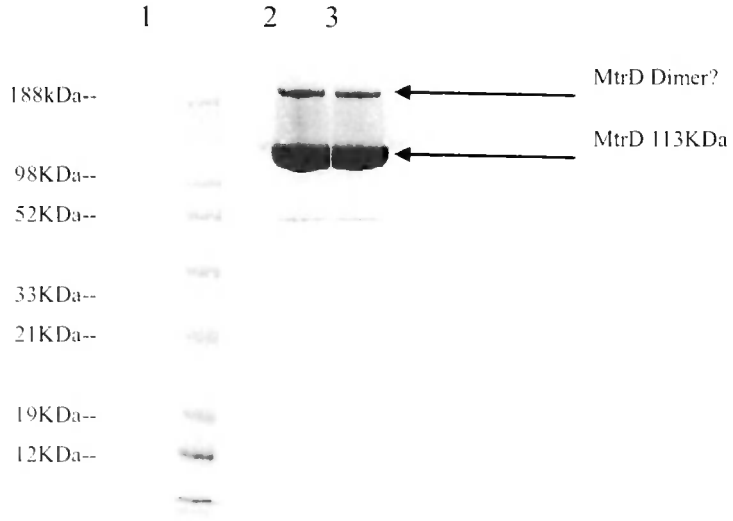

Lane1: Seeblue marker

Lane2, 3: MtrD after dialysis and being concentrated (1ul/lane)

From the SDS-PAGE gel above, MtrD sample only contains minor impurities, so further purification wasn't used in this study.

In the Blue-Native SDS-PAGE Gel, the homogeneity of MtrD is poor. Although the main part of the sample was a monomer, the dimer and trimer were still obviously visible in the gel. Related to the difficulty of crystallization of MtrD in later studies, the heterogeneity of the sample might be a major issue.

3.2.7 Sparse matrix screen

The same kits as used for MtrE were employed to do the initial screen for MtrD. Again, the hanging drop technique was used to set the trials as described before.

The plates were checked after two weeks. Lots of microcrystals appeared under condition No.8 of the MemSys™ kit (Molecular Dimensions Ltd); the formulation is 0.1M MES 30% V/V PEG 400 PH6.5.

Figure 3.17 The microcrystals produced in sparse matrix screen

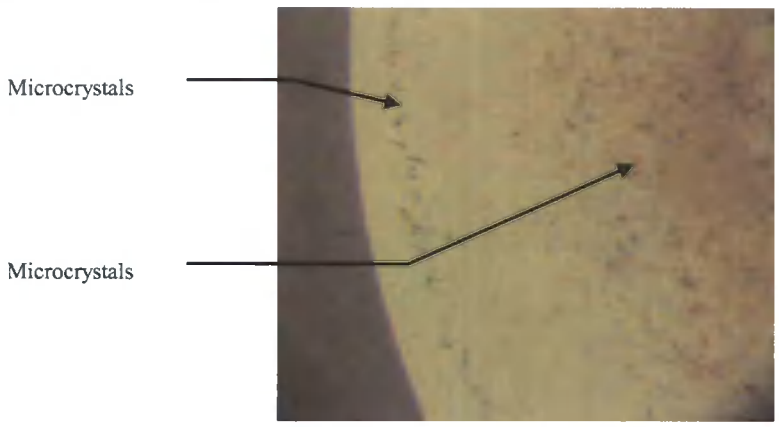

3.2.8 Optimization screen

The optimizing of conditions was based on the formulation of the sparse matrix screen; whilst the additive and detergent screens were applied. The additives and detergents were used same as MtrE which we described before. The drop in the following graph was the best one among them. It was produced under condition No.77 (50% v/v Jeffamine M-600 ® pH 7.0) from additive screen (Hampton research).

Figure 3.18 The MtrD crystals after opimization

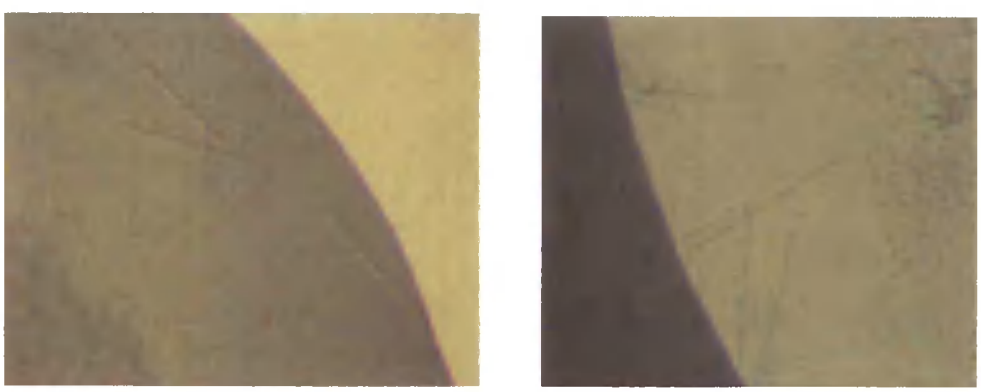

These crystals were frozen in liquid propane and sent to the ESRF for checking the diffraction. Unfortunatly, even the best one among them only diffracted to 22Å.

3.3 Discussion

The resistance to a variety of structural diverse hydrophobic agents (HAs), including antimicrobial agents in *Neisseria gonorrhoea* isolates is a global problem in the treatment of gonococcal infection. It has been reported HAs resistance in *Neisseria gonorrhoea* is mainly due to the overexpression of the Mtr (multiply transferable resistance) system (Delahay *et al.*, 1997; Hagman *et al.*, 1995). The nucleotide sequencing analysis of the *mtr* operon showed that it is composed of a regulatory gene, which encodes the transcriptional repressor MtrR, and three other genes, which encode the three membrane proteins components of an efflux pump, MtrC, MtrD and MtrE (Hagman *et al.*, 1995; Lucas *et al.*, 1995; Pan and Spratt, 1994).

Homology studies have been done to determine the function of each component of the MtrCDE system. MtrC is proposed to be a MFP, which functions co-operatively with an RND protein to transport large hydrophobic molecules across the two membranes of the Gram-negative bacterial cell envelope(Zhang *et al.*, 2007). MtrD is confirmed to be an inner membrane protein that belongs to RND family. It shows 43% identity to AcrB of *Escherichia coli* and 49% identical to MexB of *pseudomonas aeruginosa*(Hagman *et al.*, 1997). MtrE was determined to a member of the outer membrane protein family that has TolC from *E.coli* and OprM from *P.aeruginosa*(Delahay *et al.*, 1997).

Among the three components, MtrD and MtrE are particularly important in the pump function. Until now, the only known structure for an RND inner membrane protein is AcrB(Murakami *et al.*, 2002), whilst three structures of the outer membrane proteins were reported, TolC(Koronakis *et al.*, 2000), OprM (Akama *et al.*, 2004a)and VceC(Federici *et al.*, 2005). To better understand the characteristics this kind of multidrug transporter, structural analyses were carried out in this work to determine the crystal structure of the inner membrane protein MtrD and outer membrane protein MtrE.

Due to the distinct biochemical and biophysical properties of membrane proteins, their crystallization is particularly complicated, which has led to only a few structures having been solved. To achieve the crystallization of these proteins, the first requirement is to have a sufficient quantity of protein. For membrane protein, it is quite a big problem because of the toxicity of the overexpressed protein to the host strain. In this study, we employed

C43(Miroux and Walker, 1996) as the host strain and pET21a as the expressing vector. The C43 strain is derived from the C41 (DE3) strain and can overcome the toxic effects associated with overexpression of membrane proteins; pET21a vector from Novagen confers ampicillin resistance; choosing the proper restriction sites is also important because the extra amino acids tag may cause difficulties in the crystallization. The concentration of the inducer was also optimized to achieve the balance between overexpression and survival of the host strain. The cells were harvested normally after 5 hours, because for this length of growth, the cells had overexpressed the maximum amount of protein compared with the amount of cells. After purification, both MtrD and MtrE can reach 95% purity and a quantity of 0.3mg/litre culture and 0.6mg/litre culture respectively.

Choosing the detergent is another tricky question in membrane protein crystallization. There is a compromise need to be made between the long alkyl chain detergents, which make membrane protein more soluble and stable, and the short chain detergents, which compose the more hydrophilic residues for ease of crystallization. Dodecyl-β-D-maltoside (DDM) was adapted in this study due to its high success in crystallization of related proteins(Federici *et al.*, 2005; Murakami *et al.*, 2002). Due to the CMC of 0.17mM and MW of 510.6, 1×CMC is 0.0087% (w/v). 2% (w/v) of DDM was used to solubilize the membrane, while 0.2% of DDM was used in purification buffers. At the final step of purification, normally the concentrating step by ion exchange chromatography, the DDM concentration was changed to 0.1%.

Microcrystals were produced for both MtrD and MtrE from the sparse matrix screen; optimization screens were then carried out upon the condition that produced microcrystals. MtrE is the one that was investigated most deeply. After one step of optimization screen, using an additive screen and a detergent screen, the best condition so far found gave crystal that diffracted to 8Å. Although it is still too poor to solve the structure, it is a good start for this work. Compared with the outer membrane protein MtrE, the inner membrane protein MtrD was found more difficult to crystallize, which is probably because of the huge hydrophobic surface(Gotoh *et al.*, 1999; Guan *et al.*, 1999; Hagman *et al.*, 1997) and the flexibility of the molecule(Murakami *et al.*, 2006; Seeger *et al.*, 2006). Homogeneity of the sample may cause problem in crystallization as well. Because of the lacking of dynamic light scattering equipment, Blue-native electrophoresis was employed to check the homogeneity of

the MtrD and MtrE samples before applying to crystallization trials. We found that 95% of MtrE formed a trimer in the native state, while MtrD was composed of multiple oligomeric states, which may have led to the poor diffracting crystals. Another reason for the failure of the crystallization is the unrepeatable of the trials. Although the proteins were purified in exactly the same condition every time, there were still a lot of immeasurable differences between each batch of protein. The most important, alterable factor, is the detergent concentration, which would accumulate at the last step of concentrating in the ultrafiltration spin column due to the large micelle size (≈70KDa) (Strop and Brunger, 2005; Urbani and Warne, 2005; VanAken *et al.*, 1986). Except the concentration, the type of detergent is also very important. To get crystallographic quality crystals, detergents other than DDM need to be screened.

Except optimizing the purification methods, a possible means to improve the quality of the crystals is to cut off the C-terminal 6×*Histidine* tag from MtrD and MtrE. It was reported that the TolC crystals reached diffraction of 2.1Å after being treated with V8 protease which removed 43 residues at the C-termius(Koronakis *et al.*, 2000). It was suggested that these extra flexible residues can interfere with the packing of the molecules during the crystallization. Moreover, optimizing the crystallization condition again may be necessary. The condition we are using now may not be the most suitable one and can only produce crystals of poor quality. More conditions need to be tried in order to find the best one.

Although the structures of MtrD and MtrE haven't been solved in this study, it still gave us lots of information on the crystallization characteristics of these two proteins. Both MtrD and MtrE were overexpressed and purified successfully; the initial attempt at crystallization gave us the crystals that diffracted to 20Å and 7Å respectively. These will allow us to perform future structural and functional analyses.

Chapter 4 MtrC, MtrD and MtrE form a precise efflux pump and the hairpin domain of MtrC plays an important role in pump function

4.1 MIC and growth curve indicate that the MtrCDE work as a tripartite antibiotic efflux pump

4.1.1 The construct that were used in this study

In order to study the transport capability of the Mtr system, an expression vector pACYCDuet-1, which has two multiple cloning sites, was employed to express all the components. Because this vector confers chlorampenicol resistance, it doesn't have the problem of testing the transport of the antibiotics that belong to the penicillin family.

Table 4.1 the recombinant strains that were used in this study

Name	Description
control	Kam3(DE3)[pACYC Duet]
MtrC	Kam3(DE3)[pACYC Duet- MtrC(BamHI+SalI)]
MtrD	Kam3(DE3) [pACYC Duet-MtrD(Bam+SalI)]
MtrE	Kam3(DE3) [pACYC Duet-MtrE(BamHI+HindIII)]
MtrC-D	Kam3(DE3) [pACYC Duet-MtrC(BamHI+SalI)- MtrD(NdeI+XhoI)]
MtrC-E	Kam3(DE3) [pACYC Duet-MtrC(BamHI+SalI)-MtrE(NdeI+KpnI)]
MtrD-E	Kam3(DE3) [pACYC Duet-MtrE(NdeI+KpnI)-MtrD(BamHI+SalI)]
MtrC-D-E	Kam3(DE3) [pACYC Duet-MtrC-RBS SD linker-ATG MtrE(BamHI+HindIII)-MtrD(NdeI+KpnI)]
MtrE-gIII MtrC hairpin	Kam3(DE3)[pACYC Duet-MtrE(BamHI+HindIII)-gIII MtrC hairpin(NdeI+XhoI)]
MtrD-gIII MtrC hairpin	Kam3(DE3)[pACYC Duet-MtrD(BamHI+SalI)-gIII MtrC hairpin(NdeI+XhoI)]
pACYC-pET24a	Kam3(DE3)[pACYC Duet][pET24a]

MtrCDE-pET24a	Kam3(DE3)[pACYC Duet-MtrC SD linker(BamHI+EcoRI)-ATG MtrE(EcoRI+HindIII)-MtrD(NdeI+KpnI)][pET24a]
MtrCDE-gIII MtrC hairpin	Kam3(DE3)[pACYC Duet-MtrC SD linker(BamHI+EcoRI)-ATG MtrE(EcoRI+HindIII)-MtrD(NdeI+KpnI)][pET24a-gIII MtrC hairpin (NdeI+XhoI)]

The pACYC Duet- MtrC (BamHI+SalI), pACYC Duet-MtrD (BamHI+SalI) and pACYC Duet-MtrE (BamHI+HindIII) were made by ligating the *mtrC,D,E* genes into the pACYC Duet vector after digestion with the corresponding restriction endonucleases.

The construct of pACYCDuet-MtrC (BamHI+SalI)-MtrD (NdeI+XhoI) was made by ligating the fragment of *mtrC* (BamHI+SalI) into the pACYC duet vector after digesting with the same enzymes. Then *mtrD* (NdeI+XhoI) was ligated into the second multiple cloning site of pACYC Duet-mtrC (BamHI+SalI), which was digested by *NdeI* and *XhoI*. The pACYC Duet-MtrC (BamHI+SalI)-MtrE (NdeI+KpnI) and the pACYC Duet-MtrE (NdeI+KpnI)-MtrD (BamHI+SalI) constructs were made in the same manner.

Figure 4.1 Endonucleases digestion test of two constructs

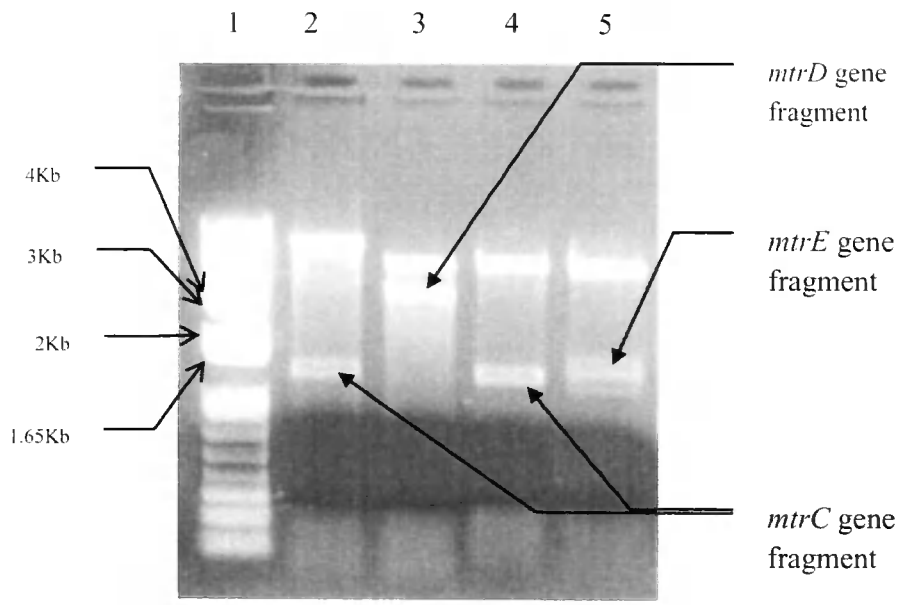

Lane1: 1Kb DNA ladder

Lane2: Kam3 (DE3) [pACYCDuet-MtrC (BamHI+SalI)-MtrD (NdeI+XhoI)] digested by *BamHI* and *SalI*

Lane3: Kam3 (DE3) [pACYCDuet-MtrC (BamHI+SalI)-MtrD (NdeI+XhoI)] digested by *NdeI* and *XhoI*

Lane 4: Kam3 (DE3) [pACYCDuet-MtrC (BamHI+SalI)-MtrE (NdeI+KpnI)] digested by *BamHI* and *SalI*

Lane 5: Kam3 (DE3) [pACYCDuet-MtrC (BamHI+SalI), MtrE (NdeI+KpnI)] digested by *NdeI* and *KpnI*

As to the [pACYCDuet-MtrC SD linker (BamHI+EcoRI)-ATG MtrE (EcoRI+HindIII)-MtrD (NdeI+KpnI)], the fragment of MtrC-RBS linker (BamHI+EcoRI) was made by PCR with the primers "MtrC BamHI F" and "MtrC SD linker EcoRI R" in table 2.7, in which GAGGAA is the Shine-Dalgarno sequence(Chen *et al.*, 1994), which is reported to be a Ribosome Binding Site sequence. Then it was ligated with pGEM-T easy vector, followed by digestion with *BamHI* and *EcoRI*. After purify the fragment by Gel Extraction, it was ligated into the pACYC Duet vector, which had been digested with the same restriction endonucleases. The second fragment of *mtrE* was made by PCR with the primers "ATG MtrE EcoRI F" and "MtrE HindIII R". One start code ATG was added to the beginning of the sequence. After release from the pGEM-T easy vector by digestion, it was connected to the pACYC Duet-MtrC-RBS linker, which was digested by *EcoRI* and *HindIII*. Finally, the fragment *mtrD* (NdeI+KpnI) was ligated into the second multiple cloning site by the same procedure.

The peiplasmic gIII-*mtrC* hairpin construct was constructed according to the following description. The primers "MtrC hairpin NcoI F" and "MtrC hairpin XhoI R" given in the table 2.7 were used to amplify the *mtrC* hairpin. Extra bases were added to put the MtrC hairpin sequence in frame. This fragment was ligated into pGEM-T vector and then digested with *NcoI* and *XhoI*. It was ligated into the pBAD-gIIIc vector that was digested with the corresponding enzymes. Another amplification was done using the "gIII NdeI F" and "MtrC hairpin XhoI R" primers and the product was ligated in the same way as above into the cloning site of the vector pACYC Duet or pET24a.

4.1.2 The minimum inhibitory concentration for different antibiotics for different *mtrCDE* constructs above

Table 4.2 MIC of some recombinant strains

	Penicillin G (μg/ml)	Tetracycline(μg/ml)	Erythromycin (μg/ml)	Nafcillin(μg/ml)
pACYC	32	4	0.5	8
mtrC	64	2	8	32
mtrD	32	16	-	64
mtrE	16	16	-	64
mtrC-mtrD	32	32	8	128
mtrC-mtrE	32	2	4	32
mtrD-mtrE	64	2	64	64

According to the data above, except for Penicillin G, the strains that express MtrD and MtrCD all had significant increase in MIC, especially for Nafcillin, which means MtrD and MtrCD can work as a efflux pump for these antibiotics.

Both Tetracycline and Nafcillin were used for the following growth curve analysis, but Nafcillin produced more pronounced differences in the growth curves.

4.1.3 Growth curve studies

4.1.3.1 A Growth curve analysis indicates that MtrCDE work as an antibiotic efflux pump

The constructs that express MtrD, MtrCD and MtrCDE were used to study the cooperation between the proteins in drug tranport. The strain Kam3 (DE3) [pACYCDuet] was used as a negative control in this study.

The concentration of Nafcillin in the culture was generally 64μg/ml, but 128μg/ml was also tested, but there was no obvious difference between them. The OD600 was tested for all the strains for 4 hours, until the cells grown to stationary phase. Each experimental test was made in triplet, by which the error bars were produced.

Figure 4.2 the growth curve of strains that overexpress various pump components

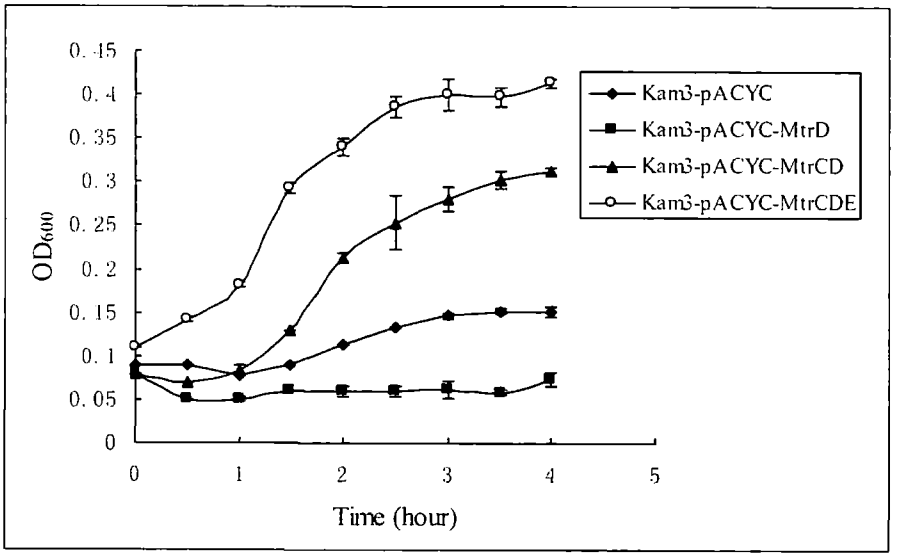

It is very clear from this graph that the growth of strain that express MtrCDE wasn't inhibited by Nafcillin, whilst the strain expressing MtrCD was partly inhibited by the antibiotic in comparison. The strain that with empty plasmid and the one expressing MtrD barely grew at all. We conclude that MtrC, MtrD and MtrE can form a stable tripartite efflux pump, which can extrude antibiotics from the cell. In the absence of the outermembrane protein MtrE, the activity of the pump was reduced, which led to limited growth in the presence of the antibiotic. This finding suggests that probably MtrCD could employ TolC to conduct defective transport. Besides this, it also showed that the membrane fusion protein MtrC plays an important role by assisting the activity of the inner membrane protein MtrD. In the absence of MtrC, apparently MtrD couldn't transport antibiotic its own.

Due to the toxic effect of overproducing membrane proteins in the host cell, which may cause different strains to grow at variable speeds even in the absence of the substrate, the growth curve data was amended to the following bar chart. OD600 was checked after 4 hours' growth. The relative growth rates were generated by dividing the average of the OD600 of three testing tubes with added Nafcillin by the OD600 of same strain without added Nafcillin.

Figure 4.3 a bar chart to show comparatively the growth of strains in the presence and absence of Nafcillin

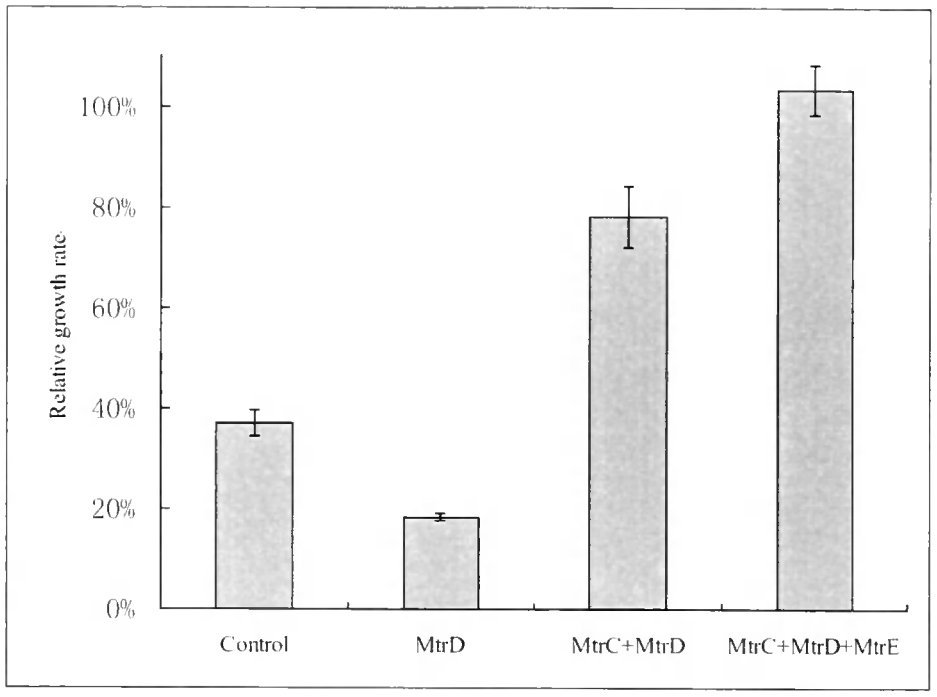

This data was produce by comparing the OD600 of all the recombinant strains with and without 64μg/ml of Nafcillin. The bars represent the ratio of growth after 4 hours of growth.

Comparing these 4 sets of data, the strain that express all three components of the MtrCDE pump grew best in the presence of Nafcillin, which is a substrate of the Mtr system. Presumably that the expression of MtrC, D and E, a whole efflux pump can be assembled to transport the antibiotic out of the cell, reducing the accumulation of the antibiotic inside the cell, enabling cell survival. Without the assistance of the outer membrane protein MtrE, the function of the pump is incomplete, which is why the growth of the strain that only express MtrCD couldn't catch up with the one expressing MtrCDE. The growth of the strain that only expresses the inner membrane protein MtrD was highly inhibited by Nafcillin, which suggests that the membrane fusion protein plays an important role in drug transport.

The same conclusion can be drawn from the bar chart comparing growth in the presence and absence of Nafcillin, that MtrCDE can form a stable tripartite efflux pump with activity of transport, and the membrane fusion protein might play a a major part in triggering the action of the pump.

4.1.3.2 The periplasmic MtrC hairpin domain didn't activate the transport of MtrD

To test if the MtrC hairpin domain could activate the transport function of MtrD, as does full length MtrC; a construct, which contains MtrD and the MtrC hairpin with N-terminal gIII signal, was employed to test the growth situation in the presence of Nafcillin.

Figure 4.4 Growth curve for strains expressing MtrC-D and MtrD-gIII MtrC hairpin

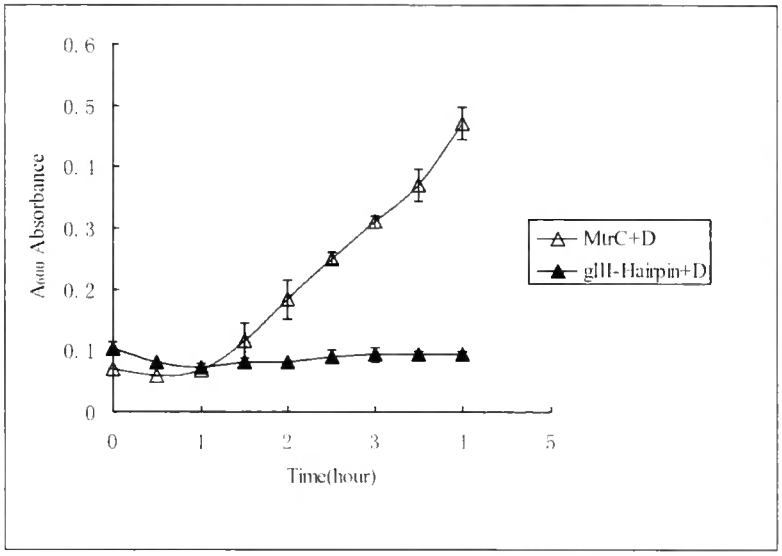

Figure 4.5 the percentage growth of cells grown in the presence and absence of Nafcillin

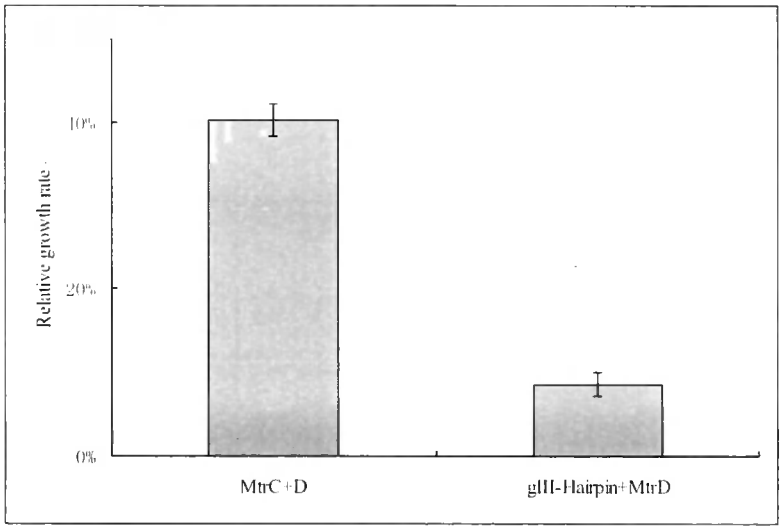

In comparison with strain overexpressing full length MtrC and MtrD, it is obvious that the periplasmic MtrC hairpin domain does not activate the transport function of MtrD, which leads to inhibitory growth in the presence of Nafcillin, or because it failed to transfer the drug

to MtrD by its own.

4.1.3.3 The opening mechanism of the outer membrane protein MtrE

To better understand the opening mechanism of the outer membrane protein MtrE, a series of growth curves were measured in the presence of Vancomycin, which is a large hydrophilic antibiotic that can't pass through the outermembrane. It can only enter cells via a channel such as that in MtrE when it is open.

Figure 4.6 growth curves and growth percentage to testify the opening of MtrE

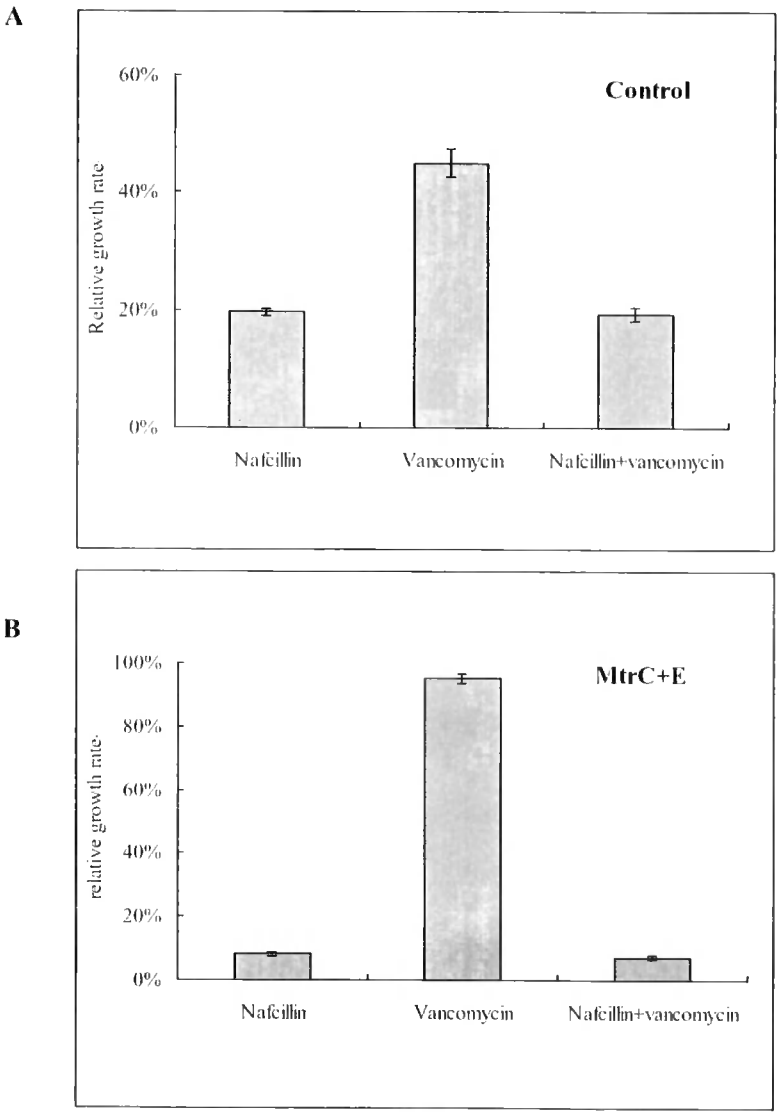

C

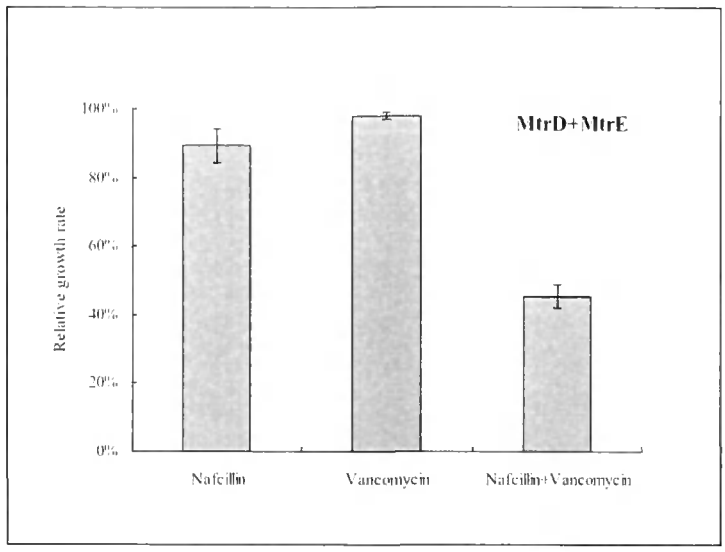

D

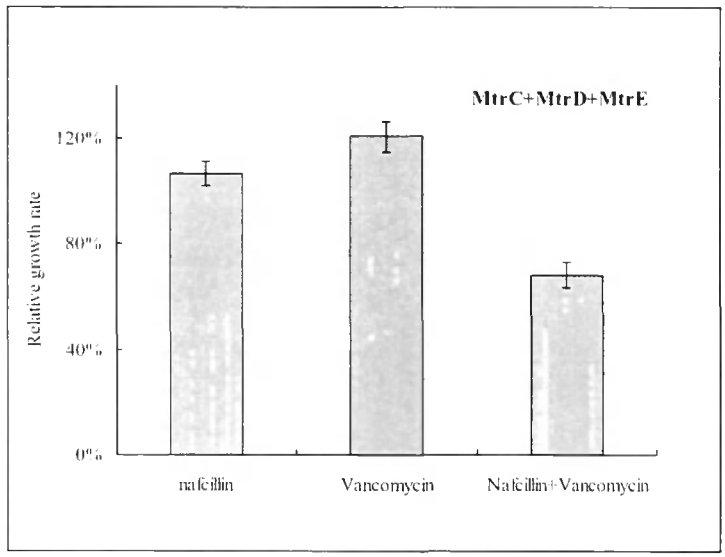

A2: percentage growth of control in the presence of Nafcillin (64μg/ml), or/and Vancomycin(150μg/ml)

B2: percentage growth of MtrCE in presence of Nafcillin (64μg/ml), or/and Vancomycin(150μg/ml)

C2: percentage growth of MtrDE in presence of Nafcillin (64μg/ml), or/and Vancomycin(150μg/ml)

D2: percentage growth of MtrCDE in presence of Nafcillin (64μg/ml), or/and Vancomycin(150μg/ml)

From the above data series we can see, the strains that doesn't express any component

of the Mtr system and those only expressing the MtrC and MtrE couldn't export the substrate Nafcillin, leading to inhibitory growth. In addition, the growth of these two strains wasn't inhibited by Vancomycin. In contrast, the strains that express MtrD and MtrE and the one expressing all the three components, grew in the presence of Nafcillin or Vancomycin. However, in the presence of both of antibiotics, the growth was obviously inhibited.

4.1.3.4 Periplasmic MtrC hairpin domain can enhance the transport action of the MtrCDE system

In order to analyse the effects of the periplasmic MtrC hairpin on the MtrCDE system activity, a recombinant strain with two vectors, pET24a that express the gIII-MtrC hairpin and pACYC Duet that express MtrCDE, was used to test the difference in growth with the strain that only expresses MtrCDE.

Figure 4.7 growth curve showing the effect of the periplasmic MtrC hairpin domain on pump activity

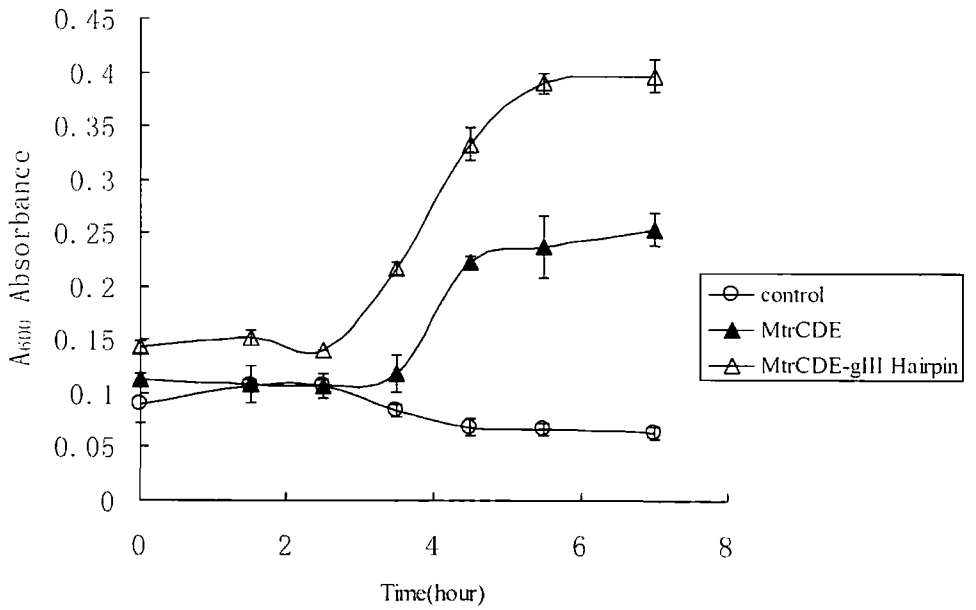

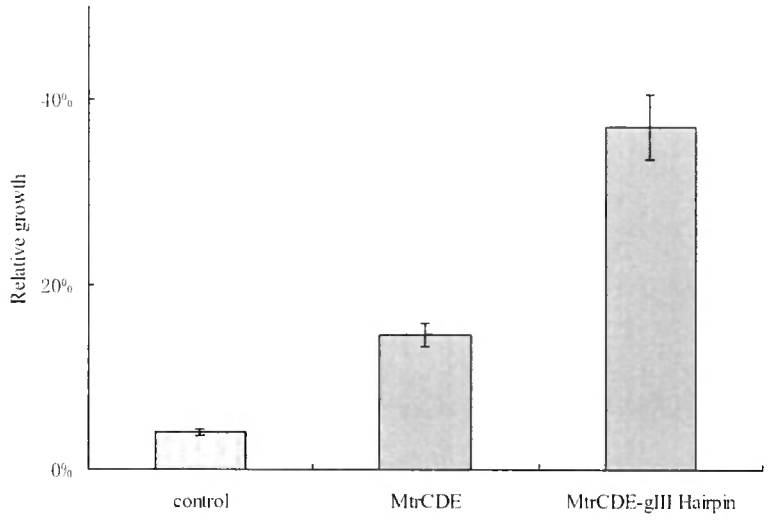

The strain Kam3(DE3) was adopted as a negative control of this analysis. In the presence of the substrate Nafcillin, the recombinant strain that overexpressed MtrCDE grew slightly slower than the one that overexpressed MtrCDE and periplasmic MtrC hairpin domain. The growth percentages also reflected the same result, which were calculated after 24 hours' of growth, comparing with the corresponding strains without Nafcillin.

4.2 Pull-Down assay indicate that the MtrCDE form a stable complex

To study the interaction of all the components of the Mtr system *in vitro*, pull down assays were carried out as described before. Two different fusion tags were adopted for the final analysis, using monoclonal antibodies to the 6×Histidine tag and S·tag. These two tags were constructed at the C-terminal of these proteins as required.

pACYC Duet –1 vector was employed again for the reason that it provides an in frame S·tag sequence.

Table 4.3 the recombinant strains that were used in Pull-Down assay

Name	Description
pACYC	BL21(DE3)[pACYCDuet]
MtrD-His	C43 [pET21a-MtrD(NdeI+XhoI)]
MtrE-His	C43 [pET21a-MtrE(NdeI+HindIII)]
MtrC-S	BL21(DE3)[pACYC-MtrC(NdeI+XhoI)]

MtrE-S	BL21(DE3)[pACYC-MtrC(NdeI+KpnI)]

The pull down assays was performed according to the principle of using a larger molecule to capture smaller ones, which can reduce the interference of the false negative that is produced by gravity and flow.

As described before, the bait protein was purified by IMAC, followed by desalted to the buffer without Imidazole. The crude membrane extract of prey protein with fusion S-tag was used without purification. After solubilised this with DDM, the two proteins were mixed together and co-purified. One negative control was set by mixing His-tag bait protein with the membrane of BL21 (DE3) [pACYCDuet], which only express dissociative S-tag; another negative control was set by mixing Ni-NTA agarose only with cell membrane containing prey protein and then washed and eluted. Finally, the western blot was used to detect the presence of both bait and prey protein.

Figure 4.8 the results of Pull Down assay

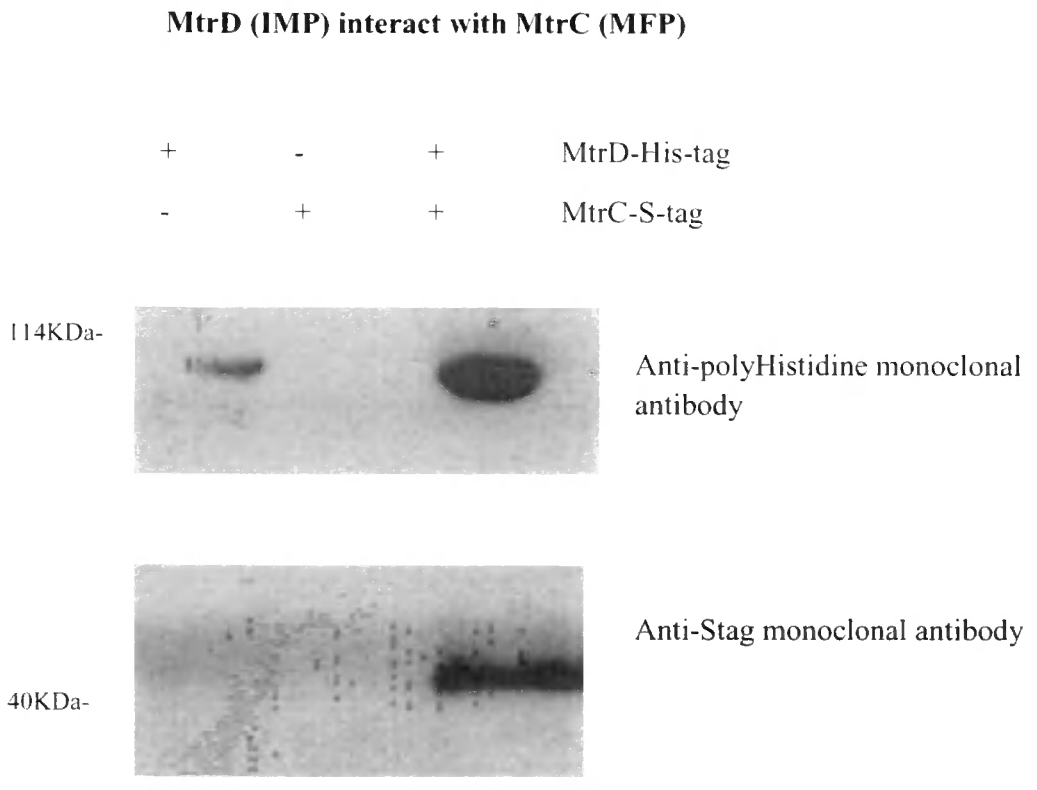

MtrE (OMP) interact with MtrC (MFP

+	-	-	+	+	MtrE-His-tag
-	+	+	+	+	MtrC-S-tag

51KDa-

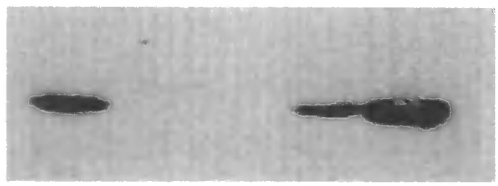

Anti-polyHistidine monoclonal antibody

40KDa-

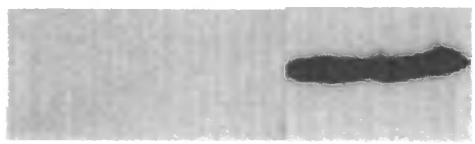

Anti-Stag monoclonal antibody

MtrD (IMP) interact with MtrE (OMP)

+	-	-	+	+	MtrD-His-tag
-	+	+	+	+	MtrE-S-tag

114KDa-

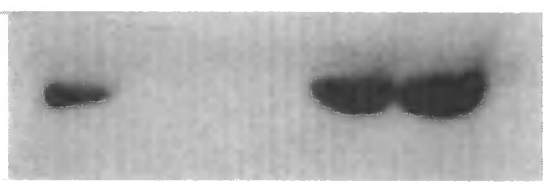

Anti-polyHistidine monoclonal antibody

51KDa
-

Anti-Stag monoclonal antibody

From the above blots we can see, that the MtrC、MtrD and MtrE can interact with each other *in vitro*. The interaction between MtrC with MtrD and MtrE appear stronger than MtrE and MtrD. It may because the interaction between the inner membrane protein and the outer membrane protein is not persistent, so they can only form a strong interaction with the assistance of the membrane fusion protein or when the transporter is somehow activated.

4.3 study of the interaction between the MtrCDE proteins by Isothermal Titration Calorimetry

4.3.1 Sample preparation for ITC

Before starting this study, some additional constructs for the membrane fusion protein MtrC were made and the variable domains of MtrC were overexpressed and purified for the purpose of analysing their interaction with the Inner membrane protein MtrD and the outer membrane protein MtrE.

4.3.1.1 N-terminal truncated MtrC ($MtrC^{truncate}$)

After aligned MtrC with its homologue MexA, the G34 of MtrC corresponds to G25 of MexA, while MexA△1-25 was reported soluble(Higgins *et al.*, 2004). To obtain a high concentration of MtrC, but at the same time maintain the concentration of detergent with the membrane, an N-terminal transmembrane domain truncated MtrC was made by deleting 34 amino acids from N-terminus of MtrC (using primers "MtrC truncate NdeI F" and "MtrC XhoI R" in table 2.7). Therefore, the MtrC was turned into a soluble protein with three main domains, the lipoyl domain, the β-barrel domain and the α-helical hairpin.

Figure 4.9 the predicted secondary structure of MtrC (generated by on-line Secondary Structure Prediction Server: Jpred 3, which based at university of Dundee)

```
MtrC      1    MAF ASKAMRAAALAAAVALALSSCGKGGDAAQGGQPAGR
               ---------IIIIIIIIIIIIIIIIIIIIIIIIIIIIIIIIII----------
```

```
MtrC      41  EAPAPVVGVVTVHPQTVALTVELPGRLESLRTADVRAQVG
              --------         ---------          -------
MtrC      81  GI IQKRLFQEGSYVRAGQPLYQIDSSTYEAGLESARAQLA
                       --------  ------    ----HHHHHHHHHHHHHHHHHH
MtrC     121  TAQATLAKADADLARYKPLVSADAISKQEYDAAVTAKRSA
              HHHHHHHHHHHHHHHHHHHHHHHHHHHH----------HHHHHHHHHHHHHHHHHH
MtrC     161  E AGV KAAQAAI KS AGI N LNRSRITAPISGFIGQSKVSEGT
              HHHHHHHHHHHHHHHHHHHHH--------                 -------
MtrC     201  LLNAGDTTVLATIRQTNPMYVNVTQSASEVMKLRRQIAEG
                ----------       ------      --------HHHHHHHH-------
MtrC     241  KLLAADGAIAVGIKFDDGTVYPEKGRLLFADPTVEESTGQ
                ---------        ---------          ------------
MtrC     281  ITLRAAVSNDQNILMPGLYVRVLMDQVAADNAFIVPQQAV
                                 -------------      ----------
MtrC     321  TRGAKDTVMIVNAQGGMEPREVTVAQQQGTNWIVTSGLKD
                ------           -----              ----      -----
MtrC     361  GDKVVVEGISIAGMTGAKKVTPKEWAPSENQAAAPQAGVQ
                ---         --------------     --------------------------
MtrC     401  TASEAKPASEAK
                -----------------
```

The strain and construct used to overexpress MtrC^{truncate} was BL21 (DE3) [pET21a-MtrC Δ(1–34) (NdeI+XhoI)]. To overexpress the protein, one colony was used to inoculate 30ml of LB broth with 100μg/ml Carbenicillin (final concentration). 3ml of overnight culture was used to inoculate 1 litre of YT-broth with Carbenicillin. 1mM of IPTG (final concentration) was added to induce the expression of the protein when the OD600 reached 0.5-0.6. The cells were harvested 3 hour after being induced.

The cells were resuspended in lysis buffer, which was Tris 20mM NaCl 300mM Glycerol 10% DTT 1mM pH 7.5. The resuspended cells were passed through French Press 2

times at a pressure of 20KPSI. The homogenate was loaded onto a Ni-NTA chelating column after the Imidazole concentration had been adjusted to 15mM. The column was connected onto an AKTA purifier and washed with the same buffer above but with 50mM of Imidazole. Finally, the protein was eluted with above buffer containing 300mM of Imidazole.

Figure 4.10 $MtrC^{truncate}$ after purified by Nickel chelating chromatography

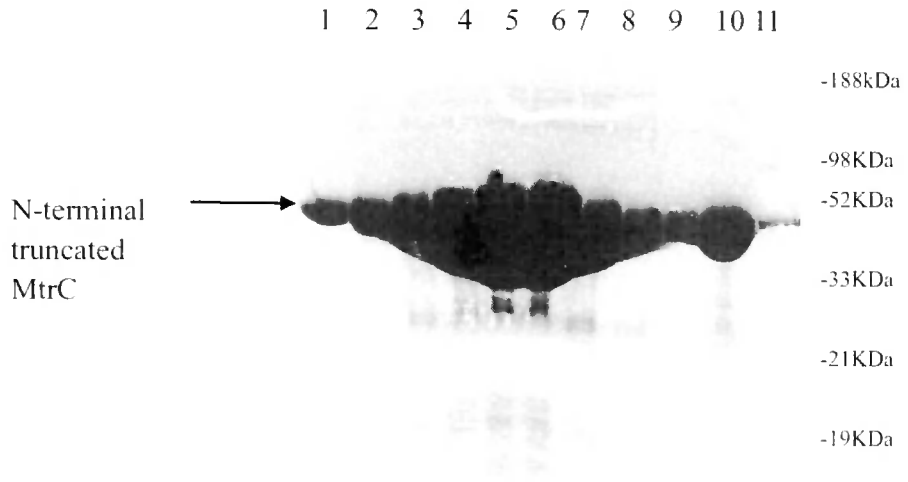

Lane 1-10: the fraction eluted from the Nickel chelating columns

Lane 11: See-Blue marker (Invitrogen)

Because the purity of the $MtrC^{truncate}$ was poor, a further gel filtration purification step was performed as following. A HiLoad 16/60 Superdex 200 gel filtration column from Amersham was equilibrated with Tris 20mM NaCl 300mM Glycerol 10% DTT 1mM pH 7.5; then 4ml of $MtrC^{truncate}$ from above was loaded onto the column using a superloop. The column was washed with the same buffer above at a the flow rate of 1ml/minute, and fractions were collected and analysized by SDS-PAGE.

Figure 4.11 Purify the $MtrC^{truncate}$ by gel filtration chromatography

Figure 4.12 MtrC^{truncate} after being purified by GF and concentrated

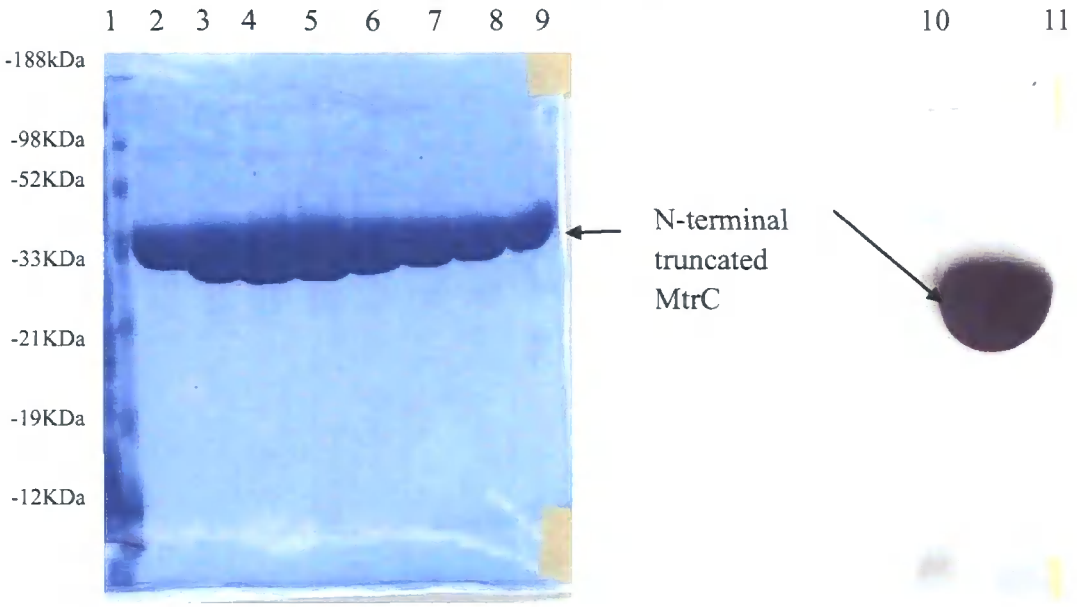

Lane 1, 10: See-Blue Marker (Invitrogen)

Lane 2-9: MtrC^{truncate} after being purified by gel filtration (20µl/lane)

Lane 11: purified MtrC^{truncate} after being concentrated (5µl/lane)

An analysis by SDS-PAGE revealed that the big peak in the graph is pure MtrC^{truncate}. The fractions were collected and concentrated using a 30kDa ultrafiltration spin column. In order to keep the same detergent concentration as for the membrane protein in ITCexperiment, DDM was added to a concentration of 0.1%, the same as for the membrane protein samples.

4.3.1.2 The construction and purification of the MtrC^{hairpin} α-helical hairpin of MtrC (MtrC^{hairpin})

Figure 4.13 Sequence alignment of the α-helical hairpin of AcrA, MexA and MtrC

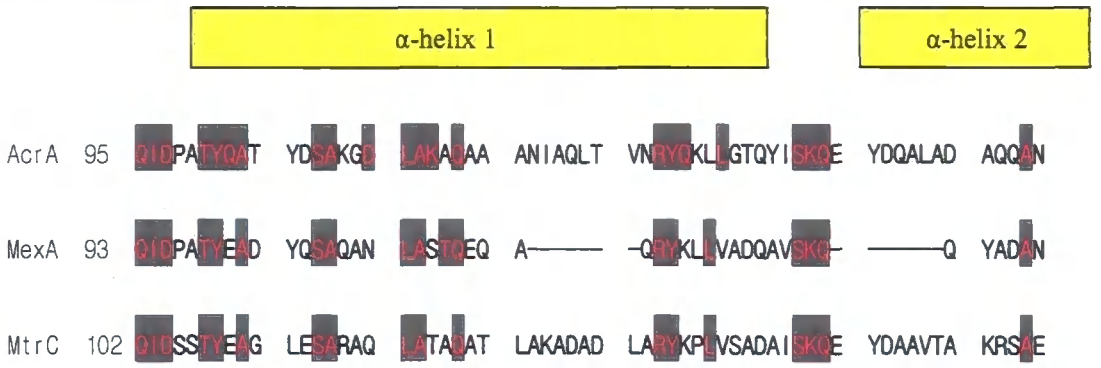

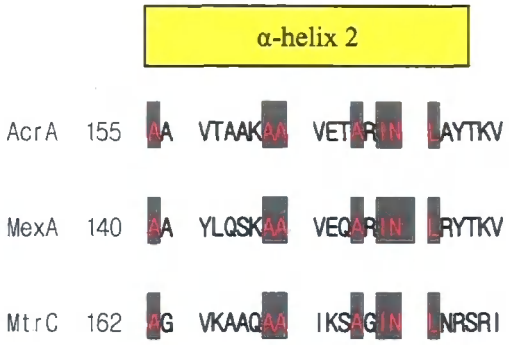

The above figure is the alignment of the α-helical hairpin of MtrC with MexA (*Pseudomonas aeruginosa*) and AcrA (*Escherichia.coli*)(Higgins *et al.*, 2004; Mikolosko *et al.*, 2006), for which the structures are known. The corresponding heptad position is shown above and the residues which are conserved are highlighted in grey and mauve.

A construct for the expressing of the $MtrC^{hairpin}$ was made using the primers "MtrC hairpin NdeI F" and "MtrC hairpin XhoI R" from table 2.7. They were designed according to the alignment above from Isoleucine (103) to Isoleucine (183). The amplified gene fragment was ligated into pET21a expression vector and was transferred to BL21 (DE3).

The recombinant strain was used to inoculate an overnight culture, and 3ml of overnight culture was used to inoculate 1 litre of YT-broth with 100μg/ml of Carbenicillin (final concentration). 1mM of IPTG was added to induce the overexpression when the OD600 reached 0.6-0.7. The cells were harvested 3 hours after being induced.

As described in Chapter 4.3.1.1, the cells were resuspended in the same buffer as $MtrC^{truncate}$ and then passed through a French Press twice. After ultracentrifugation, the supernatant was collected and loaded on a to Nickel-NTA chelating column after the Imidazole concentration had been adjusted to 10mM.

The column was connected to an AKTA purifier and washed and eluted like $MtrC^{truncate}$.

Figure 4.14 $MtrC^{hairpin}$ after purified by Nickel chelating column

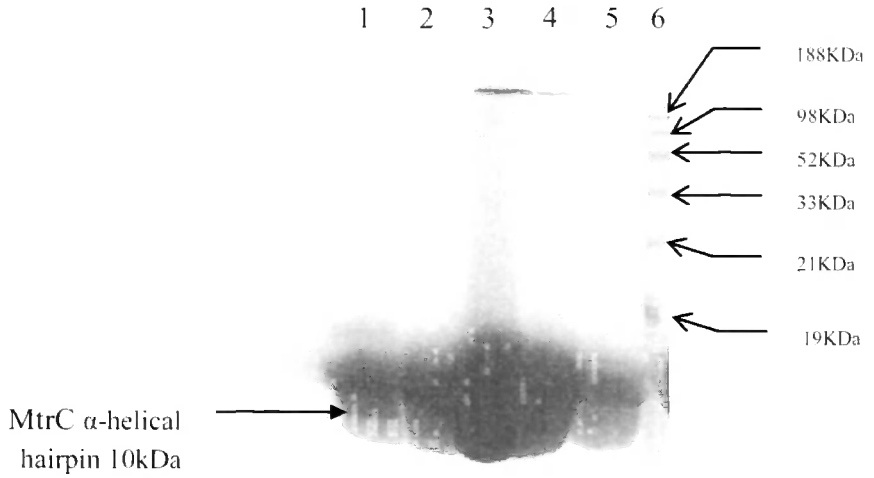

Lane 1-5: Fractions of $MtrC^{hairpin}$ purified from a Nickel chelating column

Lane 6: SeeBlue marker (Invitrogen)

The $MtrC^{hairpin}$ was also purified by gel filtration chromatography. An HiLoad 16/60 Superdex 75 gel filtration column from Amersham was employed in this study. The column was pre-equilibrated with Tris 20mM NaCl 300mM Glycerol 10% pH7.5, then the protein was loaded onto the column using a superloop. The same buffer was used to elute the protein

Figure 4.15 the Gel Filtration Chromatography of $MtrC^{hairpin}$

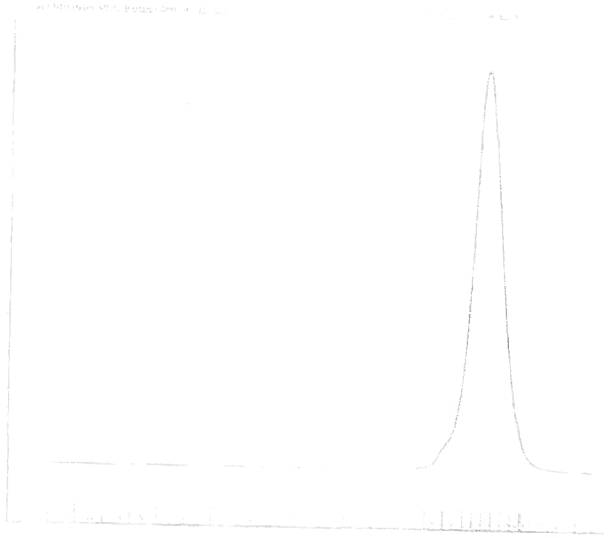

The above graph shows the elution peak for $MtrC^{hairpin}$ purified by gel filtration chromatography. Fractions were collected and analysized by 18% SDS-PAGE electrophoresis, establishing that the peak is pure hairpin

Figure 4.16 SDS-PAGE (18%) analysis of $MtrC^{hairpin}$ after being purified and concentrated

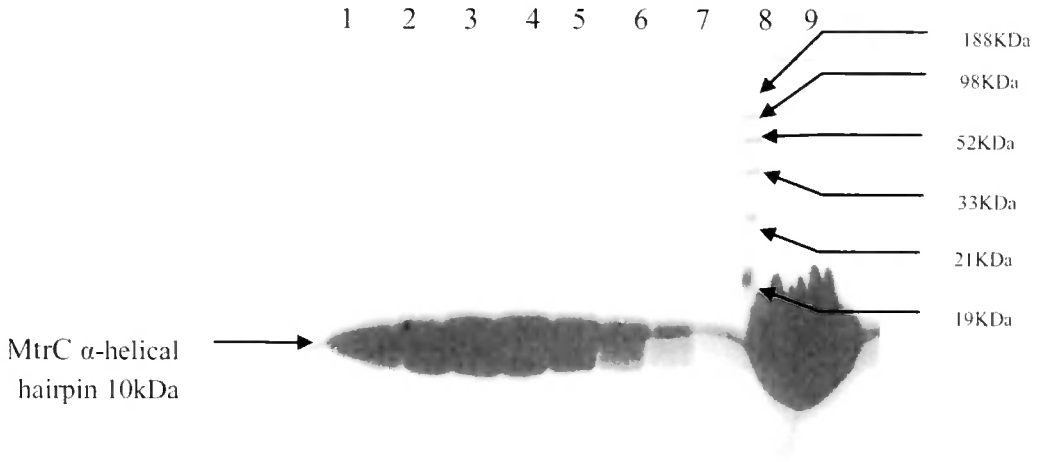

Lane 1-7: $MtrC^{hairpin}$ fractions from gel filtration chromatography

Lane 8: SeeBlue marker (Invitrogen)

Lane 9: $MtrC^{hairpin}$ after being concentrated using a 10kDa ultrafiltration spin column

The pure $MtrC^{hairpin}$ fraction was collected and concentrated using a 10kDa ultrafiltration spin column. Like $MtrC^{truncate}$, DDM was added to concentrate $MtrC^{hairpin}$ to a concentration of 0.1%.

4.3.2 ITC analysis of the interaction of the MtrCDE proteins

ITC measurements were carried out at 25°C using a VP-ITC MicroCalorimeter (MicroCal). MtrD and MtrE were in buffer Tris 20mM NaCl 300mM Glycerol 10% DDM 0.1% pH 7.5. After adding DDM to $MtrC^{truncate}$ and $MtrC^{hairpin}$ to 0.1%, they were dialysis in different dialysis cassettes at the same time with MtrD or MtrE respectively against the same buffer as above. After dialysis, the concentration of each protein was determined using a Bradford Protein assay kit.

Figure 4.17 ITC between MtrCDE

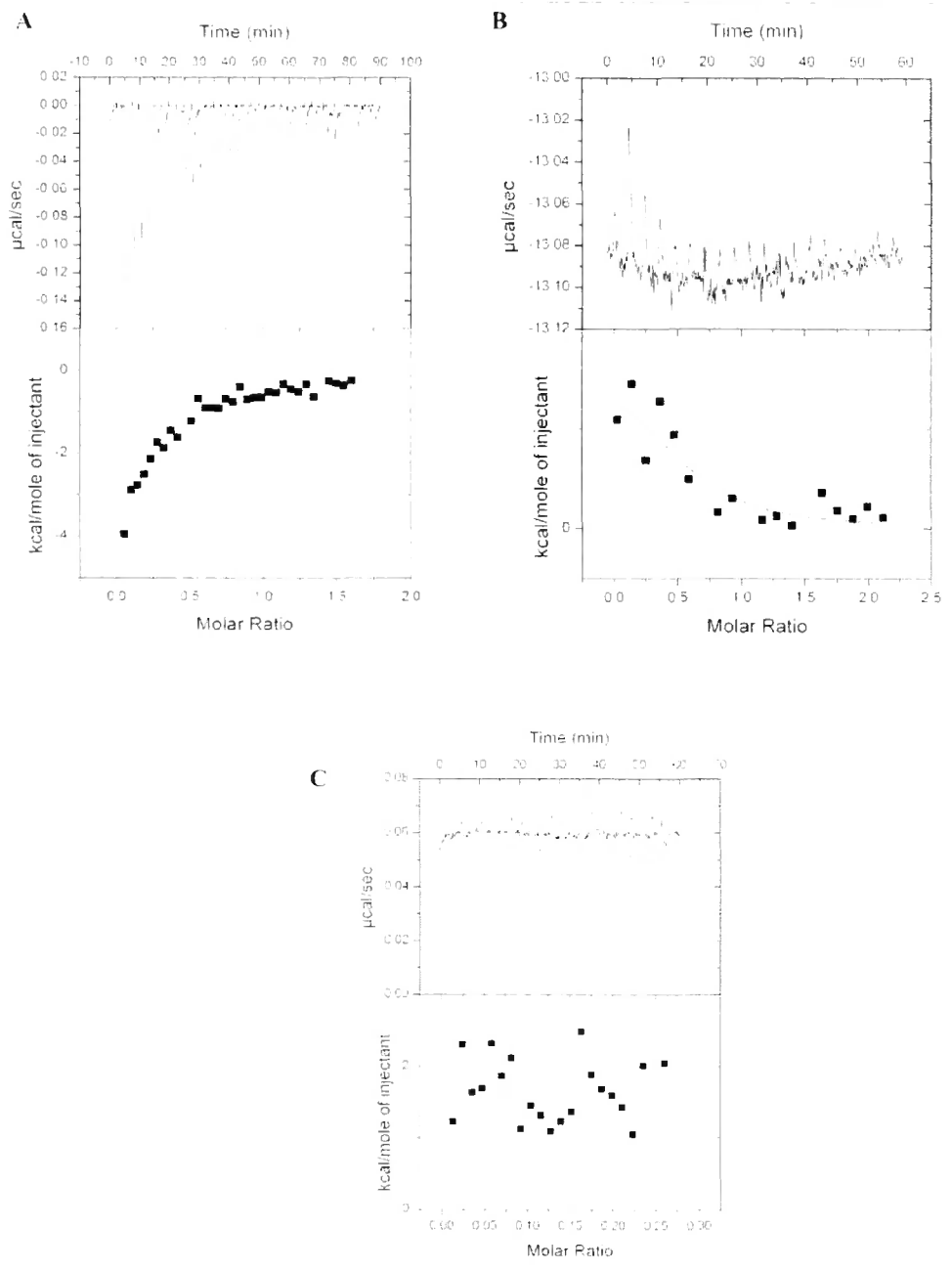

A: MtrC^{truncate} titrated into MtrE

B: MtrC^{truncate} titrated into MtrD

C: MtrE titrated into MtrD

ITC experiment were performed by stepwise titration of MtrC^{truncate} (200µM) in to the MtrE (15µM), and the heat energy change accompanying the reaction was detected upon each

injection by comparison with a reference cell. The heat changes were integrated after subtracting values obtained when MtrC was titrated into buffer (top left). The top right graph was for the titration of MtrE (15μM) into MtrD (12μM).

Figure 4.18 ITC between $MtrC^{hairpin}$ with MtrD and MtrE

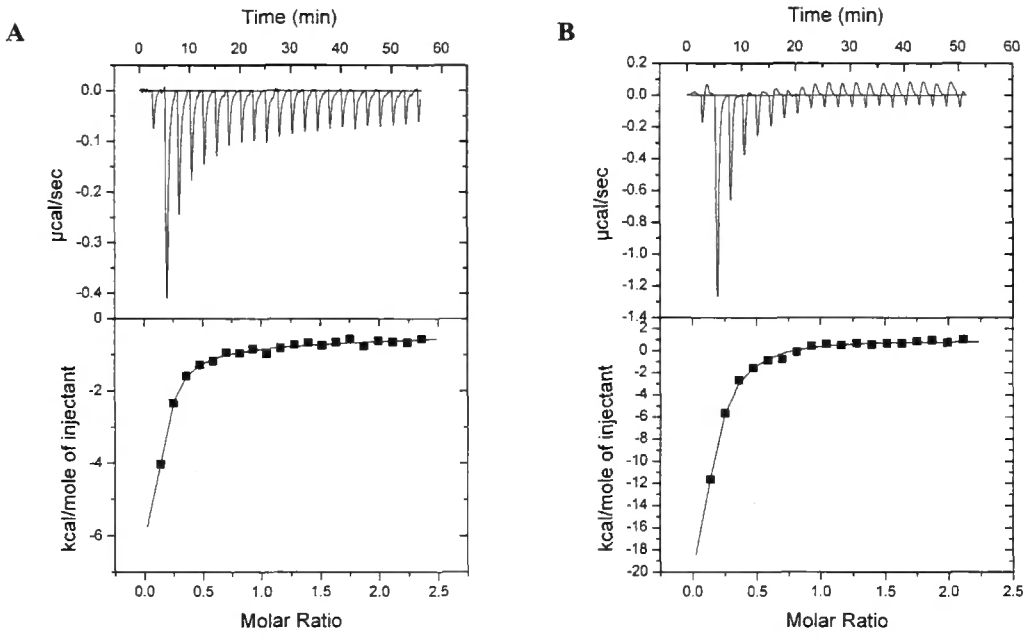

A: $MtrC^{hairpin}$ titrated into MtrE

B: $MtrC^{hairpin}$ titrated into MtrD

Similar ITC assays were carried out to study interaction of the $MtrC^{hairpin}$ with the MtrE (top left) and MtrD proteins (top right).The concentration of $MtrC^{hairpin}$ was 500 μM and the MtrE and MtrD were 15 μM and 12 μM, respectively.

Table 4.4 Thermodynamic parameters of interactions.

Protein	Phases	N	$K(M^{-1})$	$\Delta H(KCal \cdot M^{-1})$	$\Delta S(Cal \cdot M^{-1}K^{-1})$
$MtrC^{truncate}$/MtrE	1	0.258	1.0 (+ 0.50) x 10^5	-6.836	-0.01
$MtrC^{truncate}$/MtrD	1	0.238	1.2 (+ 1.2) x 10^6	1.4	32.5
$MtrC^{hairpin}$/MtrE	2	0.0915	4.6 (+ 0.61) x 10^5	-11.19	-11.4
		0.196	3.2 (+ 0.96) x 10^3	-61.49	-190
$MtrC^{hairpin}$/MtrD	2	0.0332	2.1 (+ 0.01) x 10^5	-152.4	-487
		0.663	3.1 (+ 1.22) x 10^3	266.8	906

The titration of $MtrC^{truncate}$ into MtrE is signified as $MtrC^{truncate}$/ MtrE. The number of phases indicates how many different sequential binding reactions were obtained for each titration.

When $MtrC^{truncate}$ was titrated into MtrE a weak exothermic interaction, with a K_d of 9.8M, was detected, which was characterized by a change in enthalpy (ΔH) of -6.836 kcal.mol^{-1} and entropy (ΔS) of -0.01cal.mol^{-1}.K^{-1}. In contrast, when $MtrC^{truncate}$ was titrated into MtrD, a strong endothermic reaction, with a K_d of 0.84M, was detected, which was characterized by a ΔH of 1.4 kcal.mol^{-1} and ΔS of 32.5 cal.mol^{-1}.K^{-1}. We also attempted to fit the data in each case to a two-site model: in the case of MtrE this simply indicated two sites that only had a 2-fold difference in their affinities; whilst in the case of MtrD this indicated sites with a 10-fold difference in affinity, the sum of squares of the variance of the data was greater than for a monophasic fit. In accord with our pull-down experiments that suggested that MtrD interacts weakly with MtrE, no appreciable interaction was detected by ITC. It is notable that MtrD binds MtrC an order of magnitude more strongly than MtrE binds MtrC and that this interaction is entropically driven.

ITC was used to confirm that the hairpin domain of MtrC binds to MtrE; but, interestingly, we also found that it binds to MtrD. In contrast to the binding of $MtrC^{truncate}$ to MtrD, which is an endothermic process, the binding of its $MtrC^{hairpin}$ (residues 103-183) to MtrD is an exothermic process. It is conceivable that the binding of $MtrC^{truncate}$ to MtrD is similar but only the latter endothermic process at higher molar ratios was detected; consistent with such a proposal, the baseline heat exchange for MtrD, titrated with buffer, was lower than the heat exchange at the start of the titration curve with $MtrC^{truncate}$ (data not shown). Neither the curve for the binding of the hairpin to MtrE or to MtrD could be adequately fitted to a monophasic function but both data sets could be fitted to a biphasic function, suggesting that these proteins might have both high- and low-affinity sites for the hairpin. Such finding is not fully unexpected considering the fact that both MtrE and MtrD protomers have arisen from an internal gene duplication event, and hence their trimers present a pseudo six-fold symmetry. However, whilst binding of the hairpin to both sites on MtrE were exothermic processes, with respective values for K_d, ΔH and ΔS of 2.2M, -11.2 kcal.mol^{-1} and -11.6 cal.mol^{-1}.K^{-1} for the high-affinity site, and 0.3 mM, -61.5 kcal.mol^{-1} and -190 cal.mol^{-1}.K^{-1},

respectively, for the low-affinity site; binding to the high-affinity site of MtrD was an exothermic process but to the low-affinity site an endothermic process, with values of 4.9 M, -152 kcal.mol^{-1} and -487 cal.mol^{-1}.K^{-1} and 3.3 mM, 266.8 kcal.mol^{-1} and 906 cal.mol^{-1}.K^{-1}, for the respective sites. It is noteable that the MtrC^{hairpin} is bound more tightly than MtrC^{truncate} by MtrE, whilst the MtrC^{hairpin} is bound less tightly than MtrC^{truncate} by MtrD. This is consistent with the α-helical coiled-coil domain of MtrC predominantly interacting with MtrE, whilst the β-domain of MtrC predominantly, but not exclusively, interacts with MtrD .

4.4 Circular Dichroism spectrum analysis of MtrC^{truncate} and MtrC^{hairpin}

CD spectrum analysis was performed to see if the purified MtrC^{truncate} and MtrC^{hairpin} were folded properly.

The analysis was carried out after dialysing the MtrC^{truncate} and MtrC^{hairpin} against the buffer Tris-H_2SO_4 20mM NaF 300mM pH7.5, overnight. The concentrations were caculated using a Bradford Protein Assay kit.

Figure 4.19 The CD spectrum of MtrCtruncate and MtrChairpin

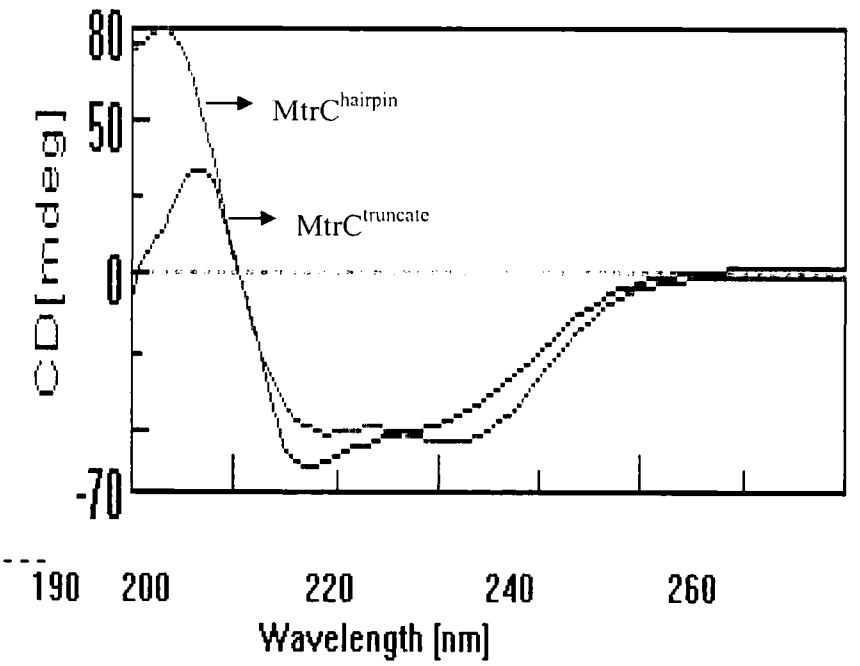

Table 4.5 Analysis of the CD spectrum data

result	Helix1	Helix2	Strand1	Strand2	Turns	Unordered	Total
$MtrC^{hairpin}$	0.707	0.284	0.000	0.009	0.000	0.000	1
	0.144	0.155	0.111	0.058	0.181	0.351	1

The secondary structure of $MtrC^{hairpin}$ was shown all α-helical structure, which resembles the secondary structure prediction and the alignment. A mixture of helix and strand was found in $MtrC^{truncate}$; from the reported homologous structures(Higgins *et al.*, 2004; Mikolosko *et al.*, 2006), it was not out of our surprise that membrane fusion proteins are composed by both α-helices and β-strands.

The data above were produced by the On Line Circular Dichroism Analysis software "DICHROWEB", which is hosted by the School of Crystallography, Birkbeck college, University of London.

4.5 Chemical cross-linking and Atomic-force-microscope (AFM) analyses of MtrCDE

The cross-linkers, EGS (spacer arm 16.1Å), DMA (spacer arm 8.6 Å) Glutaraldehyde, were used to analyses the interaction between the MtrCDE proteins. DMA is a water soluble, membrane permeable, homobifunctional imidoester cross-linker. EGS is a water insoluble, homobifunctional N-hydroxysuccinimide ester (NHS ester). Among them, EGS was the one that could cross-link the MtrCDE; DMA, on the contrary, didn't work in this study, which probably due to the shorter spacer arm it has.

Because formation of the ester between cross-linker and the amino group of the proteins renders proteins cross-linked, the free amino groups in reactions need to be eliminated. The buffer for the membrane proteins were changed to phosphate buffer by Ion Exchange chromatography, whilst the soluble N-terminal truncated MtrC and MtrC hairpin were changed into phosphate buffer at the step of gel filtration.

The stocks of DMA and EGS solution were freshly prepared in DMSO and water, to concentrations of 50mM and 100mM. The final concentrations used in this study were 20mM and 33mM. The protein samples and the cross-linker were mixed and left at room temperature

for 1 hour. The reactions were terminated by adding 100mM Tris buffer (final concentration) and mixing with loading buffer. The reactions were then heated to 100°C for 5 minutes before performing 4%-12% SDS-PAGE.

Figure 4.20 the cross-link of MtrDE with $MtrC^{hairpin}$ by EGS

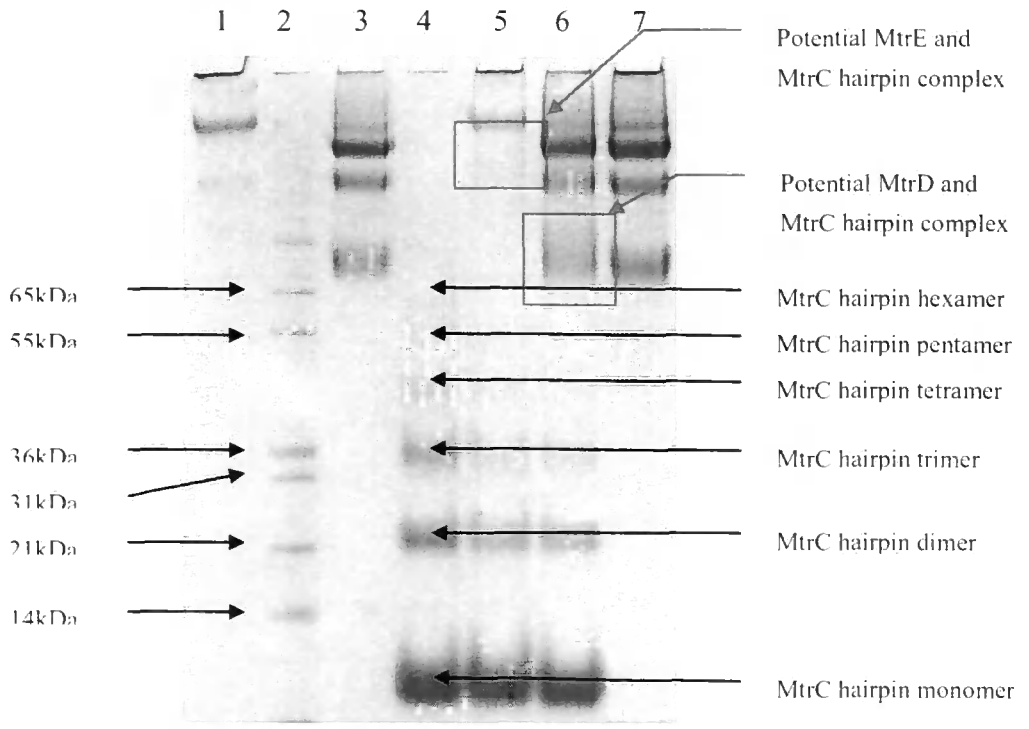

Lane 1: MtrE +EGS

Lane 2: marker

Lane 3: MtrD + EGS

Lane 4: MtrC hairpin + EGS

Lane 5: MtrC hairpin +MtrE+EGS

Lane 6: MtrC hairpin +MtrD +EGS

Lane 7: MtrD +MtrE + EGS

From the photo above, the MtrD and MtrE formed oligomers after being cross-linked by EGS. The MtrC α-helical hairpin forms up to 6 obvious bands, which represent the monomer, dimer, trimer, tetramer, pentamer and hexamer. After cross-linking the MtrC hairpin and the inner membrane protein MtrD, an extra band was shown, which may be a band for the MtrD-MtrC hairpin complex. However, the complex band of MtrE and MtrC hairpin is not

very clear. MtrD and MtrE didn't form a complex from the gel, which is reasonable because the inner membrane protein and outer membrane protein are not considered to form a stable structure.

Figure 4.21 Chemical cross-linking of MtrC with MtrD and MtrE by EGS and Gluteralderhyde

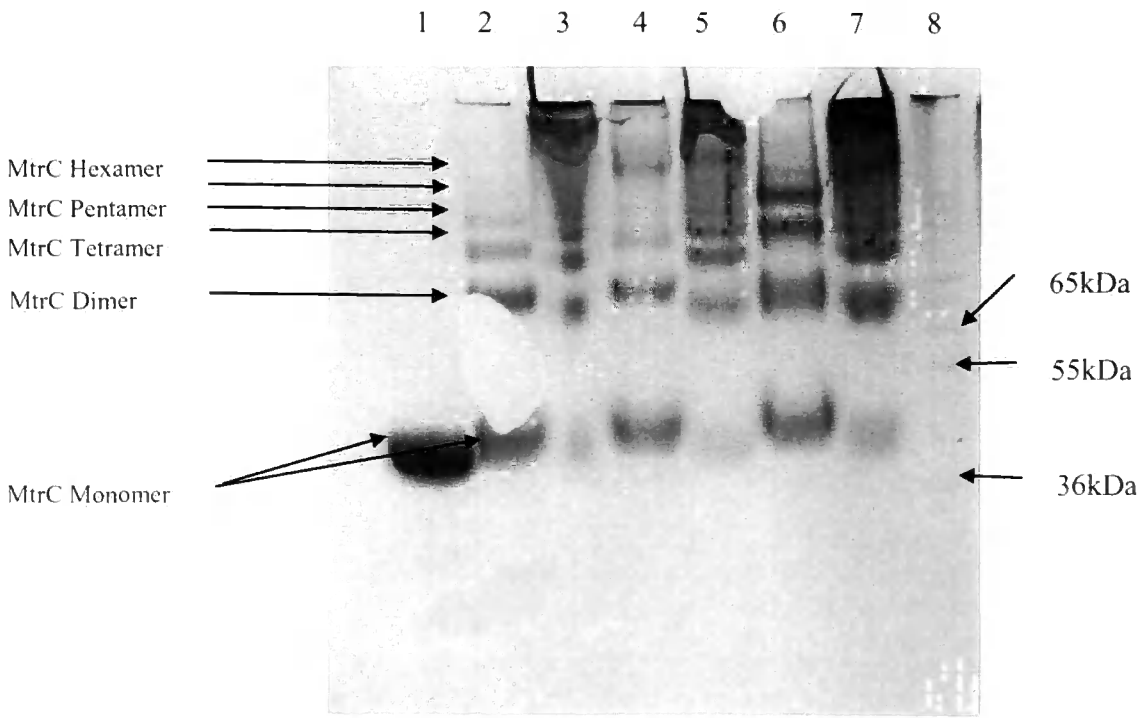

Lane 1: $MtrC^{trucated}$

Lane 2: $MtrC^{trucated}$ +EGS

Lane 3: $MtrC^{trucated}$ +Gluteralderhyde

Lane 4: MtrE+ $MtrC^{trucated}$ +EGS

Lane 5: MtrE+ $MtrC^{trucated}$ +Gluteraldehyde

Lane 6: MtrD+ $MtrC^{trucated}$ +EGS

Lane 7: MtrD+ $MtrC^{trucated}$ +Gluteralderhyde

Lane 8: Marker

After cross-linking with EGS, the $MtrC^{truncate}$ can obviously form oligomers like its α-helical hairpin domain. It could form at least 6 clear bands, which is also the same as its α-helical hairpin domain. When $MtrC^{truncate}$ was cross-linked with MtrD and MtrE, although no extra bands were found to be the potential complexes, it doesn't mean that $MtrC^{truncate}$ can

not interact with MtrD and MtrE.

Glutaraldehyde didn't work well in this study as a cross linker. The protein precipitated seriously during the cross-linking, which made the bands in the gel not clear at all. Another try with lower concentrations of glutaraldehyde needs to be performed in the future.

Figure 4.22 Cross-linking of $MtrC^{hairpin}$ with MtrD and MtrE by DMA

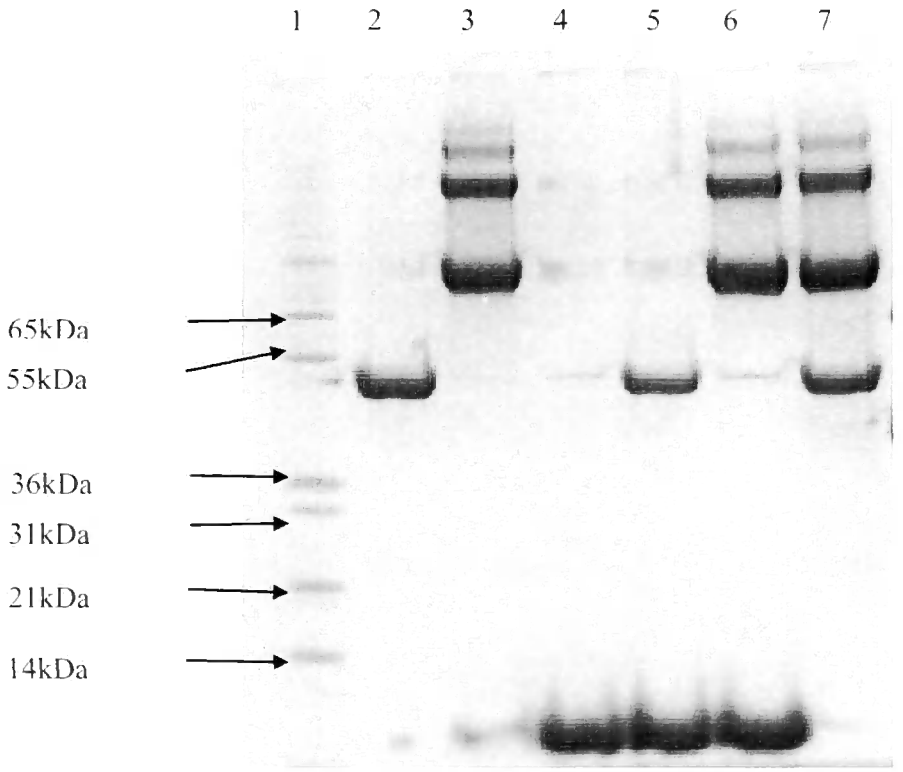

Lane 1: Marker

Lane 2: MtrE+DMA

Lane 3: MtrD+DMA

Lane 4: $MtrC^{hairpin}$+DMA

Lane 5: MtrE+ $MtrC^{hairpin}$ +DMA

Lane 6: MtrD+ $MtrC^{hairpin}$ +DMA

Lane 7: MtrD+MtrE+DMA

Using the DMA as a cross-linker, the MtrE and $MtrC^{hairpin}$ domain weren't clearly cross-linked. Moreover, there were no obvious extra bands after mixing them, which may represent the complex. Due to the short spacer arm of 8.6 Å compared with 16.1 Å for EGS, it might have attributed to the failure of DMA to cross-link MtrC hairpin.

Figure 4.23 Three dimensional imagines of MtrC hairpin domain by Atomic Force Electromicroscope (AFM) –was performed by Dr Nelson Barrera, department of Chemistry, University of Cambridge

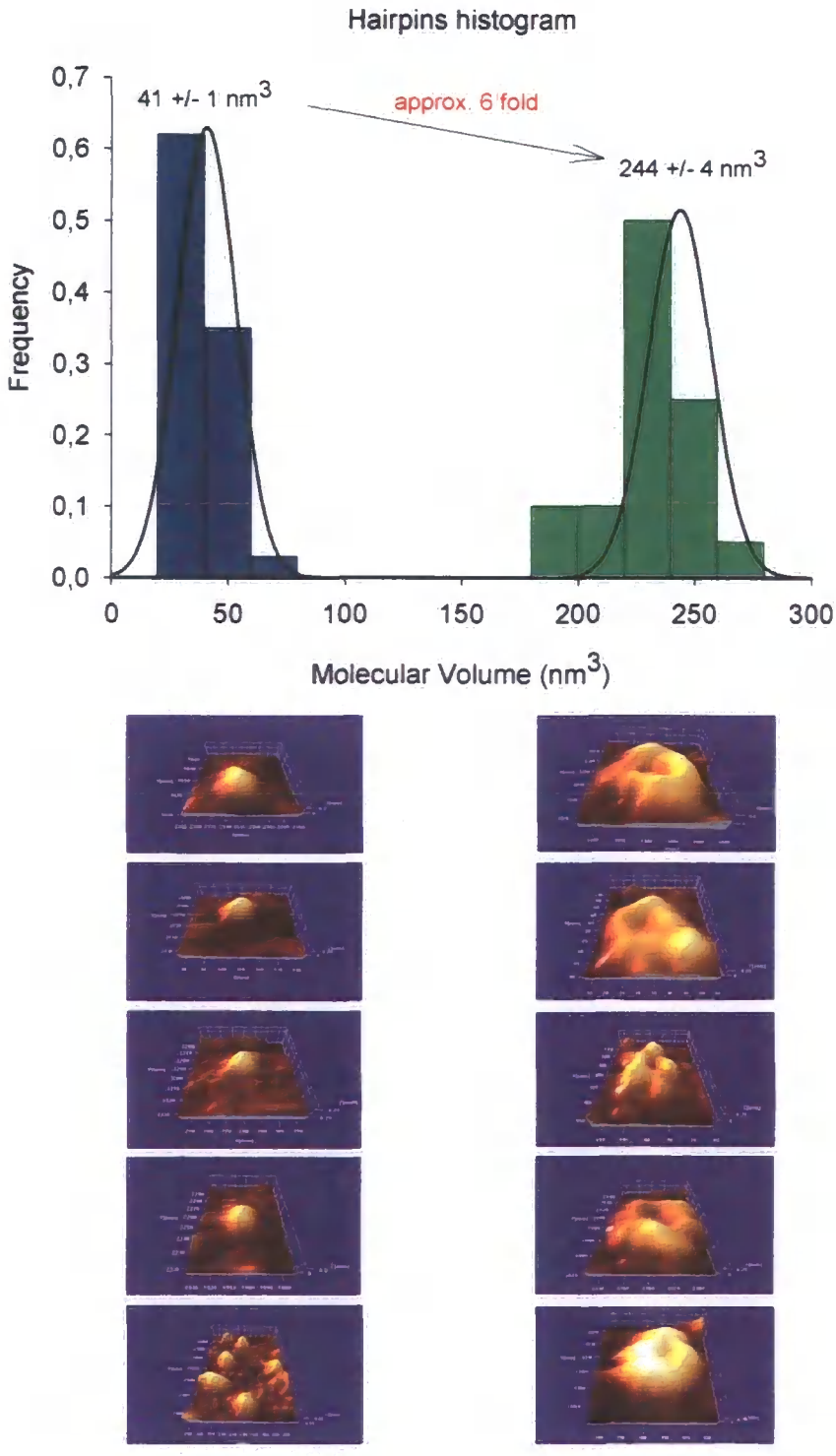

To further investigate the oligomeric state of the MtrC α-helical domain, which formed hexamers, AFM was employed to have a "deeper look" at it. The MtrC hairpin was diluted to a final concentration of 1μg/ml, and 45 μl of the sample was allowed to adsorb to freshly cleaved mica. Imaging in air was performed with a Multimode atomic force microscope (Digital Instruments, Santa Barbara, CA) in tapping mode. The silicon cantilevers containing a diamond-like extratip had a drive frequency of ≈300 kHz, a specified spring constant of 40 N/m (MikroMasch, Portland, OR) and the applied imaging force was kept as low as possible (target amplitude ≈1.6-1.8 V and amplitude set-point ≈1.3-1.5 V). The molecular volumes of the protein particles were determined from particle dimensions based on AFM images using the SPIP software (Image Metrology).

It was clear to see individual hairpins and cylindrical structure oligomers in solution by atomic-force microscopy. Frequency distribution of molecular volumes of MtrC hairpin monomers (top left) and hexamers (top right). In each case the curve indicates a fitted Gaussian function.These particles had average molecular volumes of 41 ± 1 and 243 ± 5 nm3, which is also compatible with the hexamer of MtrC hairpins.

4.6 Discussion

In gram negative bacteria, some transporters utilize a tripartite protein complex rather than a single transporter protein. These transporter systems consist of an inner membrane protein (IMP), an outer membrane protein (OMP) and a membrane fusion protein (MFP). The importance of the MFP in assembling the tripartite transporter has been reported by many research works (Mokhonov et al., 2004; Tikhonova and Zgurskaya, 2004). In order to investigate this phenomenon, we sought to determine the role of MtrC, the MFP that couples the IMP MtrD, an RND transporter, with the OMP MtrE. Three different approaches, including pull-down assays, growth curve analyses and ITC measurement were used, resemble for the existence of the stable MtrCDE complex. In pull-down assays (fig 4.8) and ITC (fig 4.17) experiments, because the previous reports of the stable interaction between MFP and IMP(Husain et al., 2004; Zgurskaya and Nikaido, 2000) or OMP(Gerken and Misra, 2004; Lobedanz *et al.*, 2007), it is not surprising that the MtrC could be co-purified with

MtrD and MtrE. However, the MtrE could be co-purified with MtrD without cross-linking was out of our expectation. This complex formed without the presence of substrate or energy supply, which indicates that the MtrD and MtrE can interact directly. This finding is in agreement with the hypothesis that the IMP directly interacts with the OMP first, then the complex is stabilized by the MFP(Tamura *et al.*, 2005). This interacton wasn't determined by ITC, probably due to the difference in the sensitivity of two experimemtal methods. The growth curve results (fig 4.2, fig 4.3) are consistent with the conclusion that MtrCDE form a functional efflux pump. We also found that MtrC enhanced the resistance to Nafcillin conferred by MtrD alone suggesting that it modulated the activity of the MtrD transporter.

By analysing the growth curves for recombinant strains which overexpressed different components of the MtrCDE system, we raised a possible mechanism of the opening of the MtrE periplasmic tunnel entrance, which is considered to be a critical event in multidrug efflux. Augustus *et al* has reported that the TolC derivative R367H, in which the intermonoer hydrogen bond between H4 and adjacent H8 from another monomer was distruped, caused the TolC to open, leading to an increased sensitivity of TolC to the large hydrophilic antibiotic, Vancomycin(Andersen *et al.*, 2002; Augustus *et al.*, 2004). Based on this principle, a series of growth curve were done to determine the opening mechanism of the MtrE. It is quite clear that due to the size of the vancomycin, it can't pass the closed periplasmic entrance of MtrE into the periplasm, which allowed the non-inhibitory growth of all the recombinant strains with the presence of vancomycin alone (fig 4.6). The presence of MtrC and MtrD, even both MtrC and MtrD, were not sufficient to trigger the opening of MtrE. In order to find the essential factor in this mechanism, the substrate Nafcillin was added to the culture along with the vancomycin. Surprisingly, the growth of the strains that overexpress MtrD and MtrE and one that expressed MtrCDE were partially inhibited, when compared with the presence of Nafcillin alone and vancomycin alone (fig 4.6). The growth inhibitory was due to the vancomycin passing through of the opened MtrE, which indicated the opening of the MtrE needed the assistance of both MtrD and substrate. However, from this result, two questions arise, firstly, is MtrC necessary for opening of MtrE? As we described above, the mutants that increase the sensitivity of TolC to vancomycin, was recently proved by crystallography can lead to a partially opened TolC (Bavro *et al.*, 2008). We propose that the interaction between

MtrD and MtrE in the presence of Nafcillin could only open the MtrE imcompletely, but it was already big enough for vancomycin to pass through, while the additional assistance of MtrC could open the MtrE completely. This proposed mechanism is highly consistant with the conclusion we got before: that the IMP interacts first with the OMP directly, and then the complex is stabilized by the MFP(Tamura *et al.*, 2005). The second question is, can MtrC alone open MtrE? Because the strain that overexpresses MtrC and MtrE didn't grow in both Nafcillin and Nafcillin with vancomycin, it is hard to decide if the growth was inhibited by the Nafcillin or Vancomycin, accordingly to make sure whether MtrE can be opened by MtrC with substrate or not. It may need to be proved by other experimental methods.

The importance of the hairpin domain of the MFP has been shown previously (Stegmeier *et al.*, 2006); apparently the function of MFP hairpin domain is to interact with the coiled-coil of the OMP and may be involve in opening the OMP channel (Krishnamoorthy *et al.*, 2008; Lobedanz *et al.*, 2007); while the C-terminal of the MFP is involved in the interaction with the IMP(Nehme *et al.*, 2004; Tikhonova *et al.*, 2002; Touze *et al.*, 2004). However, in this study, the ITC experiments showed that the α-helical hairpin domain of MtrC could interact with both IMP MtrD and the OMP MtrE (fig 4.18). To further analyses the function of the hairpin domain of MtrC, the hairpin domain was constructed with an N-terminal gIII signal sequence, to target it to the periplasm. This gIII-MtrC^{hairpin} fusion protein was co-overexpressed with MtrD and the growth situation in presence of Nafcillin was compared with the strain which can overexpress MtrD and full-length MtrC. It turned out that the growth of the strain expressing MtrD/gIII- MtrC^{hairpin} was inhibited by nafcillin, which means that the periplasmic MtrC hairpin domain can't execute the full function like full-length MtrC does. It might be that although the hairpin domain of the MFP can interact with the IMP, stablizing the IMP-OMP complex and even opening the channel of OMP, it is still not capable of performing the full function of passing the substrate to IMP without the assistance of the β-barrel domain, which has been reported to interact with the IMP (Gerken and Misra, 2004) and may take part in binding of sustrates (Borges-Walmsley *et al.*, 2003; Higgins *et al.*, 2004). After knowing the hairpin domain of MtrC can not fully assist the MtrD in substrate transport, another question arise, will the presence of the extra hairpin domain interfere in the transport function of the MtrCDE system? The periplasmic gIII- MtrC^{hairpin}

was co-overexpressed with MtrCDE to find out the answer. Interestingly, with the extra MtrC hairpin domain, the growth of the strain that overexpresses MtrCDE seemed less inhibited than the one without it (fig 4.7). This data clearly indicates that overproduction of the hairpin in the periplasm can elevated the pump function.The explanation could be, due to the finding that MFP has a flexible conformation (Mikolosko *et al.*, 2006; Vaccaro *et al.*, 2006), The MFP may emply a hing-bend motion to accomplish the function. In details, with the presence of substrate, the MFP can bind the substrate and then interact with the both IMP and OMP through the conformational change; after passing the substrate to IMP, the interaction between them is released or partially released, which leads to the weakness the the transport. Because the MtrC hairpin could interact with both MtrE and MtrD, probably hold MtrE in the open state, with the presence of extra periplasmic MtrC hairpin domain, it may confer the ability to stabilize the tripartite complex and open MtrE while the full-length MtrC works on transferring the substrates, at the same time, stabilizing the complex. The effect of the MtrC hairpin domain could be persistent because it lacks the hinge structure and can't achieve the conformational change, which makes the assembling of the pump stable and leads to the more efficient transport.

Our understanding of the oligomeric state of the MFP is still ambiguous, although forming an oligomer has been shown as a precondition of transport activity(Zgurskaya and Nikaido, 2000). The compositional stoichiometry is still uncertain, with a trimeric form found *in vivo* but a monomer form *in vitro* (Akama *et al.*, 2004b; Higgins *et al.*, 2004; Zgurskaya and Nikaido, 1999a, , 2000). In this study, *in vitro* cross-linking of MtrC was performed along with the Atomic Force Microscope (AFM) to find out the oliogmeric state of the MFP. Both $MtrC^{truncate}$ and $MtrC^{hairpin}$ showed six clear bands after being cross-linked, which indicate the presence of at least a hexamer. This result was observed better in AFM studies, showed a ring of $MtrC^{hairpin}$ domains that composed of six monomers. These results suggest that the oligomeric state of MtrC is a hexamer, which may lead to a stoichiometry of 1:2:1 (IMP:MFP:OMP) model that resembles the one proposed by Akama *et al* in 2004(Akama *et al.*, 2004b).

Chapter 5 The oligomeric state of the repressor MtrR and Characterization of MtrR when it interacts with Penicillin G and antimicrobial polypeptide LL-37

5.1 Construction and purification of MtrR

The MtrR construction described in chapter 2, for which the pET21a expression vector, was adopted again for MtrR. The gene expressing *mtrR* was amplified by primers "MtrR NdeI F" and "MtrR XhoI R" from table 2.7 with Genomic DNA of *Neisseria gonorrhoea* FA19 as template. The *E.coli* strain BL21-AI was used as the expression host this time because of its tighter regulation of expression for production of proteins using the T7 promoter.

To overexpress MtrR, one colony was used to inoculate an overnight culture and 3ml of overnight culture was used to inoculate 1 litre of YT-broth with Carbenicillin. When the OD reached 0.6-0.7, IPTG was added to a final concentration of 0.2mM and 0.04% (w/v) L-arabinose was added to induce the expression of MtrR. The temperature was then adjusted to 28°C and the cells were harvestd 3 hours after induction.

The cells were resuspended in buffer Tris 20mM NaCl 300mM Glycerol 10% pH8.0. After adding an appropriate amount of DNAase I and Proteinase inhibitor tablets, the cells were passed through French Press twice at the pressure of 20KPSI. Ultracentrifugation was performed and then the supernatant was collected.

After loading to the Nickel chelating columns, the columns were washed by Tris 20mM NaCl 300mM Glycerol 10% Imidazole 50mM pH 8.0 and the protein was eluted with the buffer above but with 300mM imidazole.

Figure 5.1 the MtrR after being purified using a Nickel chelating column

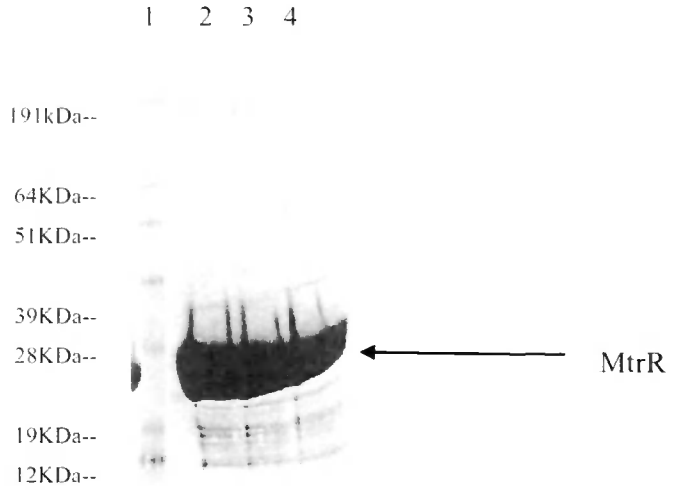

Lane 1: SeeBlue marker (Invitrogen)

Lane 2.4: MtrR fractions from Nickel chelating columns

In order to get high purity MtrR, a further gel filtration purification step was performed afterwards. An Hiload 16/60 superdex 200 prep grade gel filtration column from Amersham was equilibrated first with buffer Tris 20mM NaCl 300mM Glycerol 10% DTT 1mM pH 8.0. 5ml of MtrR protein solution was loaded onto the column using a superloop, which is designed to load a large amount of sample (up to 20ml) to chromatographic columns, then the protein was eluted with the buffer above, the fractions of two peaks were collected and analysized by SDS-PAGE electrophoresis.

Figure 5.2 the gel filtration chromatography of MtrR

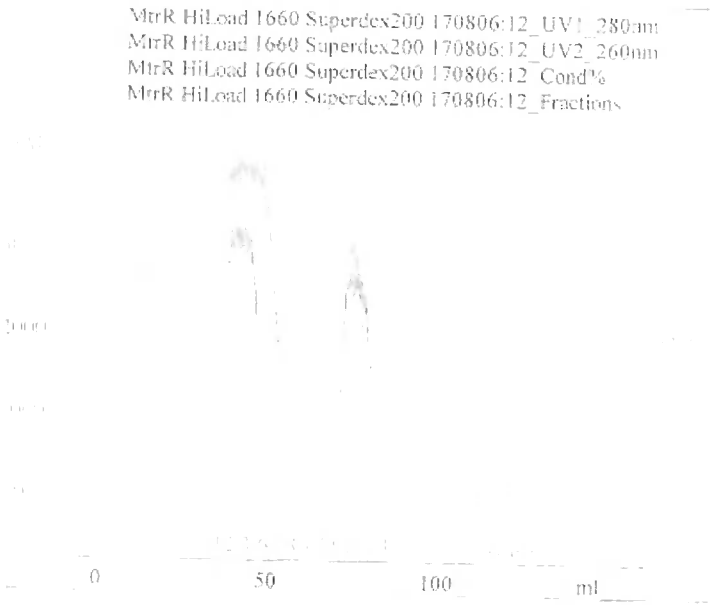

Figure 5.3 The SDS-PAGE electrophoresis analyses of fractions

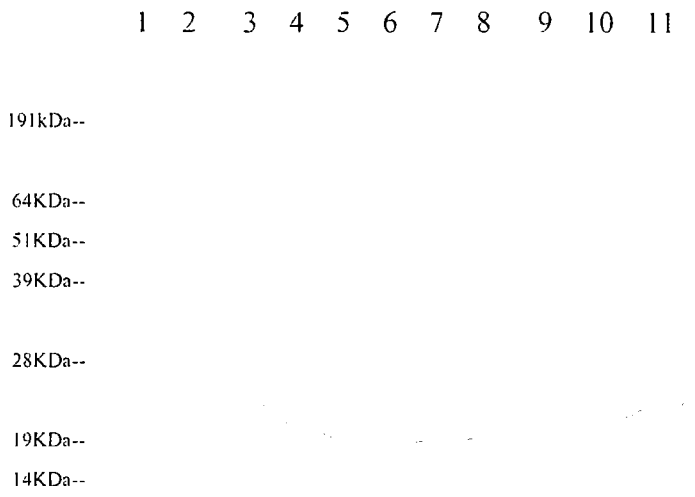

Lane 1: SeeBlue Marker (Invitrogen)

Lane 2-3: fractions of peak1

Lane 4-13: fractions of peak

From the gel, the first peak of MtrR gel filtration chromatography doesn't contain reasonable MtrR protein according to the size of the peak. This phenomenon has been found for another regulating repressor that was purified in our lab. It might due to the fact that oligomeric MtrR is able to bind the DNA from host cells, which has an absorbance at 260nm. The second peak is the pure MtrR that was used to perform the following study.

5.2 Mass spectrum analysis of MtrR

This analysis was done by Matthew F Burton in the Department of Chemistry, The mass spectrum indicated a Mr for MtrR of 25.26 kDa, which is consistent with the size of MtrR with attached 6×Histidine tag.

5.3 The oligomeric state of MtrR and cooperative bind to double-strand DNA

5.3.1 Determination of the oligomeric state of MtrR by Size Exclusion Chromatography (SEC)

A Superdex 200 PC 3.2/30 column from Amersham was adopted here for the analysis of the oligomeric state of native MtrR and when bound DNA. Initially, the column was

equilibrated with filtered and degassed buffer Tris 20mM NaCl 300mM Glycerol 10% pH 8.0. Then 50μl of sample which has been centrifuged at 13,000rpm for 10 minutes was loaded onto the column. The column was washed at a flow rate of 0.05ml/minute and the times of emergence of the samples were recorded and analysized.

Figure 5.4 Double-stranded 31-bp oligonucleotide encompassing the *mtrR*-binding site on the *mtrC* coding strand and the complementary sequence, with pseudo direct repeats underlined . (Hagman *et al.*, 1997)

5'-TTTTTATCCGTGCAATCGTGTATGTATAATG-3'

3'-AAAAATAGGCACGTTAGCACATACATATTAC-5'

Table 5.1 the standard samples for SEC

Name	Calculated MW	Log Mr	Elution volume	Kav*
Chymotrypsinogen	20.3kDa	4.31	1.94ml	0.6592
Ovalbumin	46.7kDa	4.67	1.84ml	0.5852
Adolase	182kDa	5.26	1.62ml	0.4222
Catalase	213kDa	5.33	1.58ml	0.3926
Dextran blue	-	-	1.05ml	-

*: Kav= (Ve-Vo) / (Vt-Vo)

Ve is the elution volume of each sample

Vt is the column volume, 2.4ml in this case

Vo is the void volume, which is the elution volume of Dextran blue in this case

According to the logMr and the Kav of each standard samples, a standard curve was produced and an equation for calculating the molecular mass from the elution volume derived from it.

Figure 5.5 the standard curve of SEC

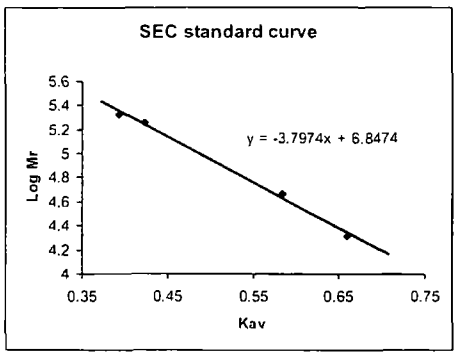

The equation for calculating the log Mr(Y axis) according to Kav (X axis) in this study is y=-3.7974x+6.8474.

To estimate the molecular mass of native MtrR and MtrR with ssDNA and dsDNA, the runs were performed as follows.

For native MtrR, 50μl of 50μM MtrR protein was loaded onto the column, and the same buffer used for the standard samples was used to elute the protein. The elution volume was recorded.

As to MtrR with ssDNA, the final concentration of MtrR (50μM) was mixed with ssDNA (20 μM) and left on ice for 15minutes.

Similarly, for dsDNA, the MtrR (50μM) was mixed with dsDNA (15μM) and left on ice for 15 minutes.

Before applying to column, all these samples were centrifuged at 13,000rpm for 10 minutes.

Figure 5.6 the size exclusion chromatography of MtrR and with ssDNA and dsDNA

Table 5.2 SEC data of native MtrR and MtrR with ssDNA and dsDNA

Name	Elution volume	Kav		Log Mr	Mr
MtrR	1.82	0.5704	by equation above	4.6814	48kDa
MtrR+ssDNA	1.89	0.6222		4.4846	30.5kDa
MtrR+dsDNA	1.66	0.4518		5.1317	135kDa

From the final Mr that we got, it is easy to see that MtrR froms a dimer in its native state; whilst a pair of dimers appear to bind to one dsDNA. Most interestingly, in the presence of ssDNA, the MtrR dimer split into a pair of monomers and forms monomer-ssDNA complex.

5.3.2 MtrR binds to operator DNA by ITC

The dsDNA that was used in SEC analysis was prepared for ITC according to the following procedure. The same 31-mer oligonucleotide and its complementary strand as the ones used in the SEC experiment above were used in this study. The two single strand oligonucleotides were annealed as described before. The dsDNA was dialysized in a different dialysis cassettes with MtrR against the buffer Tris 20mM NaCl 300mM Glycerol 10% DTT 1mM pH 8.0, overnight. The concentration of dsDNA was determined by testing the OD_{260}; then adjusting the concentration of dsDNA to 50mM with the buffer that the DNA and MtrR protein has been dialysized in.

Figure 5.7 the interaction of MtrR with 31-mer double strand oligonucleotide by ITC

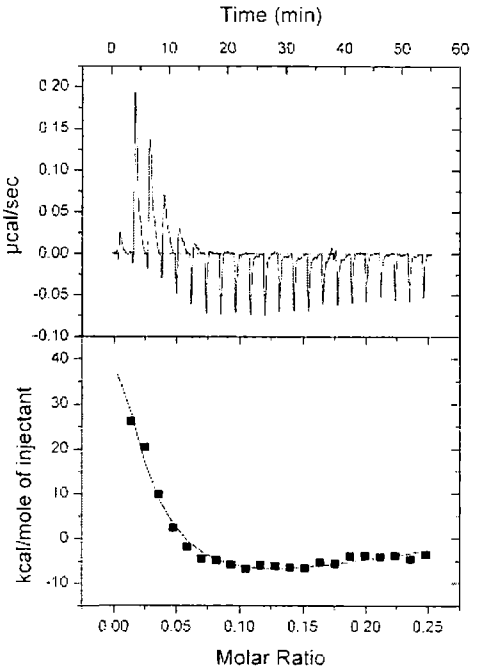

Table 5.3 Thermodynamic parameters of interaction

Protein	Phases	N	$K(M^{-1})$	$\Delta H(KCal \cdot M^{-1})$	$\Delta S(Cal \cdot M^{-1}K^{-1})$
dsDNA/MtrR	2	0.0313±0.00101	8.35×10^{7}	2.1	152
		0.204±0.0177	1.54×10^{6}	2.28	-3.48

5.4 Human antimicrobial polypeptide LL-37 binds to MtrR

5.4.1 MtrR can bind LL-37

Before applying to calorimetry analysis, the MtrR from peak two of the gel filtration chromatography (Fig 5.4) was dialysized against the buffer Tris 20mM NaCl 300mM Glycerol 10% DTT 1mM pH8.0, overnight. The buffer was collected as well as the protein for the purpose of dissolving the substrates.

Figure 5.8 the sequences of synthesized fragments of LL-37 (all the LL-37 peptide fragments were sythesized by Mr Matthew burton in the Department of Chemistry, Durham University)

Sequence of LL-37:

1 10 20 30

LLGDFFRKSKEKIGKEFKRIVQRIKDFLRNLVPRTES

LL-37 full length

Synthesized LL-37 fragments:

LLGDFFRKSKE

LL-37 NT (1-11)

FKRIVQRIKDFLR

LL-37 Core (17-29)

DFLRNLVPRTES

LL-37 CT (26-37)

Figure 5.9 LL-37 NT (1-11) titrated into MtrR

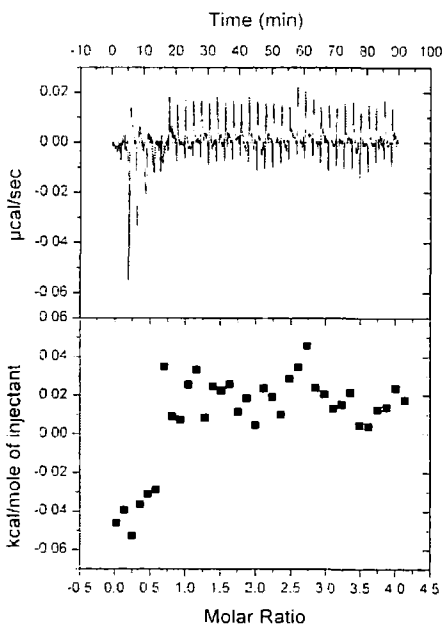

It was not surprising to find out that LL-37 NT (1-11) did not bind to MtrR from ITC. From the reported studies of LL-37, the N-terminous involves in oligomer formation instead of antimicrobial activity.

Figure 5.10 LL-37 Core (17-29) titrated into MtrR

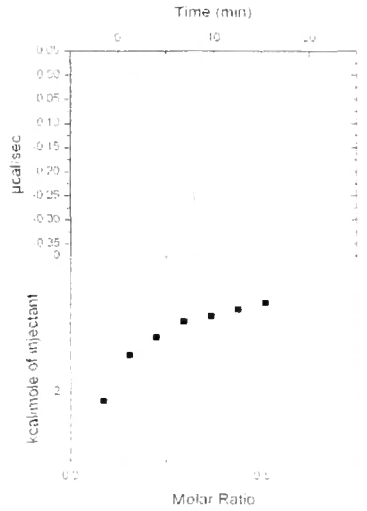

Obviously, the core part of LL-37 (17-29) can bind to MtrR from ITC. Unfortunately, the experiment wasn't accomplished due to the failure of the equipment. This needs to be conducted again once the peptide is ready; and then the thermodynamic parameter can be calculated.

Figure 5.11 LL-37 CT (26-37) titrated into MtrR

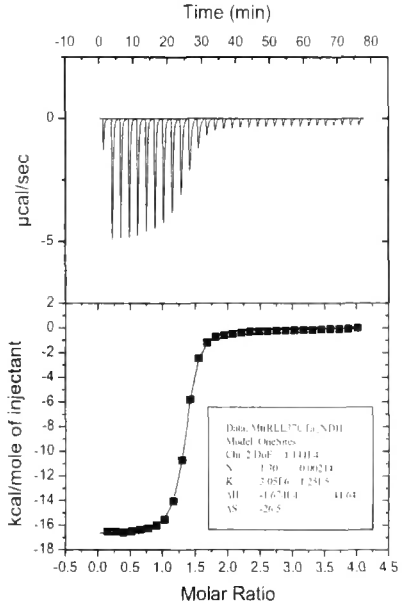

A endothermic interation was detected when 1mM of LL-37 C-terminal part (29-37) was titrated into 120μM of MtrR, with binding stoichiometry of 1.3, K_d of 0.33M , enthalpy of -16.7KCal•M^{-1} and entropy of -26.5Cal•$M^{-1}K^{-1}$.

5.4.2 LL-37 resistance is due to the overexpression of MtrCDE system

To test if the resistance to LL-37 resistance is due to MtrCDE system, a growth curve analysis was adapted to see if the pump system can export this antimicrobial polypeptide. From the above ITC data, it is already clear that the C-terminal end of LL-37 can bind MtrR. Accordingly, LL-37 CT (26-37) was used as a substrate for various recombinant strains.

Figure 5.14 growth curve of Mtr system with presence of LL-37 CT (26-37)

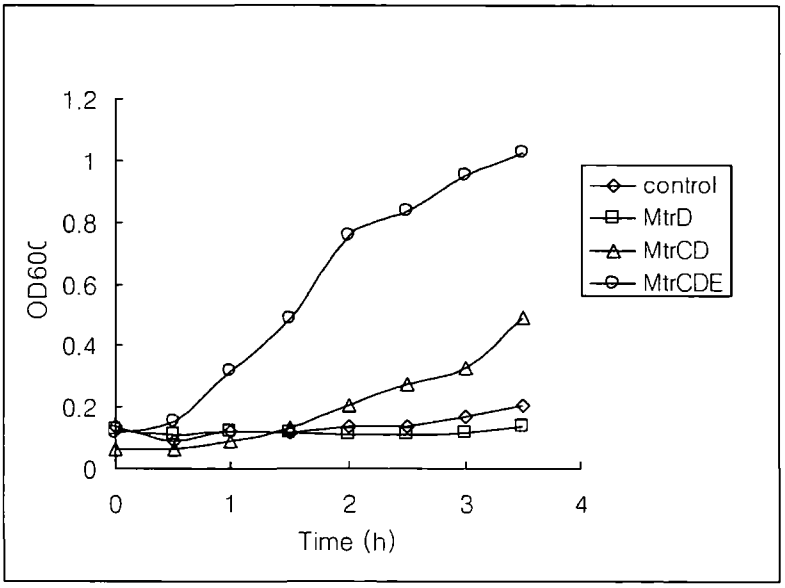

It is obvious from the growth of the control cells (Kam3/pACYC) and the one overexpress MtrD alone couldn't export the LL-37 CT, so their growth was totally inhibited. However, the strain expressing MtrC and MtrD was partially inhibited in comparison with the one that overexpress MtrCDE, which grew the fastest.

5.5 MtrR may work like a beta-lactamase

Because it has been reported that the Penicillin G (PG) resistance in *Neisseria gonorrhoea* is due to the overexpression of the Mtr system, we had the initial idea of testing

whether MtrR would bind Penicillin G. However, our ITC analysis of MtrR with PG revealed a potentially different story.

ITC was originally developed to measure binding energies and was recently introduced as a powerful tool for assaying enzyme kinetics in soluble systems and characterized by the mechanism, $E + S \Leftrightarrow ES \xrightarrow{Kcat} E + P$, Where enzyme (E) binds reversibly to the substrate (S) to form an enzyme–substrate complex (ES), which then undergoes an essentially irreversible reaction characterized by rate constant (kcat) to form product (P) and release the enzyme. As long as the enzyme is not saturated with substrate, subsequent titrations with substrate aliquots will result in increased bound enzyme concentrations in the cell and thus the differential thermal power level at each steady state will change accordingly. Once saturation is achieved, the thermal power does not change with increased substrate concentrations in the cell and instead remains constant as long as the enzymes maintain activity and the substrate to enzyme ratio remains high.

Tris-HCl buffer (Tris 20mM NaCl 300mM Glycerol 10% pH 8.0) was used initially for ITC with PG, an apparent buffer effect was found under these conditions.

Figure 5.15 Penicillin G titrated into MtrR in Tris buffer

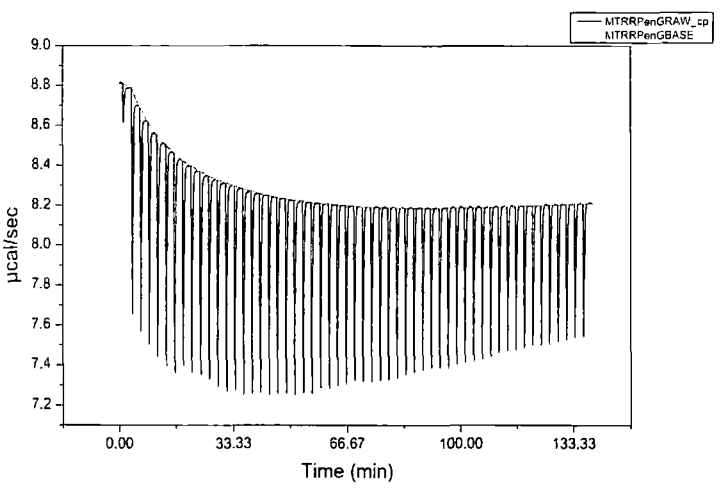

The baseline shift was caused by PG being hydrolyzed, while the buffer effect was introduced by some ingradient in the Tris-HCl buffer. A control was done to see if this was the case.

Figure 5.16 Penicillin G titrated into Tris-HCl buffer

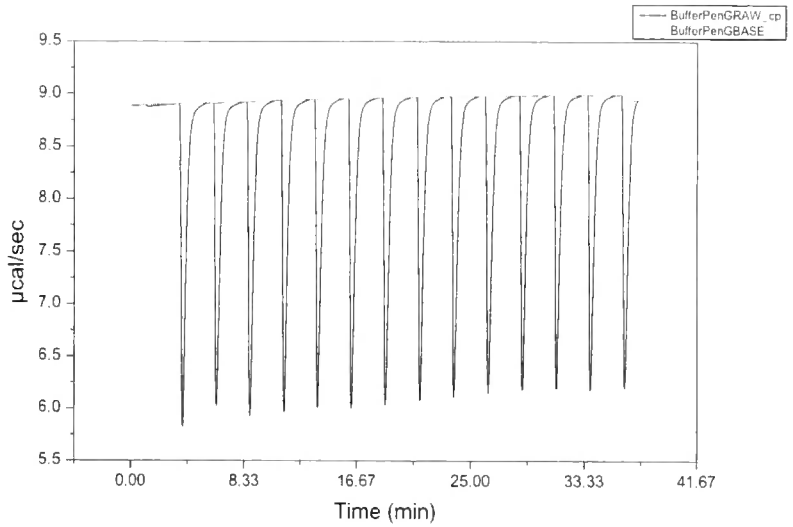

The same buffer effect appeared when the PG was titrated into Tris-HCl buffer. However, the baseline shift that appeared when titrated PG into MtrR didn't present, which suggests that PG was really hydrolyzed for some reason other than the buffer.

Phosphate buffer (Na_2HPO_4 20mM NaCl 200mM Glycerol 10% pH7.8) was then used to repeat the same titration, which was undertaken by titrating 1mM PG into 120µM MtrR at 25°C.

Figure 5.17 Enzyme-substrate reaction test of MtrR with Penicillin G by ITC with Multi Injection Method (MIM) in phosphate buffer

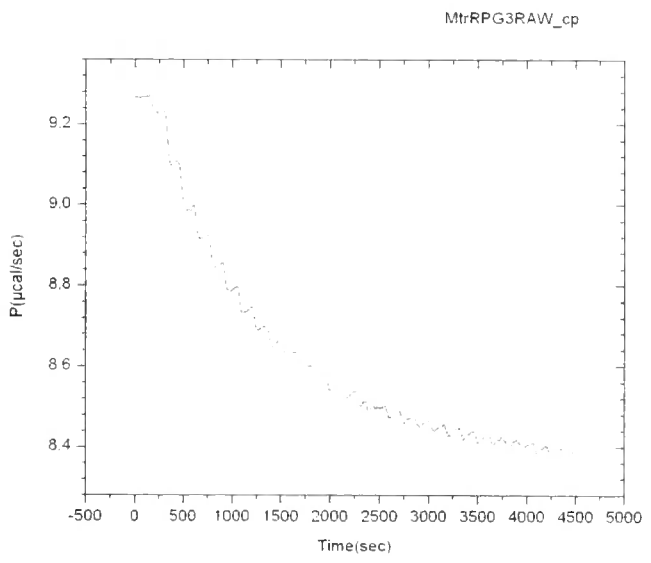

Figure 5.18 Enzyme Kinetic Parameters

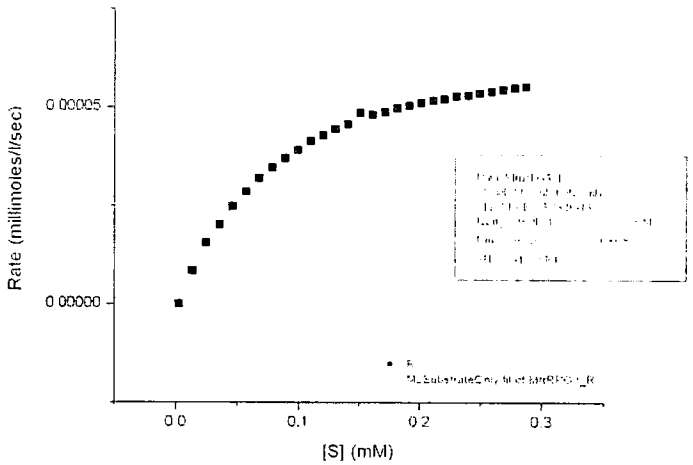

To further understand this hypothesis, His105 of MtrR was substituted to Tyr (was done by Bing Zhang, Department of Biological and Biomedical Science), which was reported to be found in Penicillin G sensitive isolates(Pan and Spratt, 1994). After titrating Penicillin G into MtrRH105Y, the Kcat, Km and Kcat/Km were shown in table 5.5.

Figure 5.19 PG titrated into MtrR H105Y

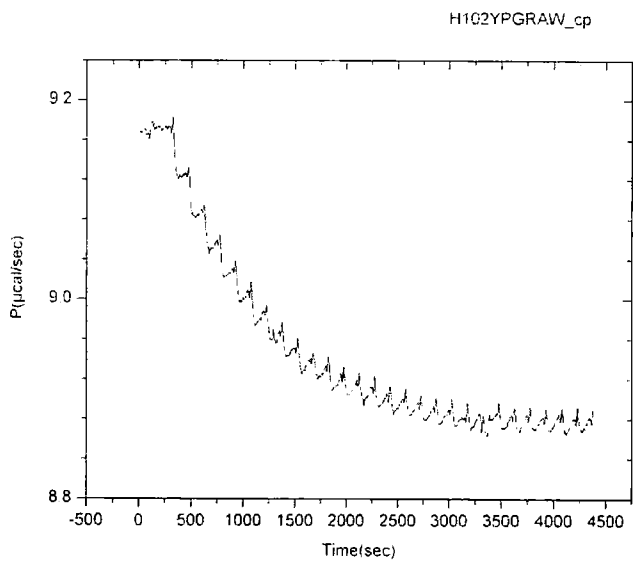

Figure 5.20 Enzyme Kinetic Parameters of MtrR H105Y with PG

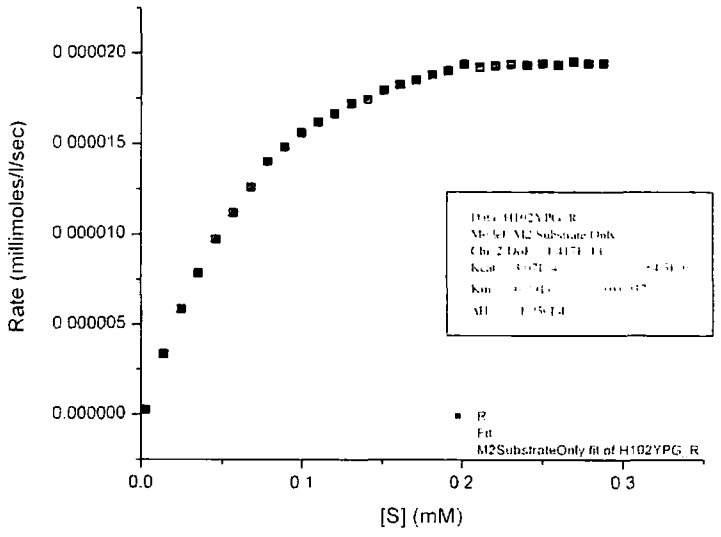

Table 5.5 Comparison of MtrR WT and MtrR H105Y

	Kcat (mM S^{-1})	Km (mM)	Kcat/Km
MtrR WT	$9.09\pm0.08\times10^{-4}$	0.12±0.0028	7.575×10^{-3}
MtrR H105Y	$3.07\pm0.045\times10^{-4}$	0.0911±0.0037	3.37×10^{-3}

The reduced Kcat/Km of MtrR H105Y showed the less activatity of mutant MtrR than wild type one.

The beta-lactamase inhibitor Clauvlanic acid was used to test if it could block the activity of MtrR. First, 1mM Clauvlanic acid was titrated into 0.1mM MtrR (in phosphate buffer) to see if they could bind to one other, then 2mM of PG was titrated directly into the mixture of MtrR with clauvlanic acid from the last titration. It showed that after binding with clauvlanic acid, MtrR is incapable of hydrolyzing Penicillin G anymore, which was reflected from the disappearance of the baseline shifting.

Figure 5.21 PG titrated into MtrR with Clavulanic acid

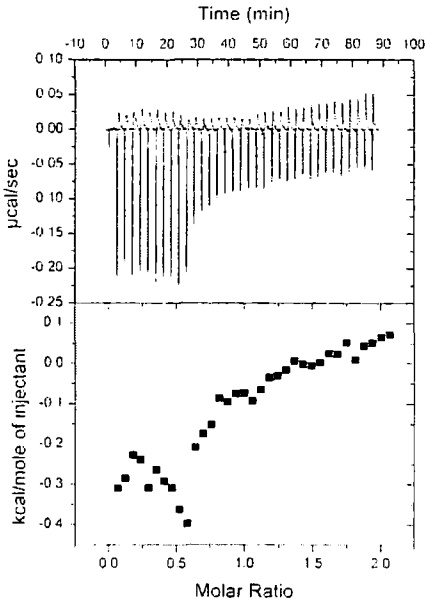

5.6 Discussion

DNA binding stoichiometry- To determine the oligomeric state of native MtrR and with its operator, Size Exclusive Chromatogrphy (SEC) was used to estimate the Mr of MtrR under non-denaturing conditions (Fig 5.6). After producing a standard curve for a series of protein with known Mr, we are able to calculate the Mr of unknown proteins according to their elution volumn. MtrR alone ran as a single protein peak, with a calculated Mr of 48 kDa that is consistent with a homodimer (with a predicted Mr of 50.5 kDa). However, upon the addition of a quartermolar concentration of dsDNA, the peak shifted forward, indicating that it forms complex with DNA. This complex had a calculated Mr of 135 kDa, consistent with the formation of a tetramer (4 protomer×25.26kDa=101KDa, 31bp×660Da/bp=25.5kDa, 126.5kDa in total), as would be expected if a pair of MtrR dimers bound to the DNA. The difference can be explaned to the non-globular overall structure of the MtrR-dsDNA complex. This result is consistent with previous work on MtrR(Hoffmann *et al.*, 2005), in which fluorescence polarization assay and Dynamic Light Scattering were used to determine the stoichiometry that MtrR employs. This DNA binding stoichiometry is the same as that utilized by TetR family member QacR(Schumacher *et al.*, 2002) but different to the other two

members, TetR which binds one dimer (Orth *et al.*, 2000) and EthR which putatively binds four dimers (Dover *et al.*, 2004). Interestingly, we found that MtrR could bind ssDNA (e.g. either strand of the promoter dsDNA) to form a complex that had a calculated Mr of 30.5 kDa, suggesting that the dimer interface was destabilised by the presence of the ssDNA.

The C-terminal fragments of LL-37 is the part that binds to MtrR- Antimicrobial peptides and their precursor molecules form the central part of human and mammalian inate immunity against both Gram-positive and Gram-negative bacteria, fungi and viruses. There are two groups of antimicrobial peptides, defensins and cathelincidins, which contribute to the peptide based defense in mammals. Defensins contain conserved cysteine residues in their sequences and exhibit characteristic β-sheet structures stabilized by intramolecular disulfide bonds(Shafer *et al.*, 1998), whilst cathelicidins are characterized by highly conserved cathelin-like pro-sequences and variable carboxyl-terminal sequences(Gennaro and Zanetti, 2000; Zanetti *et al.*, 1995). LL-37, the only cathelicidin-derived antimicrobial peptide found in humans, is a 37-residues, amphipathic helical peptide that has been shown to exhibit a broad spectrum of antimicrobial activity. The structure of LL-37 was reported as a helix-turn-helix conformation, with K12 located at the break point between the N-terminal and C-terminal helices (Hung *et al.*, 1998; Porcelli *et al.*, 2008). It has been reported that LL-37 resistance in *Neisseria gonorrhoe* is due to the *mtr* efflux system(Shafer *et al.*, 1998). Moreover, the *mtr* system was also reported to be involved in the LL-37 resistance in *Neisseria meningitides*(Tzeng et al., 2005). Our results from growth curve studies also support this report. The growth of the strain that expressed MtrCDE wasn't inhibited by LL-37, which means that MtrCDE can form a precise efflux pump to export this oligo peptide. To understand which part of LL-37 that can bind MtrR, the transcriptional repressor of the *mtr* system, a series of LL-37 fragments were synthesized and titrated into MtrR in a calorimeter. Unfortunately, these ITC experiments haven't been accomplished due to the failure of synthesiser. From the data already got, we can tell that the C-terminal part of LL-37 (17-37) can bind MtrR, whilst the N-terminal fragment (1-11) can't. This result resembles previous research that reported the C-terminal part of LL-37 has the antibacterial activity, while N-terminal has not (Buchaklian and Klug, 2006; Nagaoka *et al.*, 2002). Another important point is, that our results may bive rise to a new mechanism for amphipathic

α-helical antimicrobial peptides, which is different from the present hypothesis that LL-37 interrupts the cell membrane by its integration *via* a "barrel-stave" model or a carpet model(Henzler Wildman *et al.*, 2003; Porcelli *et al.*, 2008). If LL-37 can bind to MtrR, this possibly suggests another unknown mechanism of LL-37 antimicrobial activity other than disruption of cell membrane.

MtrR may work as a β-lactamase- This is still an ongoing work and needs to be conformed. The β-lactamase family of enzymes degrade β-lactam antibiotics and are found widely disseminated amongst Gram-positive and Gram-negative bacteria. They are excreted into the periplasm in Gram-negative bacteria. The catalytic mechanisms by which these enzymes inactivate β-lactam antibiotics are through the hydrolysis of the amide bond of the β-lactam ring (Frere, 1995; Livermore, 1995). In this study, because the MtrR was shown to belong to Penicillin G resistance *N.gonorrhoeae* by Mass Spectrometry, which has a Histidine at 105, our initial aim was to test for the interaction of MtrR with penicillin G by ITC. Surprisingly, the results looked like enzyme-hydrolysis reaction (fig 5.17), characterised by Kcat, Km and Kcat/Km with values of $9.09\pm0.08\times10^{-4}$mM S^{-1}, 0.12±0.0028 mM and 7.575×10^{-3} respectively. Moreover, this catalystical reaction could be inhibitated by the β-lactamase inhibitor clavulanic acid (fig 5.19, fig 5.20). The Penicillin G in the MtrR-PG mixture was analysized by mass spectrometry after eliminating the protein, and compared with pure Penicillin G, these studies revealed that the β-lactam ring was all hydrolyzed to the open form, while those of latter were only partially opened (was done by Matthew Burton, Department of Chemistry, data not shown). To further test this hypothesis, His105 of MtrR was substituted to Tyr, which was reported to be found in Penicillin G sensitive isolates(Pan and Spratt, 1994). After titrating Penicillin G into MtrRH105Y, the Kcat, Km and Kcat/Km values were $3.07\pm0.045\times10^{-4}$ mM S^{-1}, 0.0911±0.0037mM and 3.37×10^{-3} respectively, indicating that MtrRH105Y is less efficient than MtrRWT at hydrolyzing Penicillin G.

For the reason that the hydrolyzing activity of MtrR can be inhibited by clauvlanic acid, it might classify in Class A/D beta-lactamase, which are penicillinases, cephalosporinases, inhibited by clavulanic acid and act by a serine-based mechanism. According to this, the future work should focus on the alignment of MtrR with know beta-lactamase in same group. After finding the conserved motifs of MtrR with other beta-lactamases, mutagenesis can be

used to determine the importance of these conserved motifs.

Although all the data so far showed the beta-lactamase activity of MtrR, there is still adoubt about this finding, for example, how is it necessary to hydrolyze Penicillin G in cytoplasm while Penicillin disrupt the cell wall sythesis by binding to penicillin-Binging -Protein in periplasm? Does Penicillin G dissociate MtrR from the *mtr* promoter, enabling transcription of the MtrCDE system like other repressor? Unfortunatly, owing to time constraints, further biochemical studies could not be conducted to elucidate this clearly, but it will be an interesting direction for futher work.

Chapter 6 Final discussion

In Gram-negative bacteria, the tripartite-pumps that consist of an IMP and an OMP, as well as a periplasmic MFP, compose a pump that can span across the inner and the outer membranes, are considered to be involved in the extrusion of cytotoxic compounds, such as antibiotics and other antimicrobial compounds. To further understand how these proteins are assembled we have characterized the Neisserial MtrCDE pump, which is an important contributor in conferring resistance to penicillin and structural diverse hydrophobic agents (HAs), such as drugs, dyes, detergents and host-derived compounds (fatty acids and bile salts), as well as some cationic antimicrobial peptides, such as PC-8 and LL-37(Shafer et al., 1998; Tzeng et al., 2005)

Crystallization attempts of the Inner membrane protein MtrD and the Outer membrane protein MtrE-These two membrane protein were overexpressed and purified successfully using the non-ionic detergent DDM. A sparse matrix screen was used for establishing initial conditions and better quality crystals were produced by optimization screens, with the best crystals of MtrD and MtrE shown to diffract to 20Å and 8 Å respectively. Although we didn't elucidate the crystal structures for MtrD and MtrE yet, crystallisation trials have successfully yielded crystals that bring us a step closer to realising this potential. It is anticipated that successful structural determination will elucidate the mechanism by which MtrE interacts with its cognate antiporter MtrD. The crystal structure will also provide insights into how these three components assemble together and act as a functional efflux pump.

MtrCDE form a functional tripartite efflux pump- Using pull-down assays and ITC experiments, the MFP MtrC was shown to bind both the IMP MtrD and the OMP MtrE. In growth curve studies, the resistance of MtrD transformant could be elevated by the presence of MtrC and it was further enhanced by MtrE, indicating MtrCDE could form an extruding pump. Interestingly, the α-helical hairpin domain of MtrC binds to both MtrD and MtrE. The hairpin bound to a high-affinity site on MtrE, with a slightly greater affinity than MtrC, and with a similar affinity to MtrD, suggesting the hairpin domain is the primary domain

interacting with MtrE, while the β barrel domain and lipoyl domain is largely responsible for the high-affinity binding of MtrC to MtrD. In order to study the opening mechanism of the OMP MtrE, Vancomycin was introduced into growth curve analyses. The results showed that the presence of both the IMP MtrD and the substrates Nafcillin are required for opening of MtrE.

The MtrC hairpin domain forms a hexameric structure- The formation of the MFP oligomers has been shown as a precondition of transport activity(Zgurskaya and Nikaido, 2000). To find out the stoichiometry of binding, we used EGS as a cross-linker to test for interactions between MtrC hairpins, establishing that a number of complexes could be trapped up to and including the hexamer. Similarly, cross-linking NT-MtrC indicated that it can form hexamers. AFM images revealed that the hairpins are assembled into a cylindrical structure, which could accommodate the MtrE trimer, assuming this has similar dimensions to TolC. These results indicate that the oligomeric the MFP is an hexamer, which may lead to a stoichiometry of 1:2:1 (IMP:MFP:OMP) for the pump assembly, which resembles the one proposed by Akama et al in 2004(Akama et al., 2004b).

A possible tetrameric state for DNA-bound MtrR- Through analytical SEC, the Mr of both apo and DNA-bound forms of MtrR were calculated to be ~48kDa and ~135 kDa, which would be consistent with apo MtrR forming a dimer and a pair of dimers binding to ds DNA. Interestingly, when bound to single strand DNA, the MtrR dimer split into monomers. This result is consistent with the previous work on MtrR(Hoffmann et al., 2005). This DNA binding stoichiometry is the same as another TetR family member, QacR(Schumacher et al., 2002).

The C-terminal fragments of LL-37 can bind to MtrR- ITC was used to test for the interaction between MtrR and a vaiety of LL-37 fragments. It has been reported that LL-37 resistance in *Neisseria gonorrhoe* is due to the *mtr* efflux system(Shafer *et al.*, 1998). N-terminal 1-11), core (17-29) and C-terminal (26-37) of LL-37 were sythesised in the Department of Chemistry and tested for binding to MtrR. We showed that the C-terminal part of LL-37 is the active part in binding MtrR, with an approximate binding stiochiometry of 1:1.

This work hasn't reached a final conclusion yet, but it is anticipated that we can work out the binding domain of MtrR with this α-helical antimicrobial peptide, as well as how LL-37 regulates the expression of the *mtr* system.

MtrR may work as a ß-lactamase-This is still an ongoing work. Based on the result of catalytical reaction of Penicillin G with MtrR and that its enzymatic activity can be inhibited by β-lactamase inhibitor, we assume that MtrR works as a β-lactamase. Less activity was found for MtrRH105Y, which was reported to belong to a Penicillin G sensitive strain. Previous works have shown decreased hypersusceptibility to Penicillin that is caused by the mutantions in MtrR, but after testing the MtrR-Penicillin G interaction by ITC, stopped flow, electrophoretic mobility shift assay and Size Exlusion Chromatography, we could neither get any evidence that Penicillin binds to MtrR, nor Penicillin G could dissociate the MtrR-DNA complex. We have tested the growth of cells expressing MtrCDE, in presence of Penicillin G; these cells were unable to grow like those that don't overexpress drug pumps, indicating that theMtrCDE drug pump couldn't export Penicillin. Drawing us to further conclude, although more evidence are needed to prove our hypothesis, that MtrR acts as a β-lactamase, raised a possible mechanism of β-lactam resistance in bacteria.

Reference

Abramson, J., Smirnova, I., Kasho, V., Verner, G., Kaback, H.R., and Iwata, S. (2003) Structure and mechanism of the lactose permease of Escherichia coli. *Science* **301**: 610-615.

Aires, J.R., and Nikaido, H. (2005) Aminoglycosides are captured from both periplasm and cytoplasm by the AcrD multidrug efflux transporter of Escherichia coli. *J Bacteriol* **187**: 1923-1929.

Akama, H., Kanemaki, M., Yoshimura, M., Tsukihara, T., Kashiwagi, T., Yoneyama, H., Narita, S., Nakagawa, A., and Nakae, T. (2004a) Crystal structure of the drug discharge outer membrane protein, OprM, of Pseudomonas aeruginosa: dual modes of membrane anchoring and occluded cavity end. *J Biol Chem* **279**: 52816-52819.

Akama, H., Matsuura, T., Kashiwagi, S., Yoneyama, H., Narita, S., Tsukihara, T., Nakagawa, A., and Nakae, T. (2004b) Crystal structure of the membrane fusion protein, MexA, of the multidrug transporter in Pseudomonas aeruginosa. *J Biol Chem* **279**: 25939-25942.

Aleksandrov, A., Schuldt, L., Hinrichs, W., and Simonson, T. (2008) Tet repressor induction by tetracycline: a molecular dynamics, continuum electrostatics, and crystallographic study. *J Mol Biol* **378**: 896-910.

Andersen, C., Koronakis, E., Bokma, E., Eswaran, J., Humphreys, D., Hughes, C., and Koronakis, V. (2002) Transition to the open state of the TolC periplasmic tunnel entrance. *Proc Natl Acad Sci U S A* **99**: 11103-11108.

Aramaki, H., Yagi, N., and Suzuki, M. (1995) Residues important for the function of a multihelical DNA binding domain in the new transcription factor family of Cam and Tet repressors. *Protein Eng* **8**: 1259-1266.

Augustus, A.M., Celaya, T., Husain, F., Humbard, M., and Misra, R. (2004) Antibiotic-sensitive TolC mutants and their suppressors. *J Bacteriol* **186**: 1851-1860.

Azzaria, M., Schurr, E., and Gros, P. (1989) Discrete mutations introduced in the predicted nucleotide-binding sites of the mdr1 gene abolish its ability to confer multidrug resistance. *Mol Cell Biol* **9**: 5289-5297.

Bavro, V.N., Pietras, Z., Furnham, N., Perez-Cano, L., Fernandez-Recio, J., Pei, X.Y., Misra, R., and Luisi, B. (2008) Assembly and channel opening in a bacterial drug efflux machine. *Mol Cell* **30**: 114-121.

Bayly, A.M., Berglez, J.M., Patel, O., Castelli, L.A., Hankins, E.G., Coloe, P., Hopkins Sibley, C., and Macreadie, I.G. (2001) Folic acid utilisation related to sulfa drug resistance in Saccharomyces cerevisiae. *FEMS Microbiol Lett* **204**: 387-390.

Bayly, A.M., and Macreadie, I.G. (2002) Folic acid antagonism of sulfa drug treatments. *Trends Parasitol* **18**: 49-50.

Berens, C., Pfleiderer, K., Helbl, V., and Hillen, W. (1995) Deletion mutagenesis of Tn 10 Tet repressor--localization of regions important for dimerization and inducibility in vivo. *Mol Microbiol* **18**: 437-448.

Berens, C., Schnappinger, D., and Hillen, W. (1997) The role of the variable region in Tet repressor for inducibility by tetracycline. *J Biol Chem* **272**: 6936-6942.

Borbat, P.P., Surendhran, K., Bortolus, M., Zou, P., Freed, J.H., and McHaourab, H.S. (2007) Conformational motion of the ABC transporter MsbA induced by ATP hydrolysis. *PLoS Biol* **5**: e271.

Borges-Walmsley, M.I., Beauchamp, J., Kelly, S.M., Jumel, K., Candlish, D., Harding, S.E., Price, N.C., and Walmsley, A.R. (2003) Identification of oligomerization and drug-binding domains of the membrane fusion protein EmrA. *J Biol Chem* **278**: 12903-12912.

Boyle-Vavra, S., Carey, R.B., and Daum, R.S. (2001) Development of vancomycin and lysostaphin resistance in a methicillin-resistant Staphylococcus aureus isolate. *J Antimicrob Chemother* **48**: 617-625.

Browne, B.L., McClendon, V., and Bedwell, D.M. (1996) Mutations within the first LSGGQ motif of Ste6p cause defects in a-factor transport and mating in Saccharomyces cerevisiae. *J Bacteriol* **178**: 1712-1719.

Buchaklian, A.H., Funk, A.L., and Klug, C.S. (2004) Resting state conformation of the MsbA homodimer as studied by site-directed spin labeling. *Biochemistry* **43**: 8600-8606.

Buchaklian, A.H., and Klug, C.S. (2006) Characterization of the LSGGQ and H motifs from the Escherichia coli lipid A transporter MsbA. *Biochemistry* **45**: 12539-12546.

Butler, P.J., Ubarretxena-Belandia, I., Warne, T., and Tate, C.G. (2004) The Escherichia coli multidrug transporter EmrE is a dimer in the detergent-solubilised state. *J Mol Biol* **340**: 797-808.

Cases, I., de Lorenzo, V., and Ouzounis, C.A. (2003) Transcription regulation and environmental adaptation in bacteria. *Trends Microbiol* **11**: 248-253.

Cattoir, V. (2004) [Efflux-mediated antibiotics resistance in bacteria]. *Pathol Biol (Paris)* **52**: 607-616.

Chen, H., Bjerknes, M., Kumar, R., and Jay, E. (1994) Determination of the optimal aligned spacing between the Shine-Dalgarno sequence and the translation initiation codon of Escherichia coli mRNAs. *Nucleic Acids Res* **22**: 4953-4957.

Chen, J., Sharma, S., Quiocho, F.A., and Davidson, A.L. (2001) Trapping the transition state of an ATP-binding cassette transporter: evidence for a concerted mechanism of maltose transport. *Proc Natl Acad Sci U S A* **98**: 1525-1530.

Chen, Y.J., Pornillos, O., Lieu, S., Ma, C., Chen, A.P., and Chang, G. (2007) X-ray structure of EmrE supports dual topology model. *Proc Natl Acad Sci U S A* **104**: 18999-19004.

Das, D., Xu, Q.S., Lee, J.Y., Ankoudinova, I., Huang, C., Lou, Y., DeGiovanni, A., Kim, R., and Kim, S.H. (2007) Crystal structure of the multidrug efflux transporter AcrB at 3.1A resolution reveals the N-terminal region with conserved amino acids. *J Struct Biol* **158**: 494-502.

Dastidar, V., Mao, W., Lomovskaya, O., and Zgurskaya, H.I. (2007) Drug-induced conformational changes in multidrug efflux transporter AcrB from Haemophilus influenzae. *J Bacteriol* **189**: 5550-5558.

Daus, M.L., Grote, M., Muller, P., Doebber, M., Herrmann, A., Steinhoff, H.J., Dassa, E., and Schneider, E. (2007) ATP-driven MalK dimer closure and reopening and conformational changes of the "EAA" motifs are crucial for function of the maltose ATP-binding cassette transporter (MalFGK2). *J Biol Chem* **282**: 22387-22396.

Davidson, A.L., and Maloney, P.C. (2007) ABC transporters: how small machines do a big job. *Trends Microbiol* **15**: 448-455.

Dawson, R.J., and Locher, K.P. (2006) Structure of a bacterial multidrug ABC transporter. *Nature* **443**: 180-185.

Delahay, R.M., Robertson, B.D., Balthazar, J.T., Shafer, W.M., and Ison, C.A. (1997) Involvement of the gonococcal MtrE protein in the resistance of Neisseria gonorrhoeae to toxic hydrophobic agents. *Microbiology* **143 (Pt 7)**: 2127-2133.

Dong, J., Yang, G., and McHaourab, H.S. (2005) Structural basis of energy transduction in the transport cycle of MsbA. *Science* **308**: 1023-1028.

Dover, L.G., Corsino, P.E., Daniels, I.R., Cocklin, S.L., Tatituri, V., Besra, G.S., and Futterer, K. (2004) Crystal structure of the TetR/CamR family repressor Mycobacterium tuberculosis EthR implicated in ethionamide resistance. *J Mol Biol* **340**: 1095-1105.

Eckford, P.D., and Sharom, F.J. (2008) Functional characterization of Escherichia coli MsbA: interaction with nucleotides and substrates. *J Biol Chem* **283**: 12840-12850.

Elkins, C.A., and Nikaido, H. (2002) Substrate specificity of the RND-type multidrug efflux pumps AcrB and AcrD of Escherichia coli is determined predominantly by two large periplasmic loops. *J Bacteriol* **184**: 6490-6498.

Elkins, C.A., and Nikaido, H. (2003) Chimeric analysis of AcrA function reveals the importance of its C-terminal domain in its interaction with the AcrB multidrug efflux pump. *J Bacteriol* **185**: 5349-5356.

Eswaran, J., Hughes, C., and Koronakis, V. (2003) Locking TolC entrance helices to prevent protein translocation by the bacterial type I export apparatus. *J Mol Biol* **327**: 309-315.

Federici, L., Du, D., Walas, F., Matsumura, H., Fernandez-Recio, J., McKeegan, K.S., Borges-Walmsley, M.I., Luisi, B.F., and Walmsley, A.R. (2005) The crystal structure of the outer membrane protein VceC from the bacterial pathogen Vibrio cholerae at 1.8 A resolution. *J Biol Chem* **280**: 15307-15314.

Fernandez-Recio, J., Walas, F., Federici, L., Venkatesh Pratap, J., Bavro, V.N., Miguel, R.N., Mizuguchi, K., and Luisi, B. (2004) A model of a transmembrane drug-efflux pump from Gram-negative bacteria. *FEBS Lett* **578**: 5-9.

Fontana, R., Canepari, P., Lleo, M.M., and Satta, G. (1990) Mechanisms of resistance of enterococci to beta-lactam antibiotics. *Eur J Clin Microbiol Infect Dis* **9**: 103-105.

Frenois, F., Engohang-Ndong, J., Locht, C., Baulard, A.R., and Villeret, V. (2004) Structure of EthR in a ligand bound conformation reveals therapeutic perspectives against tuberculosis. *Mol Cell* **16**: 301-307.

Frere, J.M. (1995) Beta-lactamases and bacterial resistance to antibiotics. *Mol Microbiol* **16**: 385-395.

Gennaro, R., and Zanetti, M. (2000) Structural features and biological activities of the cathelicidin-derived antimicrobial peptides. *Biopolymers* **55**: 31-49.

Gerken, H., and Misra, R. (2004) Genetic evidence for functional interactions between TolC and AcrA proteins of a major antibiotic efflux pump of Escherichia coli. *Mol Microbiol* **54**: 620-631.

Gil, H., Platz, G.J., Forestal, C.A., Monfett, M., Bakshi, C.S., Sellati, T.J., Furie, M.B., Benach, J.L., and Thanassi, D.G. (2006) Deletion of TolC orthologs in Francisella tularensis identifies roles in multidrug resistance and virulence. *Proc Natl Acad Sci U S A* **103**: 12897-12902.

Goldberg, M., Pribyl, T., Juhnke, S., and Nies, D.H. (1999) Energetics and topology of CzcA, a cation/proton antiporter of the resistance-nodulation-cell division protein family. *J Biol Chem* **274**: 26065-26070.

Gotoh, N., Kusumi, T., Tsujimoto, H., Wada, T., and Nishino, T. (1999) Topological analysis of an RND family transporter, MexD of Pseudomonas aeruginosa. *FEBS Lett* **458**: 32-36.

Grkovic, S., Brown, M.H., Roberts, N.J., Paulsen, I.T., and Skurray, R.A. (1998) QacR is a repressor protein that regulates expression of the Staphylococcus aureus multidrug efflux pump QacA. *J Biol Chem* **273**: 18665-18673.

Grkovic, S., Brown, M.H., Schumacher, M.A., Brennan, R.G., and Skurray, R.A. (2001) The staphylococcal QacR multidrug regulator binds a correctly spaced operator as a pair of dimers. *J Bacteriol* **183**: 7102-7109.

Grkovic, S., Brown, M.H., and Skurray, R.A. (2002) Regulation of bacterial drug export systems. *Microbiol Mol Biol Rev* **66**: 671-701, table of contents.

Guan, L., Ehrmann, M., Yoneyama, H., and Nakae, T. (1999) Membrane topology of the xenobiotic-exporting subunit, MexB, of the MexA,B-OprM extrusion pump in Pseudomonas aeruginosa. *J Biol Chem* **274**: 10517-10522.

Guan, L., and Nakae, T. (2001) Identification of essential charged residues in transmembrane segments of the multidrug transporter MexB of Pseudomonas aeruginosa. *J Bacteriol* **183**: 1734-1739.

Guan, L., Mirza, O., Verner, G., Iwata, S., and Kaback, H.R. (2007) Structural determination of wild-type lactose permease. *Proc Natl Acad Sci U S A* **104**: 15294-15298.

Hagman, K.E., Pan, W., Spratt, B.G., Balthazar, J.T., Judd, R.C., and Shafer, W.M. (1995) Resistance of Neisseria gonorrhoeae to antimicrobial hydrophobic agents is modulated by the mtrRCDE efflux system. *Microbiology* **141 (Pt 3)**: 611-622.

Hagman, K.E., and Shafer, W.M. (1995) Transcriptional control of the mtr efflux system of Neisseria gonorrhoeae. *J Bacteriol* **177**: 4162-4165.

Hagman, K.E., Lucas, C.E., Balthazar, J.T., Snyder, L., Nilles, M., Judd, R.C., and Shafer, W.M. (1997) The MtrD protein of Neisseria gonorrhoeae is a member of the resistance/nodulation/division protein family constituting part of an efflux system. *Microbiology* **143 (Pt 7)**: 2117-2125.

Hanaki, H., Labischinski, H., Inaba, Y., Kondo, N., Murakami, H., and Hiramatsu, K. (1998) Increase in glutamine-non-amidated muropeptides in the peptidoglycan of vancomycin-resistant Staphylococcus aureus strain Mu50. *J Antimicrob Chemother* **42**: 315-320.

Hasdemir, U. (2007) [The role of cell wall organization and active efflux pump systems in multidrug resistance of bacteria]. *Mikrobiyol Bul* **41**: 309-327.

Hearn, E.M., Gray, M.R., and Foght, J.M. (2006) Mutations in the central cavity and periplasmic domain affect efflux activity of the resistance-nodulation-division pump EmhB from Pseudomonas fluorescens cLP6a. *J Bacteriol* **188**: 115-123.

Hecht, B., Muller, G., and Hillen, W. (1993) Noninducible Tet repressor mutations map from the operator binding motif to the C terminus. *J Bacteriol* **175**: 1206-1210.

Henssler, E.M., Scholz, O., Lochner, S., Gmeiner, P., and Hillen, W. (2004) Structure-based design of Tet repressor to optimize a new inducer specificity. *Biochemistry* **43**: 9512-9518.

Henzler Wildman, K.A., Lee, D.K., and Ramamoorthy, A. (2003) Mechanism of lipid bilayer disruption by the human antimicrobial peptide, LL-37. *Biochemistry* **42**: 6545-6558.

Higgins, M.K., Bokma, E., Koronakis, E., Hughes, C., and Koronakis, V. (2004) Structure of the periplasmic component of a bacterial drug efflux pump. *Proc Natl Acad Sci U S A* **101**: 9994-9999.

Hinrichs, W., Kisker, C., Duvel, M., Muller, A., Tovar, K., Hillen, W., and Saenger, W. (1994) Structure of the Tet repressor-tetracycline complex and regulation of antibiotic resistance. *Science* **264**: 418-420.

Hoffmann, K.M., Williams, D., Shafer, W.M., and Brennan, R.G. (2005) Characterization of the multiple transferable resistance repressor, MtrR, from Neisseria gonorrhoeae. *J Bacteriol* **187**: 5008-5012.

Hollenstein, K., Dawson, R.J., and Locher, K.P. (2007a) Structure and mechanism of ABC transporter proteins. *Curr Opin Struct Biol* **17**: 412-418.

Hollenstein, K., Frei, D.C., and Locher, K.P. (2007b) Structure of an ABC transporter in complex with its binding protein. *Nature* **446**: 213-216.

Hung, L.W., Wang, I.X., Nikaido, K., Liu, P.Q., Ames, G.F., and Kim, S.H. (1998) Crystal structure of the ATP-binding subunit of an ABC transporter. *Nature* **396**: 703-707.

Husain, F., Humbard, M., and Misra, R. (2004) Interaction between the TolC and AcrA proteins of a multidrug efflux system of Escherichia coli. *J Bacteriol* **186**: 8533-8536.

Hvorup, R.N., Goetz, B.A., Niederer, M., Hollenstein, K., Perozo, E., and Locher, K.P. (2007) Asymmetry in the structure of the ABC transporter-binding protein complex BtuCD-BtuF. *Science* **317**: 1387-1390.

Ip, H., Stratton, K., Zgurskaya, H., and Liu, J. (2003) pH-induced conformational changes of AcrA, the membrane fusion protein of Escherichia coli multidrug efflux system. *J Biol Chem* **278**: 50474-50482.

Jeng, W.Y., Ko, T.P., Liu, C.I., Guo, R.T., Liu, C.L., Shr, H.L., and Wang, A.H. (2008) Crystal structure of IcaR, a repressor of the TetR family implicated in biofilm formation in Staphylococcus epidermidis. *Nucleic Acids Res* **36**: 1567-1577.

Jha, S., Karnani, N., Dhar, S.K., Mukhopadhayay, K., Shukla, S., Saini, P., Mukhopadhayay, G., and Prasad, R. (2003) Purification and characterization of the N-terminal nucleotide binding domain of an ABC drug transporter of Candida albicans: uncommon cysteine 193 of Walker A is critical for ATP hydrolysis. *Biochemistry* **42**: 10822-10832.

Johnson, S.R., Sandul, A.L., Parekh, M., Wang, S.A., Knapp, J.S., and Trees, D.L. (2003) Mutations causing in vitro resistance to azithromycin in Neisseria gonorrhoeae. *Int J Antimicrob Agents* **21**: 414-419.

Jones, P.M., and George, A.M. (2002) Mechanism of ABC transporters: a molecular dynamics simulation of a well characterized nucleotide-binding subunit. *Proc Natl Acad Sci U S A* **99**: 12639-12644.

Kaback, H.R. (2005) Structure and mechanism of the lactose permease. *C R Biol* **328**: 557-567.

Kasahara, T., and Kasahara, M. (2003) Transmembrane segments 1, 5, 7 and 8 are required for high-affinity glucose transport by Saccharomyces cerevisiae Hxt2 transporter. *Biochem J* **372**: 247-252.

Kawabe, T., Fujihira, E., and Yamaguchi, A. (2000) Molecular construction of a multidrug exporter system, AcrAB: molecular interaction between AcrA and AcrB, and cleavage of the N-terminal signal sequence of AcrA. *J Biochem* **128**: 195-200.

Kedracka-Krok, S., Gorecki, A., Bonarek, P., and Wasylewski, Z. (2005) Kinetic and thermodynamic studies of tet repressor-tetracycline interaction. *Biochemistry* **44**: 1037-1046.

Korkhov, V.M., and Tate, C.G. (2008) Electron crystallography reveals plasticity within the drug binding site of the small multidrug transporter EmrE. *J Mol Biol* **377**: 1094-1103.

Koronakis, V., Sharff, A., Koronakis, E., Luisi, B., and Hughes, C. (2000) Crystal structure of the bacterial membrane protein TolC central to multidrug efflux and protein export. *Nature* **405**: 914-919.

Krell, T., Teran, W., Mayorga, O.L., Rivas, G., Jimenez, M., Daniels, C., Molina-Henares, A.J., Martinez-Bueno, M., Gallegos, M.T., and Ramos, J.L. (2007) Optimization of the palindromic order of the TtgR operator enhances binding cooperativity. *J Mol Biol* **369**: 1188-1199.

Krishnamoorthy, G., Tikhonova, E.B., and Zgurskaya, H.I. (2008) Fitting periplasmic membrane fusion proteins to inner membrane transporters: mutations that enable Escherichia coli AcrA to function with Pseudomonas aeruginosa MexB. *J Bacteriol* **190**: 691-698.

Lanig, H., Othersen, O.G., Beierlein, F.R., Seidel, U., and Clark, T. (2006) Molecular dynamics simulations of the tetracycline-repressor protein: the mechanism of induction. *J Mol Biol* **359**: 1125-1136.

Li, X.Z., and Poole, K. (2001) Mutational analysis of the OprM outer membrane component of the MexA-MexB-OprM multidrug efflux system of Pseudomonas aeruginosa. *J Bacteriol* **183**: 12-27.

Livermore, D.M. (1995) beta-Lactamases in laboratory and clinical resistance. *Clin Microbiol Rev* **8**: 557-584.

Lobedanz, S., Bokma, E., Symmons, M.F., Koronakis, E., Hughes, C., and Koronakis, V. (2007) A periplasmic coiled-coil interface underlying TolC recruitment and the assembly of bacterial drug efflux pumps. *Proc Natl Acad Sci U S A* **104**: 4612-4617.

Locher, K.P., Lee, A.T., and Rees, D.C. (2002) The E. coli BtuCD structure: a framework for ABC transporter architecture and mechanism. *Science* **296**: 1091-1098.

Loo, T.W., Bartlett, M.C., and Clarke, D.M. (2002) The "LSGGQ" motif in each nucleotide-binding domain of human P-glycoprotein is adjacent to the opposing walker A sequence. *J Biol Chem* **277**: 41303-41306.

Lucas, C.E., Hagman, K.E., Levin, J.C., Stein, D.C., and Shafer, W.M. (1995) Importance of lipooligosaccharide structure in determining gonococcal resistance to hydrophobic antimicrobial agents resulting from the mtr efflux system. *Mol Microbiol* **16**: 1001-1009.

Mao, W., Warren, M.S., Black, D.S., Satou, T., Murata, T., Nishino, T., Gotoh, N., and Lomovskaya, O. (2002) On the mechanism of substrate specificity by resistance nodulation division (RND)-type multidrug resistance pumps: the large periplasmic loops of MexD from Pseudomonas aeruginosa are involved in substrate recognition. *Mol Microbiol* **46**: 889-901.

Masaoka, Y., Ueno, Y., Morita, Y., Kuroda, T., Mizushima, T., and Tsuchiya, T. (2000) A two-component multidrug efflux pump, EbrAB, in Bacillus subtilis. *J Bacteriol* **182**: 2307-2310.

Middlemiss, J.K., and Poole, K. (2004) Differential impact of MexB mutations on substrate selectivity of the MexAB-OprM multidrug efflux pump of Pseudomonas aeruginosa. *J Bacteriol* **186**: 1258-1269.

Mikolosko, J., Bobyk, K., Zgurskaya, H.I., and Ghosh, P. (2006) Conformational flexibility in the multidrug efflux system protein AcrA. *Structure* **14**: 577-587.

Miroux, B., and Walker, J.E. (1996) Over-production of proteins in Escherichia coli: mutant hosts that allow synthesis of some membrane proteins and globular proteins at high levels. *J Mol Biol* **260**: 289-298.

Mirza, O., Guan, L., Verner, G., Iwata, S., and Kaback, H.R. (2006) Structural evidence for induced fit and a mechanism for sugar/H+ symport in LacY. *Embo J* **25**: 1177-1183.

Mokhonov, V.V., Mokhonova, E.I., Akama, H., and Nakae, T. (2004) Role of the membrane fusion protein in the assembly of resistance-nodulation-cell division multidrug efflux pump in Pseudomonas aeruginosa. *Biochem Biophys Res Commun* **322**: 483-489.

Murakami, S., Nakashima, R., Yamashita, E., and Yamaguchi, A. (2002) Crystal structure of bacterial multidrug efflux transporter AcrB. *Nature* **419**: 587-593.

Murakami, S., Nakashima, R., Yamashita, E., Matsumoto, T., and Yamaguchi, A. (2006) Crystal structures of a multidrug transporter reveal a functionally rotating mechanism. *Nature* **443**: 173-179.

Murray, D.S., Schumacher, M.A., and Brennan, R.G. (2004) Crystal structures of QacR-diamidine complexes reveal additional multidrug-binding modes and a novel mechanism of drug charge neutralization. *J Biol Chem* **279**: 14365-14371.

Nagaoka, I., Hirota, S., Niyonsaba, F., Hirata, M., Adachi, Y., Tamura, H., Tanaka, S., and Heumann, D. (2002) Augmentation of the lipopolysaccharide-neutralizing activities of human cathelicidin CAP18/LL-37-derived antimicrobial peptides by replacement with hydrophobic and cationic amino acid residues. *Clin Diagn Lab Immunol* **9**: 972-982.

Nehme, D., Li, X.Z., Elliot, R., and Poole, K. (2004) Assembly of the MexAB-OprM multidrug efflux system of Pseudomonas aeruginosa: identification and characterization of mutations in mexA compromising MexA multimerization and interaction with MexB. *J Bacteriol* **186**: 2973-2983.

Ninio, S., Rotem, D., and Schuldiner, S. (2001) Functional analysis of novel multidrug transporters from human pathogens. *J Biol Chem* **276**: 48250-48256.

Ninio, S., Elbaz, Y., and Schuldiner, S. (2004) The membrane topology of EmrE - a small multidrug transporter from Escherichia coli. *FEBS Lett* **562**: 193-196.

Okada, U., Kondo, K., Hayashi, T., Watanabe, N., Yao, M., Tamura, T., and Tanaka, I. (2008) Structural and functional analysis of the TetR-family transcriptional regulator SCO0332 from Streptomyces coelicolor. *Acta Crystallogr D Biol Crystallogr* **64**: 198-205.

Oldham, M.L., Khare, D., Quiocho, F.A., Davidson, A.L., and Chen, J. (2007) Crystal structure of a catalytic intermediate of the maltose transporter. *Nature* **450**: 515-521.

Orelle, C., Dalmas, O., Gros, P., Di Pietro, A., and Jault, J.M. (2003) The conserved glutamate residue adjacent to the Walker-B motif is the catalytic base for ATP hydrolysis in the ATP-binding cassette transporter BmrA. *J Biol Chem* **278**: 47002-47008.

Orth, P., Cordes, F., Schnappinger, D., Hillen, W., Saenger, W., and Hinrichs, W. (1998) Conformational changes of the Tet repressor induced by tetracycline trapping. *J Mol Biol* **279**: 439-447.

Orth, P., Schnappinger, D., Sum, P.E., Ellestad, G.A., Hillen, W., Saenger, W., and Hinrichs, W. (1999) Crystal structure of the tet repressor in complex with a novel tetracycline, 9-(N,N-dimethylglycylamido)-6-demethyl-6-deoxy-tetracycline. *J Mol Biol* **285**: 455-461.

Orth, P., Schnappinger, D., Hillen, W., Saenger, W., and Hinrichs, W. (2000) Structural basis of gene regulation by the tetracycline inducible Tet repressor-operator system. *Nat Struct Biol* 7: 215-219.

Pan, W., and Spratt, B.G. (1994) Regulation of the permeability of the gonococcal cell envelope by the mtr system. *Mol Microbiol* **11**: 769-775.

Pao, S.S., Paulsen, I.T., and Saier, M.H., Jr. (1998) Major facilitator superfamily. *Microbiol Mol Biol Rev* **62**: 1-34.

Patel, O., Satchell, J., Baell, J., Fernley, R., Coloe, P., and Macreadie, I. (2003) Inhibition studies of sulfonamide-containing folate analogs in yeast. *Microb Drug Resist* **9**: 139-146.

Payen, L.F., Gao, M., Westlake, C.J., Cole, S.P., and Deeley, R.G. (2003) Role of carboxylate residues adjacent to the conserved core Walker B motifs in the catalytic cycle of multidrug resistance protein 1 (ABCC1). *J Biol Chem* **278**: 38537-38547.

Philippon, A., Arlet, G., and Jacoby, G.A. (2002) Plasmid-determined AmpC-type beta-lactamases. *Antimicrob Agents Chemother* **46**: 1-11.

Pinkett, H.W., Lee, A.T., Lum, P., Locher, K.P., and Rees, D.C. (2007) An inward-facing conformation of a putative metal-chelate-type ABC transporter. *Science* **315**: 373-377.

Porcelli, F., Verardi, R., Shi, L., Henzler-Wildman, K.A., Ramamoorthy, A., and Veglia, G. (2008) NMR structure of the cathelicidin-derived human antimicrobial peptide LL-37 in dodecylphosphocholine micelles. *Biochemistry* **47**: 5565-5572.

Ramos, J.L., Martinez-Bueno, M., Molina-Henares, A.J., Teran, W., Watanabe, K., Zhang, X., Gallegos, M.T., Brennan, R., and Tobes, R. (2005) The TetR family of transcriptional repressors. *Microbiol Mol Biol Rev* **69**: 326-356.

Rapp, M., Seppala, S., Granseth, E., and von Heijne, G. (2007) Emulating membrane protein evolution by rational design. *Science* **315**: 1282-1284.

Reichmann, P., Konig, A., Marton, A., and Hakenbeck, R. (1996) Penicillin-binding proteins as resistance determinants in clinical isolates of Streptococcus pneumoniae. *Microb Drug Resist* **2**: 177-181.

Rotem, D., and Schuldiner, S. (2004) EmrE, a multidrug transporter from Escherichia coli, transports monovalent and divalent substrates with the same stoichiometry. *J Biol Chem* **279**: 48787-48793.

Rouquette-Loughlin, C.E., Balthazar, J.T., Hill, S.A., and Shafer, W.M. (2004) Modulation of the mtrCDE-encoded efflux pump gene complex of Neisseria

meningitidis due to a Correia element insertion sequence. *Mol Microbiol* **54**: 731-741.

Rouquette, C., Harmon, J.B., and Shafer, W.M. (1999) Induction of the mtrCDE-encoded efflux pump system of Neisseria gonorrhoeae requires MtrA, an AraC-like protein. *Mol Microbiol* **33**: 651-658.

Sahin-Toth, M., le Coutre, J., Kharabi, D., le Maire, G., Lee, J.C., and Kaback, H.R. (1999) Characterization of Glu126 and Arg144, two residues that are indispensable for substrate binding in the lactose permease of Escherichia coli. *Biochemistry* **38**: 813-819.

Sahin-Toth, M., Karlin, A., and Kaback, H.R. (2000) Unraveling the mechanism of the lactose permease of Escherichia coli. *Proc Natl Acad Sci U S A* **97**: 10729-10732.

Sahin-Toth, M., and Kaback, H.R. (2001) Arg-302 facilitates deprotonation of Glu-325 in the transport mechanism of the lactose permease from Escherichiacoli. *Proc Natl Acad Sci U S A* **98**: 6068-6073.

Schlor, S., Schmidt, A., Maier, E., Benz, R., Goebel, W., and Gentschev, I. (1997) In vivo and in vitro studies on interactions between the components of the hemolysin (HlyA) secretion machinery of Escherichia coli. *Mol Gen Genet* **256**: 306-319.

Schneider, E., Wilken, S., and Schmid, R. (1994) Nucleotide-induced conformational changes of MalK, a bacterial ATP binding cassette transporter protein. *J Biol Chem* **269**: 20456-20461.

Scholz, O., Kostner, M., Reich, M., Gastiger, S., and Hillen, W. (2003) Teaching TetR to recognize a new inducer. *J Mol Biol* **329**: 217-227.

Schuldiner, S. (2007) When biochemistry meets structural biology: the cautionary tale of EmrE. *Trends Biochem Sci* **32**: 252-258.

Schumacher, M.A., Miller, M.C., Grkovic, S., Brown, M.H., Skurray, R.A., and Brennan, R.G. (2001) Structural mechanisms of QacR induction and multidrug recognition. *Science* **294**: 2158-2163.

Schumacher, M.A., Miller, M.C., Grkovic, S., Brown, M.H., Skurray, R.A., and Brennan, R.G. (2002) Structural basis for cooperative DNA binding by two dimers of the multidrug-binding protein QacR. *Embo J* **21**: 1210-1218.

Schumacher, M.A., Miller, M.C., and Brennan, R.G. (2004) Structural mechanism of the simultaneous binding of two drugs to a multidrug-binding protein. *Embo J* **23**: 2923-2930.

Seeger, M.A., Schiefner, A., Eicher, T., Verrey, F., Diederichs, K., and Pos, K.M. (2006) Structural asymmetry of AcrB trimer suggests a peristaltic pump mechanism. *Science* **313**: 1295-1298.

Seeger, M.A., von Ballmoos, C., Eicher, T., Brandstatter, L., Verrey, F., Diederichs, K., and Pos, K.M. (2008) Engineered disulfide bonds support the functional rotation mechanism of multidrug efflux pump AcrB. *Nat Struct Mol Biol* **15**: 199-205.

Sennhauser, G., Amstutz, P., Briand, C., Storchenegger, O., and Grutter, M.G. (2007) Drug export pathway of multidrug exporter AcrB revealed by DARPin inhibitors. *PLoS Biol* **5**: e7.

Shafer, W.M., Qu, X., Waring, A.J., and Lehrer, R.I. (1998) Modulation of Neisseria gonorrhoeae susceptibility to vertebrate antibacterial peptides due to a member of the resistance/nodulation/division efflux pump family. *Proc Natl Acad Sci U S A* **95**: 1829-1833.

Smith, P.C., Karpowich, N., Millen, L., Moody, J.E., Rosen, J., Thomas, P.J., and Hunt, J.F. (2002) ATP binding to the motor domain from an ABC transporter drives formation of a nucleotide sandwich dimer. *Mol Cell* **10**: 139-149.

Soskine, M., Adam, Y., and Schuldiner, S. (2004) Direct evidence for substrate-induced proton release in detergent-solubilized EmrE, a multidrug transporter. *J Biol Chem* **279**: 9951-9955.

Soskine, M., Mark, S., Tayer, N., Mizrachi, R., and Schuldiner, S. (2006) On parallel and antiparallel topology of a homodimeric multidrug transporter. *J Biol Chem* **281**: 36205-36212.

Spurlino, J.C., Lu, G.Y., and Quiocho, F.A. (1991) The 2.3-A resolution structure of the maltose- or maltodextrin-binding protein, a primary receptor of bacterial active transport and chemotaxis. *J Biol Chem* **266**: 5202-5219.

Stegmeier, J.F., Polleichtner, G., Brandes, N., Hotz, C., and Andersen, C. (2006) Importance of the adaptor (membrane fusion) protein hairpin domain for the functionality of multidrug efflux pumps. *Biochemistry* **45**: 10303-10312.

Steiner-Mordoch, S., Soskine, M., Solomon, D., Rotem, D., Gold, A., Yechieli, M., Adam, Y., and Schuldiner, S. (2008) Parallel topology of genetically fused EmrE homodimers. *Embo J* **27**: 17-26.

Strop, P., and Brunger, A.T. (2005) Refractive index-based determination of detergent concentration and its application to the study of membrane proteins. *Protein Sci* **14**: 2207-2211.

Szentpetery, Z., Kern, A., Liliom, K., Sarkadi, B., Varadi, A., and Bakos, E. (2004) The role of the conserved glycines of ATP-binding cassette signature motifs of MRP1 in the communication between the substrate-binding site and the catalytic centers. *J Biol Chem* **279**: 41670-41678.

Takahata, S., Senju, N., Osaki, Y., Yoshida, T., and Ida, T. (2006) Amino acid substitutions in mosaic penicillin-binding protein 2 associated with reduced susceptibility to cefixime in clinical isolates of Neisseria gonorrhoeae. *Antimicrob Agents Chemother* **50**: 3638-3645.

Takatsuka, Y., and Nikaido, H. (2006) Threonine-978 in the transmembrane segment of the multidrug efflux pump AcrB of Escherichia coli is crucial for drug transport as a probable component of the proton relay network. *J Bacteriol* **188**: 7284-7289.

Takatsuka, Y., and Nikaido, H. (2007) Site-directed disulfide cross-linking shows that cleft flexibility in the periplasmic domain is needed for the multidrug efflux pump AcrB of Escherichia coli. *J Bacteriol* **189**: 8677-8684.

Tamura, N., Murakami, S., Oyama, Y., Ishiguro, M., and Yamaguchi, A. (2005) Direct interaction of multidrug efflux transporter AcrB and outer membrane channel TolC detected via site-directed disulfide cross-linking. *Biochemistry* **44**: 11115-11121.

Tanaka, M., Nakayama, H., Huruya, K., Konomi, I., Irie, S., Kanayama, A., Saika, T., and Kobayashi, I. (2006) Analysis of mutations within multiple genes associated with resistance in a clinical isolate of Neisseria gonorrhoeae with reduced ceftriaxone susceptibility that shows a multidrug-resistant phenotype. *Int J Antimicrob Agents* **27**: 20-26.

Tate, C.G., Kunji, E.R., Lebendiker, M., and Schuldiner, S. (2001) The projection structure of EmrE, a proton-linked multidrug transporter from Escherichia coli, at 7 A resolution. *Embo J* **20**: 77-81.

Tate, C.G., Ubarretxena-Belandia, I., and Baldwin, J.M. (2003) Conformational changes in the multidrug transporter EmrE associated with substrate binding. *J Mol Biol* **332**: 229-242.

Teran, W., Krell, T., Ramos, J.L., and Gallegos, M.T. (2006) Effector-repressor interactions, binding of a single effector molecule to the operator-bound TtgR homodimer mediates derepression. *J Biol Chem* **281**: 7102-7109.

Tikhonova, E.B., Wang, Q., and Zgurskaya, H.I. (2002) Chimeric analysis of the multicomponent multidrug efflux transporters from gram-negative bacteria. *J Bacteriol* **184**: 6499-6507.

Tikhonova, E.B., and Zgurskaya, H.I. (2004) AcrA, AcrB, and TolC of Escherichia coli Form a Stable Intermembrane Multidrug Efflux Complex. *J Biol Chem* **279**: 32116-32124.

Touze, T., Eswaran, J., Bokma, E., Koronakis, E., Hughes, C., and Koronakis, V. (2004) Interactions underlying assembly of the Escherichia coli AcrAB-TolC multidrug efflux system. *Mol Microbiol* **53**: 697-706.

Toyoshima, C., and Inesi, G. (2004) Structural basis of ion pumping by Ca2+-ATPase of the sarcoplasmic reticulum. *Annu Rev Biochem* **73**: 269-292.

Trias, J., and Nikaido, H. (1990a) Protein D2 channel of the Pseudomonas aeruginosa outer membrane has a binding site for basic amino acids and peptides. *J Biol Chem* **265**: 15680-15684.

Trias, J., and Nikaido, H. (1990b) Outer membrane protein D2 catalyzes facilitated diffusion of carbapenems and penems through the outer membrane of Pseudomonas aeruginosa. *Antimicrob Agents Chemother* **34**: 52-57.

Tzeng, Y.L., Ambrose, K.D., Zughaier, S., Zhou, X., Miller, Y.K., Shafer, W.M., and Stephens, D.S. (2005) Cationic antimicrobial peptide resistance in Neisseria meningitidis. *J Bacteriol* **187**: 5387-5396.

Ubarretxena-Belandia, I., Baldwin, J.M., Schuldiner, S., and Tate, C.G. (2003) Three-dimensional structure of the bacterial multidrug transporter EmrE shows it is an asymmetric homodimer. *Embo J* **22**: 6175-6181.

Urbani, A., and Warne, T. (2005) A colorimetric determination for glycosidic and bile salt-based detergents: applications in membrane protein research. *Anal Biochem* **336**: 117-124.

Vaccaro, L., Koronakis, V., and Sansom, M.S. (2006) Flexibility in a drug transport accessory protein: molecular dynamics simulations of MexA. *Biophys J* **91**: 558-564.

VanAken, T., Foxall-VanAken, S., Castleman, S., and Ferguson-Miller, S. (1986) Alkyl glycoside detergents: synthesis and applications to the study of membrane proteins. *Methods Enzymol* **125**: 27-35.

Veal, W.L., Yellen, A., Balthazar, J.T., Pan, W., Spratt, B.G., and Shafer, W.M. (1998) Loss-of-function mutations in the mtr efflux system of Neisseria gonorrhoeae. *Microbiology* **144 (Pt 3)**: 621-627.

Veal, W.L., Nicholas, R.A., and Shafer, W.M. (2002) Overexpression of the MtrC-MtrD-MtrE efflux pump due to an mtrR mutation is required for chromosomally mediated penicillin resistance in Neisseria gonorrhoeae. *J Bacteriol* **184**: 5619-5624.

Venkatesan, P., and Kaback, H.R. (1998) The substrate-binding site in the lactose permease of Escherichia coli. *Proc Natl Acad Sci U S A* **95**: 9802-9807.

Walker, J.E., Saraste, M., Runswick, M.J., and Gay, N.J. (1982) Distantly related sequences in the alpha- and beta-subunits of ATP synthase, myosin, kinases and other ATP-requiring enzymes and a common nucleotide binding fold. *Embo J* **1**: 945-951.

Ward, A., Reyes, C.L., Yu, J., Roth, C.B., and Chang, G. (2007) Flexibility in the ABC transporter MsbA: Alternating access with a twist. *Proc Natl Acad Sci U S A* **104**: 19005-19010.

Warner, D.M., Folster, J.P., Shafer, W.M., and Jerse, A.E. (2007) Regulation of the MtrC-MtrD-MtrE efflux-pump system modulates the in vivo fitness of Neisseria gonorrhoeae. *J Infect Dis* **196**: 1804-1812.

Weinglass, A.B., Soskine, M., Vazquez-Ibar, J.L., Whitelegge, J.P., Faull, K.F., Kaback, H.R., and Schuldiner, S. (2005) Exploring the role of a unique carboxyl residue in EmrE by mass spectrometry. *J Biol Chem* **280**: 7487-7492.

Willmott, C.J., and Maxwell, A. (1993) A single point mutation in the DNA gyrase A protein greatly reduces binding of fluoroquinolones to the gyrase-DNA complex. *Antimicrob Agents Chemother* **37**: 126-127.

Yamanaka, H., Morisada, N., Miyano, M., Tsuge, H., Shinoda, S., Takahashi, E., and Okamoto, K. (2004) Amino-acid residues involved in the expression of the activity of Escherichia coli TolC. *Microbiol Immunol* **48**: 713-722.

Yerushalmi, H., Lebendiker, M., and Schuldiner, S. (1995) EmrE, an Escherichia coli 12-kDa multidrug transporter, exchanges toxic cations and H+ and is soluble in organic solvents. *J Biol Chem* **270**: 6856-6863.

Yerushalmi, H., and Schuldiner, S. (2000) An essential glutamyl residue in EmrE, a multidrug antiporter from Escherichia coli. *J Biol Chem* **275**: 5264-5269.

Yerushalmi, H., Mordoch, S.S., and Schuldiner, S. (2001) A single carboxyl mutant of the multidrug transporter EmrE is fully functional. *J Biol Chem* **276**: 12744-12748.

Yin, Y., He, X., Szewczyk, P., Nguyen, T., and Chang, G. (2006a) Structure of the multidrug transporter EmrD from Escherichia coli. *Science* **312**: 741-744.

Yin, Y., Jensen, M.O., Tajkhorshid, E., and Schulten, K. (2006b) Sugar binding and protein conformational changes in lactose permease. *Biophys J* **91**: 3972-3985.

Yoneyama, H., Maseda, H., Kamiguchi, H., and Nakae, T. (2000) Function of the membrane fusion protein, MexA, of the MexA, B-OprM efflux pump in Pseudomonas aeruginosa without an anchoring membrane. *J Biol Chem* **275**: 4628-4634.

Zaitseva, J., Jenewein, S., Jumpertz, T., Holland, I.B., and Schmitt, L. (2005) H662 is the linchpin of ATP hydrolysis in the nucleotide-binding domain of the ABC transporter HlyB. *Embo J* **24**: 1901-1910.

Zaitseva, J., Oswald, C., Jumpertz, T., Jenewein, S., Wiedenmann, A., Holland, I.B., and Schmitt, L. (2006) A structural analysis of asymmetry required for catalytic activity of an ABC-ATPase domain dimer. *Embo J* **25**: 3432-3443.

Zanetti, M., Gennaro, R., and Romeo, D. (1995) Cathelicidins: a novel protein family with a common proregion and a variable C-terminal antimicrobial domain. *FEBS Lett* **374**: 1-5.

Zarantonelli, L., Borthagaray, G., Lee, E.H., Veal, W., and Shafer, W.M. (2001) Decreased susceptibility to azithromycin and erythromycin mediated by a novel mtr(R) promoter mutation in Neisseria gonorrhoeae. *J Antimicrob Chemother* **47**: 651-654.

Zgurskaya, H.I., and Nikaido, H. (1999a) Bypassing the periplasm: reconstitution of the AcrAB multidrug efflux pump of Escherichia coli. *Proc Natl Acad Sci U S A* **96**: 7190-7195.

Zgurskaya, H.I., and Nikaido, H. (1999b) AcrA is a highly asymmetric protein capable of spanning the periplasm. *J Mol Biol* **285**: 409-420.

Zgurskaya, H.I., and Nikaido, H. (2000) Cross-linked complex between oligomeric periplasmic lipoprotein AcrA and the inner-membrane-associated multidrug efflux pump AcrB from Escherichia coli. *J Bacteriol* **182**: 4264-4267.

Zhang, Z., Ma, C., Pornillos, O., Xiu, X., Chang, G., and Saier, M.H., Jr. (2007) Functional characterization of the heterooligomeric EbrAB multidrug efflux transporter of Bacillus subtilis. *Biochemistry* **46**: 5218-5225.